CHARACTERIZATION OF PH AND ION REGULATORY PROTEINS IN LARVAL MOSQUITOES

By

KRISTIN ELIZABETH SMITH

A DISSERTATION PRESENTED TO THE GRADUATE SCHOOL
OF THE UNIVERSITY OF FLORIDA IN PARTIAL FULFILLMENT
OF THE REQUIREMENTS FOR THE DEGREE OF
DOCTOR OF PHILOSOPHY

UNIVERSITY OF FLORIDA

2009

To my loving and supportive family

ACKNOWLEDGMENTS

I thank the family and friends who have supported and encouraged me throughout the last five years. I thank my mother and father for always believing in me and never letting me forget it. I could not have done without their encouragement and advice. I thank my other half, Robbie, for being an ear to talk to, a shoulder to cry on, and a friend with whom to celebrate my accomplishments and lament my failures. I thank the members of my committee as well as the faculty, staff and students of Whitney for sharing their time, expertise, and opinions, thereby helping me accomplish much of what is written herein. Finally, I thank my advisor, Prof. Paul Linser for his support, both financial and emotional, and for allowing me the freedom to expand my science in the directions which fit my interests.

TABLE OF CONTENTS

page

LIST OF TABLES

LIST OF FIGURES

LIST OF ABBREVIATIONS

AE	Anion exchanger
AMG	Anterior midgut
AP	Alkaline phosphatase
AR	Anterior rectum
ASW	Artificial seawater
CA	Carbonic anhydrase
CA-RP	Carbonic anhydrase-related protein
DAR	Dorsal anterior rectal
DEPC	Diethylpyrocarbonate
DIDS	4,4'-diisothiocyanostilbene-2,2'- disulfonic acid
ds	Double-stranded
FBS	Fetal bovine serum
FITC	Fluorescein isothiocyanate
GC	Gastric caeca
GPI	Glycosylphosphatidylinositol
HG	Hindgut
mg	milligram
ML	multiple label
MR4	Malaria Research and Reference Reagent Resource Center
MT	Malpighian tubule
NAT	Nutrient amino acid transporter
NaP	Sodium phosphate
NBC	Sodium/bicarbonate cotransporter
NGS	Normal goat serum

NHE	Sodium hydrogen exchanger
Pen-strep	Penicillin-streptomycin
PM	Peritrophic matrix
PMG	Posterior midgut
PR	Posterior rectum
Pre-Inc	Pre-incubation medium
QPCR	Quantitative PCR
RACE	Rapid amplification of cDNA ends
RNAi	RNA interference
ROI	Region of interest
RT	reverse transcription
SIET	Self-referencing ion-selective electrode technique
siRNA	Small interfering RNA
SLC	Solute carrier
ss	Single-stranded
TBS	Tris-buffered saline
TEAHCL	Triethanolamide hydrochloride
TR	Transitional region
TRITC	Tetramethyl Rhodamine Iso-Thiocyanate
USDA	United States Department of Agriculture

Abstract of Dissertation Presented to the Graduate School
of the University of Florida in Partial Fulfillment of the
Requirements for the Degree of Doctor of Philosophy

CHARACTERIZATION OF PH AND ION REGULATORY PROTEINS IN LARVAL MOSQUITOES

By

Kristin Elizabeth Smith
May 2009

Chair: Paul Linser
Major: Medical Sciences- Molecular Cell Biology

Mosquitoes have long been a major cause of human morbidity and mortality, and as a result, worldwide efforts are underway to control these disease vectors. Evidence suggests that targeting the larval stages of the mosquito lifecycle in addition to the adult stage may facilitate vector control. In order to specifically and safely target mosquito larvae using control methods, a thorough understanding of the biological systems crucial for larval survival is necessary. Here I characterize proteins that influence larvae's ability to tightly control the pH within their alimentary canal, as well as proteins involved in their ability to adapt to varying environmental conditions. Uncovering the methods of pH and ion regulation employed by larvae in both of these processes could lead to the discovery of novel targets and new and improved larvicides.

First, I report the cloning and characterization of novel carbonic anhydrase transcripts from the larval *Anopheles gambiae* alimentary canal. Mosquito larvae generate a highly alkaline pH in a restricted area of the alimentary canal, and carbonic anhydrase is a crucial enzyme for the generation and maintenance of this pH. Characterization of mRNA expression and protein distribution in the case of one CA, AgCA9, reveal an alternate pathway for bicarbonate/carbonate transport into the lumen of the alimentary canal, updating the current model for larval pH regulation. Additionally, RNA interference work in an *An. gambiae* larval

cell line demonstrates that AgCA9 is a protein capable of being manipulated by RNAi and suggests that this technique can be used to silence a CA in live mosquito larvae.

Finally, antibody immunolocalization of AgCA9 reveals a novel subset of cells in the rectum of anopheline larvae. I characterize the cells of this rectum using immunohistochemistry, physiology, and pharmacology and use this data to develop a putative model of ion regulation in the anopheline rectum. This model supports my current hypothesis that anopheline larvae shift protein distribution to change the primary function of the rectum from absorption, in larvae reared in fresh water, to secretion, in larvae reared in saline water. Additionally, this work emphasizes the differences in rectal structure and protein regulation between anophelines and culicines, and suggests that these two subfamilies may be employ very different adaptive and regulatory strategies.

CHAPTER 1
INTRODUCTION

Significance

Mosquitoes (Diptera: Culicidae) are hosts to a number of pathogens including parasites, bacteria, viruses, and fungi. The Culicidae includes two subfamilies which comprise relevant disease vectors: the Anophelinae (including the *Anopheles* genus), and the Culicinae (including *Aedes*, *Culex*, and *Ochlerotatus* genera). Members of both subfamilies spread pathogens through the infectious bite of the adult female and were responsible for more human death and disease in the 17th through 20th centuries than all other causes combined (Gubler, 1991). Malaria is the worst of all vector-borne diseases and one of the top three killers among communicable diseases, infecting 500 million people worldwide, and killing at least two million people each year (The World Health Report, 1996; Sachs and Malaney, 2002). For these reasons, mosquitoes have been named the greatest menace of all disease-transmitting insects (The World Health Report, 1996), and worldwide efforts to control mosquito populations have been either implemented or proposed.

Mosquito control. Most mosquito control methods target the adult stage; however, evidence suggests that targeting larval stages in concert may vastly improve the efficacy of control strategies (Killeen et al., 2002a; Killeen et al., 2002b). Mosquito larvae develop from eggs laid in standing water or on sites that will be flooded, and hatch within a few days to a week. The juvenile mosquito passes through four aquatic larval instars, distinguishable by size, before pupating and emerging as a winged adult (Clements, 1992) (Figure 1-1). At any given time, the vast majority of mosquitoes on Earth are in the larval stage, an important phase in the insect's life cycle. Development during this period is critical for the emergence of healthy adults capable of reproducing and spreading disease. It is also during the larval stages that mosquitoes

are perhaps the most susceptible to control. Unlike adults that can avoid intervention by changing their location (i.e. flying away), larvae are strictly aquatic and confined to the body of water in which they were hatched (Killeen et al., 2002a). For these reasons, the larval stages of the mosquito lifecycle are ideal targets for control methods. Indeed, evidence supports the idea that targeting the larval stages in a rigorous, well managed manner may facilitate vector control (Killeen et al., 2002a; Killeen et al., 2002b).

Currently, effective larvacides are available; however, the increasing occurrence of vector resistance to insecticides necessitates a constant search for new control methods. An ideal larvacide targets a protein or pathway that is both essential for larval mosquito viability and unique to mosquitoes so as not to affect other wildlife. To find such putative targets, a detailed understanding of larval biology is needed. To date, very little research is dedicated to the biology and physiology of larval mosquitoes, or to the biological processes necessary for larval survival. Two particularly important processes for larval survival are the generation and maintenance of a luminal pH gradient, and the regulation of hemolymph osmolarity in unstable ionic environments.

pH Regulation in the Larval Alimentary Canal

One of the most intriguing aspects of mosquito biology is the ability of larvae to generate and maintain a luminal pH in excess of 10.5 in a specific region of the alimentary canal (Dadd, 1975; Zhuang et al., 1999). This is one of the highest pHs known to exist in a biological system; the use of this high pH to initiate digestion sharply contrasts most other organisms which initiate digestion in conditions that are more acidic, and can reach a pH equivalent to battery acid (~ pH 1.0) in certain situations. Because of the relative uniqueness of this mosquito characteristic, proteins responsible for the regulation of this pH may serve as targets for specific larvacides.

The larval alimentary canal is an epithelial tube one cell thick and composed of seven main regions listed here in order from anterior to posterior: the foregut, gastric caeca (GC), anterior midgut (AMG), posterior midgut (PMG), Malpighian tubules (MT), ileum and rectum (Figure 1-2). The pH of the alimentary canal lumen ranges from pH 6.5 in the rectum (Clark et al., 2007) to 7.5 in the GC and PMG to 10.5 in the AMG (Dadd, 1975) (see Figure 1-2). The highly alkaline pH is restricted to the AMG and exists in the absence of any morphological barriers between it and the near neutral pH values of the GC and PMG lumina. The alkaline AMG may have a role in the dissociation of tannin-protein complexes that are found in the phytophagous diet of insect larvae (Berenbaum, 1980).

Whereas larvae maintain a luminal pH of up to 10.5, they regulate their hemolymph to a constant pH of approximately 7.5 (Clark et al., 2004). Mosquitoes have an open circulatory system, common to arthropods, which allows the hemolymph to circulate freely throughout the insect and bathe the alimentary canal epithelial cells directly on their basal side. It is still largely a mystery how the cells of the AMG can be exposed to a nearly neutral pH in the hemolymph on their basal side while maintaining a pH as high as 10.5 on their apical side. The alimentary canal cells must exhibit a tightly regulated system of ion balance in order to function in such an extreme environment.

Structure of the Larval Alimentary Canal

Each alimentary canal region has a structure and gene expression pattern specialized for certain aspects of larval digestion as well as for biological processes including pH and ion regulation (Neira et al., 2008). The GC are eight blind expansions of the alimentary canal and are composed of four cell types: (1) resorbing/secreting cells, (2) ion-transporting cells, (3) caecal membrane-secreting cells, and (4) imaginal cells. These cell types can be found in distinct regions of the GC or intermixed, depending on the species (Volkmann and Peters, 1989).

Additionally, the cells of the GC secrete a fine granular substance, referred to as the caecal membrane, which separates the GC lumen from the rest of the alimentary canal (Clements, 1992). Recent evidence suggests a major role for the GC in protein metabolism (Neira et al., 2008).

The AMG cells possess short apical microvilli with abundant mitochondria in the apical cytoplasm and an extensive basal labyrinth which extends throughout most of the cell (Clements, 1992). The presence of small microvilli suggests that this region is not involved in major transport processes, and in support of this the AMG appears to express very few transcripts associated with transport compared to the other regions of the alimentary canal (Neira et al., 2008; K. E. Smith, unpublished data). However, microarray-based evidence indicates a role for this region in lipid metabolism and absorption (Neira et al., 2008). Additionally, the AMG lumen is highly alkaline (pH>10), suggesting an involvement of the cells in the generation and maintenance of this pH, and will be discussed in detail in the next section. The AMG is separated from the food bolus by a multilayered matrix composed mostly of chitin and carbohydrate. This "peritrophic matrix" extends from the foregut through the rectum, thus creating the endoperitrophic space, or the area within the peritrophic matrix, and the ectoperitrophic space, or the area between the peritrophic matrix and the epithelial cells (see Figure 1-2; Clements, 1992).

The AMG is separated from the PMG by a brief transitional region. Although little information is currently available regarding functions of this region, the transitional cells exhibit a distinct response to the *Bacillus thuringiensis isrealensis* CryVB toxin (Clark et al., 1999), suggesting that this region is distinct from either the AMG or PMG. The PMG cells possess long apical microvilli and abundant mitochondria in the apical cytoplasm with a less developed basal

labyrinth than the AMG (Clements, 1992). This region plays a major role in digestion and absorption of both protein and carbohydrates (Neira et al., 2008).

Five MTs open into the alimentary canal and comprise two cell types, primary cells and stellate cells. The MTs function similar to human kidneys by producing a primary urine. This urine is then passed posteriorly through the ileum, a muscular tube composed mostly of squamous cells, and into the rectum. The rectum modifies the primary urine, having a major role in ion regulation. This role is supported by the structure of the rectal cells, which possess tightly packed apical lamellae and an extensive basal labyrinth (Meredith and Phillips, 1973).

The various cells of the alimentary canal work together to maintain larval health in a constantly changing environment. Presently, a detailed understanding of the mechanisms driving digestion and pH regulation in the regions of the alimentary canal is lacking; however, evidence supports roles for members of the carbonic anhydrase family (CAs) (Corena et al., 2002; Seron et al., 2004; Strange and Phillips, 1984; T. J. Seron, personal communication), and for the membrane-bound Cl^-/HCO_3^- anion exchanger family (AEs; Strange and Phillips, 1984; Strange et al., 1984; Boudko et al., 2001a).

Current Model of Alimentary Canal Alkalization

The current model for larval alimentary canal alkalization was modified from that of *Manduca sexta*, the tobacco hornworm. Like mosquito larvae, caterpillars generate a highly alkaline pH in their alimentary canal, in some cases exceeding pH 12. *M. sexta* generates this pH by the action of an H^+ V-ATPase, which hyperpolarizes the membranes of specialized goblet cells (Harvey et al., 1983), thereby driving the transport of luminal H^+ for cellular K^+ (Wieczorek et al., 1991; Azuma et al., 1995). This system is sufficient to support a pH of 11 with CO_3^{2-} (carbonate) as the counterion (Azuma et al., 1995).

Similarly, larval mosquitoes energize ion transport in the alimentary canal by the action of an H^+ V-ATPase (Filippova et al., 1998; Zhuang et al., 1999; Boudko et al., 2001b), which uses ATP to generate a proton gradient across a membrane. In the GC and PMG, V-ATPase localizes to the apical membrane of the epithelial cells (Zhuang et al., 1999), hyperpolarizing the membrane and providing a supply of H^+ ions to the lumen. The alkaline pH in the AMG of mosquito larvae is expected to be buffered, like *M. sexta*, by CO_3^{2-}. Indeed, CA in the cytoplasm of the epithelial cells (Corena et al., 2002) catalyzes the conversion of carbon dioxide (CO_2) to bicarbonate (HCO_3^-) and a proton (H^+). Plasma membrane anion exchangers on the apical membrane may facilitate the electroneutral transport of $HCO3^-$ into the lumen in exchange for Cl^-. HCO_3^- has a pKa of 6.3 and is sufficient to buffer the near neutral pH of the GC and AMG. By contrast, in the AMG, the V-ATPase localizes to the basal membrane (Zhuang et al., 1999), and generates a net flux of protons out of the lumen (Boudko et al., 2001b). This may result in luminal HCO_3- losing an H^+, thereby forming CO_3^{2-} which has a pKa exceeding 10.0. When paired with a strong cation such as K^+ or Na^+, CO_3^{2-} could buffer the highly alkaline AMG lumen.

Ion Regulation in Mosquito Larvae

A second biological process which is crucial for larval survival, but which has been largely overlooked in many species, is ion regulation. Larval mosquitoes are aquatic organisms that live in habitats of varying salinities ranging from rain pools and streams to salt marshes and hypersaline lakes. The majority of mosquito species live in fresh water, having variable tolerance for low levels of salinity, whereas approximately 5% live in either brackish or saline water (O'Meara, 1976; Clements, 1992). A major challenge faced by all mosquito larvae is the tendency for these habitats to fluctuate widely in salinity due to such occurrences as rainfall or evaporation (Clements, 1992). For most larvae to survive in waters which are at times greatly

hyper- or hypo-osmotic to their hemolymph, they must possess highly developed systems for regulating the absorption and excretion of ions.

Larval rectum: A key organ responsible for ion regulation in larval mosquitoes is the rectum. The rectum modifies urine produced by the MT prior to excretion based on the ionic needs of the larva, resorbing essential nutrients and excreting excess salts and waste products. Because larvae depend on ion regulation for survival, the recta of several culicine genera have been studied in detail (Ramsay, 1950; Asakura, 1970; Meredith and Phillips, 1973; Bradley and Phillips, 1975, Bradley and Phillips, 1977). However, little data has been published describing the recta of anophelines. Because anopheline mosquitoes account for 100% of the world's human malaria vectors and are vectors for many other deadly diseases, it is critical to understand the processes necessary for their survival (including ion regulation and adaptation). This knowledge can foster the development of novel techniques to reduce the population of these vectors both specifically and safely.

Specific Aims

I predict that proteins intimately involved in both pH- and ion- regulation could be targeted in the production of specific and efficient larvacides. Based on this prediction, the goals of this project were to (1) expand the current physiological model of alimentary canal alkalization in mosquito larvae, and (2) develop a better understanding of ion regulation in anopheline larvae. The objectives for each of these goals are outlined in the following specific aims:

1. Clone, characterize, and localize the expression of members of the Cl^-/HCO_3^- transporter gene family in the larval mosquito alimentary canal (addressed in Appendix A)

2. Clone, characterize, and localize the expression of members of the carbonic anhydrase gene family in larval mosquito alimentary canal (addressed in Chapter 3)

3. Determine the specific role of members of the carbonic anhydrase family on larval alkalization using RNA interference (addressed in Chapter 4)

4. Characterize the rectal cell types in the larval anopheline mosquito (addressed in Chapters 5 and 6)

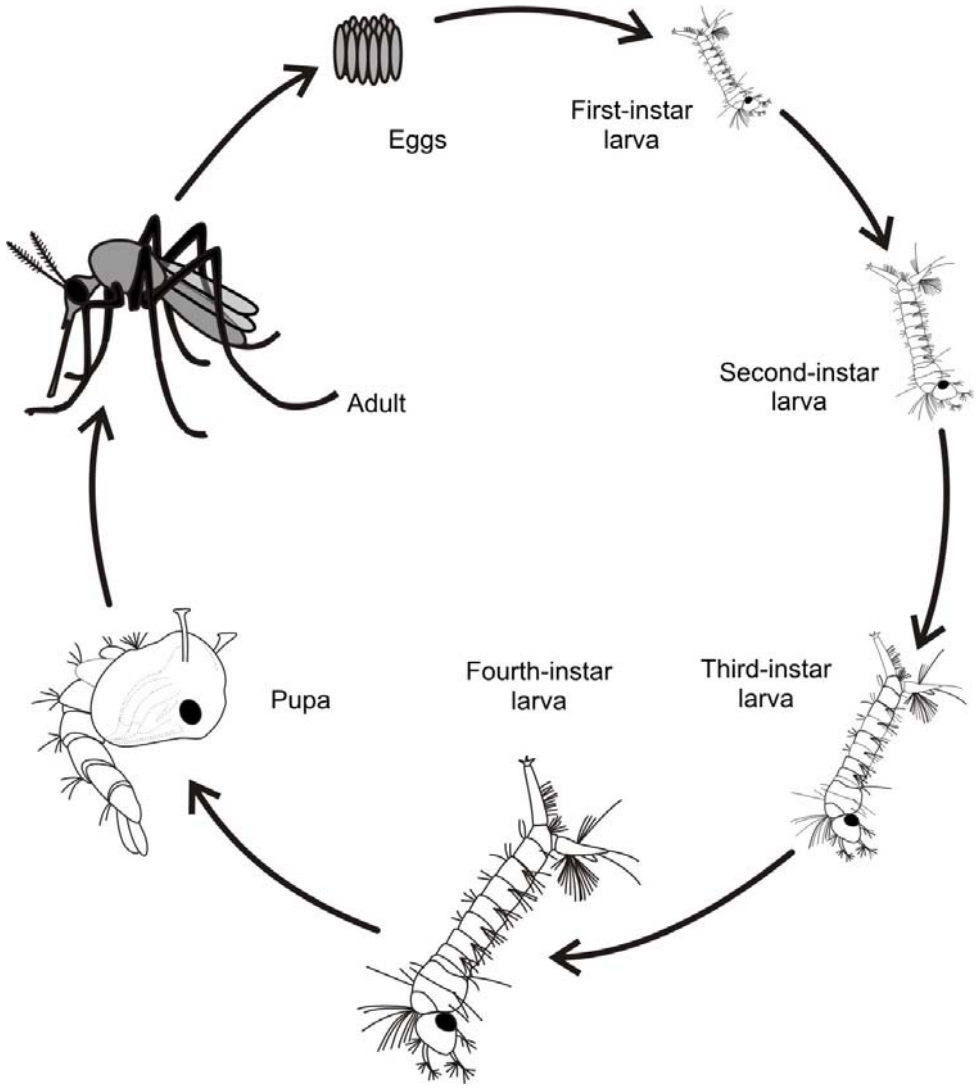

Figure 1-1. Mosquito life cycle. Mosquitoes hatch from eggs and pass through four aquatic larval instar stages before pupating and emerging as a winged adult.

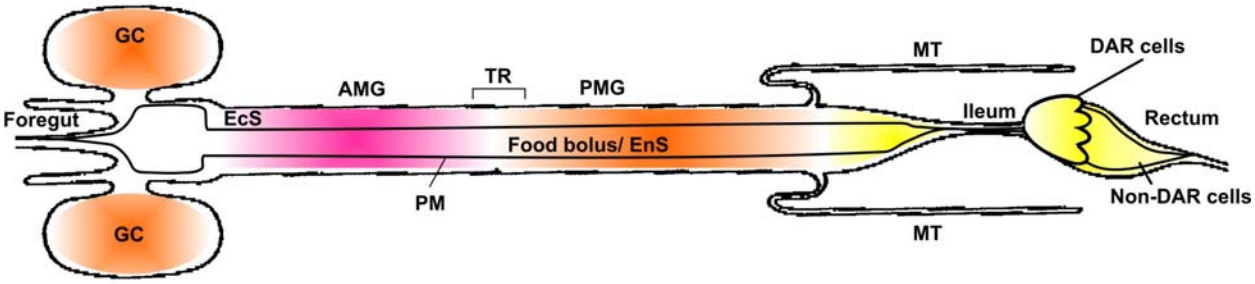

Figure 1-2. Structure of the larval alimentary canal. The larval alimentary canal consists of the forgut, gastric caeca (GC), anterior midgut (AMG), transitional region (TR), posterior midgut (PMG), Malpighian tubules (MT), ileum and rectum. The rectum is further divided into DAR and non-DAR cells. The alimentary canal is lined with the peritrophic matrix (PM) which separates the lumen into the ectoperitrophic space (EcS) and endoperitrophic space (EnS). The pH within the alimentary canal ranges from approximately 6.5 (yellow) in the rectum to 7.5 (orange) in the GC and PMG to 10.5 (red) in the AMG.

CHAPTER 2
MATERIALS AND METHODS

Artificial Sea Water (ASW)

100% artificial sea water (ASW): 420 mmol l^{-1} NaCl; 9 mmol l^{-1} KCl; 12 mmol l^{-1} $CaCl_2.H_2O$; 23 mmol l^{-1} $MgCl_2.6H2O$; 26 mmol l^{-1} $MgSO_4.7H2O$; and 2 mmol l^{-1} $NaHCO_3$ in milli-Q water (Millipore, Billerica, MA, USA), pH 8.1, osmolarity: 860 mosmol l^{-1} as measured using a 5500 vapor pressure osmometer (Wescor, Logan, UT, USA). All dilutions of the 100% ASW stock were made using milli-Q water.

Experimental Insects

Anopheles albimanus (STECLA), *Anopheles gambiae* (SS G3), *Anopheles farauti* (FAR1), and *Anopheles stephensi* (STE2) were hatched from eggs supplied by MR4 (The Malaria Research and Reference Reagents Resource Center) at the Centers for Disease Control and Prevention in Atlanta, GA, USA (http://www.malaria.atcc.org) and maintained as described in the supplier manual (www2.ncid.cdc.gov/vector/vector.html).

Ochlerotatus taeniorhynchus, *Aedes aegypti*, *Aedes albopictus* , and *Anopheles quadrimaculatus* were hatched from eggs supplied by the USDA (United States Department of Agriculture) in Gainesville, FL.

An. aquasalis were hatched from eggs and reared to fourth-instar in 10% artificial ASW by Dr. Luciano Moreira at The Oswaldo Cruz Institute in Rio de Janeiro, Brazil.

Unless otherwise stated, all larvae were reared in identical fresh water conditions (milli-Q water) at a density of approximately 100 larvae per 200 ml water. Additionally, certain species were hatched and reared in dilutions of ASW: *An. albimanus* (50% ASW), *An. gambiae* (10%, 20%, 30%, and 40% ASW, and acclimated to 60% ASW from milli-Q water by increasing the salinity by 10% each day beginning day 1 post hatch), *Oc. taeniorhynchus* (100% ASW), and *Ae.*

aegypti (40% ASW). Unless otherwise stated, all larvae were used at the early fourth-instar stage. Anopheline larvae were fed every other day with a dusting of ground TetraMin™ fish flakes (Tetra; Melle, Germany). Culicine larvae were fed every other day with a mixture of brewer's yeast and liver powder (2:3) (MP Biomedicals Inc., Solon, OH, USA).

I evaluated the fresh-water species *Ae. aegypti* (n=2 egg batches) and *An. gambiae* (n=3 egg batches), for larval size and mortality rates when reared in fresh water, 30% and 40% ASW. Mortality rates were determined by isolating 100 newly hatched first-instar larvae into a separate container and counting the surviving larvae daily. This continued until larvae reached fourth-instar (*An. gambiae*) or until the first pupa was observed (*Ae. aegypti*).

Ag55 Cell Line

The Ag55 cell line (Pudney et. al., 1979) was obtained from Kimberly Keene (Colorado State University). The cells were grown in 75 cm^2 flasks (Fisher Scientific, Pittsburgh, PA, USA) at 28°C in Leibovitz's L-15 media (Sigma-Aldrich, St. Louis, MO, USA) with 10% fetal bovine serum (FBS, Atlantic Biologicals, Norcross, GA, USA) and 1% Penicillin-Streptomycin solution (pen-strep; Sigma-aldrich). The cell media were changed every other day.

Isolation of RNA

To isolate RNA from mosquito tissues or cells, one of two reagents were used: TRI reagent® - RNA / DNA / Protein isolation reagent (Molecular Research Center, Inc; Cincinnati, OH, USA) and RNAqueous® Kit (Applied Biosystems/Ambion, Austin, TX, USA).

For TRI reagent samples, 50-100 mg of tissue, or cells grown on a culture dish <10 cm^2, were homogenized in one ml of TRI REAGENT and incubated at room temperature for five minutes to permit complete dissociation of nucleoprotein complexes. The homogenate was then supplemented with 0.2 ml chloroform, vortexed for 15 seconds, incubated at room temperature for 15 minutes, and centrifuged 12,000g for 15 minutes at 4°C. The aqueous phase contained the

RNA and was transferred to a separate tube. The DNA and protein remained in the interface and organic phases and were stored at 4°C for subsequent isolation of protein (see next section). The RNA was precipitated by combining with 0.5 ml isopropanol, incubated at room temperature for ten minutes, and centrifuged at 12,000g for eight minutes at 4°C. The supernatant was removed and the RNA pellet washed with one ml 75% ethanol for five minutes at 4°C. The supernatant again was removed and the RNA was air-dried for ten minutes under a fume-hood. RNA was resuspended in 0.5% SDS and incubated for 15 minutes at 55°C.

For RNAqueous samples, 1-75 mg, or cells grown on a culture dish < 60 cm^2 were homogenized in lysis buffer (10µl mg^{-1} tissue). An equal volume of 64% ethanol was add to the lysate and mixed gently. The lysate/ethanol mixture was applied to a Filter Cartridge assembled in a Collection Tube and centrifuged at 15,000g for one minute. The RNA was washed three times by applying 700 µl Wash Solution #1 once, and 500 µl Wash Solution #2/3 two successive times, centrifuging at 15,000g for one minute between each wash solution. The RNA was centrifuged an additional minute at 500g to ensure all wash solution was removed before the RNA was eluted twice with 50 µl Elution Solution preheated to 70°C. RNA was then precipitated with one-half volume LiCl Precipitation Solution, incubated for 30 minutes at -20°C, and centrifuged for 30 minutes at top speed. The supernatant was removed and the pellet was washed with cold 70% ethanol in diethylpyrocarbonate (DEPC) treated water and centrifuged for 30 minutes at top speed. The supernatant was removed and the pellet air-dried for ten minutes under a fume-hood. The pellet was resuspended in DEPC treated water.

All RNA was treated with DNase following extraction to ensure removal of genomic DNA. DNase I (10 Units/ml RNA; New England Biolabs, Ipswich, MA, USA) and 10x DNase reaction buffer (1/10 final reaction volume) was combined with RNA and the mixture was

incubated at 37°C for 30 minutes. To inactivate DNase I, EDTA was added to a final concentration of 5 mmol l^{-1} and the reaction was incubated at 70°C for ten minutes. RNA was stored at -20°C until use.

Isolation of Protein

Protein was isolated from samples using TRI reagent® - RNA / DNA / Protein isolation reagent (Molecular Research Center, Inc.). Protocol was followed for RNA isolation (see above section) for 50-100 mg of tissue, or cells grown on a culture dish <10 cm^2, until the step involving separation of aqueous and organic phases. The aqueous phase was removed and the organic phase was saved for isolation of protein. First the DNA was precipitated by mixing the organic phase with 0.3 mls of 100% ethanol, incubating at room temperature for three minutes, and pelleting the DNA at 2,000g for five minutes at 4°C. The phenol-ethanol supernatant was removed and aliquoted 0.5 mls per tube. Three volumes of acetone were added to each aliquot; the samples were incubated for ten minutes at room temperature and centrifuged at 12,000g for ten minutes at 4°C. The following was performed three consecutive times: the protein pellet was dispersed in 0.5 ml of 0.3 mol l^{-1} guanidine hydrochloride in 95% ethanol + 2.5 % glycerol (V:V) using a small conical Teflon pestle (Fisher K749515-0000) attached to a mechanical stirrer (~30 sec @ 800-1000 RPM). Following dispersal, another 0.5 ml aliquot of the guanidine hydrochloride/ethanol/glycerol wash solution was added and the sample was incubated for ten minutes at room temperature. The protein was pelleted again at 8,000g for five minutes.

The protein was washed one final time in one ml of ethanol containing 2.5 % glycerol (V:V), incubated at room temperature for ten minutes, and pelleted at 8,000g for five minutes. The alcohol was decanted, and the tube was inverted to dry for 7-10 min at room temperature. The pellet was resuspended in a solution of 1% SDS.

Cloning of AgCAs and AgAEs

Generation of cDNA Collections

Extracted RNA was precipitated by combining with 8 mol l^{-1} lithium chloride (1/10 final reaction volume) and 100% ethanol (2.5x final reaction volume) and incubating at -20°C for 30 minutes, centrifuging at top speed for 30 minutes, removing supernatant, and washing with 70% ethanol in DEPC-treated water. The RNA was then centrifuged for 20 minutes at top speed, the supernatant was removed and RNA was air-dried under a fume hood for 20 minutes. The RNA was then resuspended in 6 µl DEPC-treated water and run (1.0 µl) on a 1% agarose gel to ensure RNA quality.

cDNA collections were generated as described in Matz (2003). See Table 2-1 for all primer names referred to in this section and their corresponding sequences. The first strand synthesis reaction was prepared by combining 5.0 µl RNA with 1.0 µl TRSa primer (10 µmol l^{-1}) and heating to 65°C for three minutes. To this was added 2.0 µl 5x first-strand buffer (Superscript™ II RT, Invitrogen, Carlsbad, CA, USA), 1.0 µl DTT (0.1 mol l^{-1}), 1.0 µl TS-oligo primer (5 µmol l^{-1}), 0.5 µl dNTPs (10 mmol l^{-1} each dNTP), and 1.0 µl superscript II reverse transcriptase (Invitrogen). This was incubated for one hour at 42°C followed by three minutes at 65°C and quick-cooled on ice.

cDNA was amplified by combining 1.5 µl of a 1:5 dilution of first-strand DNA, 3.0 µl 10x advantage2 PCR buffer (Clontech, Mountain View, CA, USA), 1.0 µl dNTPs (10 mmol l^{-1} each dNTP), 1.5 µl TRSa primer (2 µmol l^{-1}), 1.5 µl TS-PCR primer (2 µmol l^{-1}), 1 µl advantage II polymerase (Clontech), and 20 µl DEPC treated water. The mixture was cycled 17 times at 94°C for 40 seconds, 65°C for one minute, and 72°C for five minutes.

Cloning of Internal Fragments

Primers were designed to an internal region of each gene as predicted by Ensembl (www.ensembl.org). These primers were used in a PCR reaction to amplify the message from cDNA collections made to include the entire larval alimentary canal. Once amplified, the PCR product was sequenced using the ABI Prism Big Dye Terminator Cycle Sequencing Kit (Applied Biosystems, Foster City, CA, USA) and the reaction products were analyzed on an ABI Prism 310 Genetic Analyzer. This known sequence was used to design gene specific primers for the rapid amplification of cDNA ends (RACE).

Rapid Amplification of cDNA Ends (RACE)

RACE (Zhang and Frohman, 1997; modified by Matz et al., 1999) was used to determine the 3' and 5' ends using cDNA collections which were generated as described above. For all primer names listed in this section and corresponding sequences see Table 2-1. First, specific primers (5_1, 3_1, 5_2, 3_2) were designed for each gene of interest. RACE was performed in two stages; three reactions were set up in the first stage: 5' RACE, 3' RACE, and a control. To each tube 2 µl 10x advantage PCR buffer (Clontech), 0.5 µl dNTP mix (10 mmol l^{-1} of each dNTP), 1.0 µl first strand cDNA (diluted 1:5 in water), 0.5 µl advantage DNA polymerase (Clontech), and 16 µl sterile water were added. To the 5' RACE tube 1.0 µl 5_1 (2 µmol l^{-1}) and 1.0 µl 5_prox (2 µmol l^{-1}) were added. To the 3' RACE tube 1.0 µl 3_1 (2 µmol l^{-1}) and 1.0 µl 3_prox (2 µmol l^{-1}) were added. To the control tube 1.0 µl 5_1 (2 µmol l^{-1}) and 1.0 µl 3_1 (2 µmol l^{-1}) were added. PCR program: 94°C for 40 seconds, X°C (specific to the primer) for three minutes, 72°C for two minutes. This program was run for 22-25 cycles.

The second stage of RACE consisted of a nested PCR and required four tubes: 3' Nested, 3' control, 5' Nested, 5' control. A master mix was made consisting of 8.0 µl 10x advantage buffer (Clontech), 2.0 µl dNTP mix (10 mmol l^{-1} each dNTP), 4.0 µl Udist (2 µmol l^{-1}), 2 µl

advantage DNA polymerase (Clontech), and 60 µl sterile water. This master mix was dispensed into two tubes, 38 µl each. To one tube was added 2 µl of the first stage 3' RACE cDNA diluted 1:50. To the second tube was added 2 µl of the first stage 5' RACE diluted 1:50. Each of these two mixtures was divided into two tubes, 19 µl each. One of the resulting mixtures contained the Udist primer alone and served as a negative control. To the other, 1 µl of the corresponding RACE primer (2 µmol l^{-1}; 3_2 primer to the 3' Nested PCR tube, 5_2 primer to the 5' Nested PCR tube). PCR program: 12-20 cycles of 94°C for 40 seconds, X°C (specific to the primer) for three minutes, and 72°C for two minutes.

Cloning of Full-Length Gene Product

Once the full sequence for each gene was determined, gene specific primers were designed to amplify the full length cDNA product (Table 2-2). The full length gene was ligated into the pCR4-TOPO vector (Invitrogen) and transformed into Top10 chemically-competent bacterial cells (Invitrogen) for sequence confirmation as described above.

Protein Alignments

To generate a protein alignment, sequences were combined in a notebook document in FastA format. The sequences were aligned in ClustalX (Larkin et al., 2007) and visualized using Genedoc (Nicholas et al., 1997). Similarity groups were enabled using the default scoring matrix, Blosum 62 matrix. Regions with high similarity are highlighted in black (100%). Regions of lesser similarity are highlighted in grey (>80%) and light grey (>60%).

Calculation of Percent Identity

To calculate the percent identity between AgAE3 and other AgAEs, a protein alignment was made between AgAE3 and either AgAE1 or AgAE2 as described above. The number of identical residues was then divided by the number of residues in the longest sequence. The resulting fraction was multiplied by 100 to give a final percentage.

Detection of CA Activity

CA activity was detected in the alimentary canal of early fourth-instar *An. gambiae* larvae using Hansson's method (Hansson, 1967) as described by Brown (Brown, 1980) (Figure 3-1). Briefly, early fourth-instar *An. gambiae* larvae were fixed by injection into the haemocoel of a 2.5% gluteraldehyde solution and immersed in the same solution for 30 minutes at room temperature. Twelve μm sections were cut at -20°C using a Leica Cryostat CM 3050S (Leica, Bannockburn, IL, USA) and mounted on gelatin-coated slides. Using a slide basket, slides were immersed in incubation solution (1.75 mmol l^{-1} $CoSO_4$, 11.7 mmol l^{-1} KH_2PO_4, 157.0 mmol l^{-1} $NaHCO_3$, and 53.0 mmol l^{-1} H_2SO_4 in milli-Q water) briefly and then removed to permit adequate aeration of sections. This was repeated for approximately ten minutes, allowing 20-30 seconds to elapse between immersions. The slides were then rinsed in milli-Q water and immersed in blackening reagent (0.5% ammonium sulfide) for five minutes. The slides were again rinsed in milli-Q water and mounted in 60% glycerol in PBS. The addition of the carbonic anhydrase inhibitor, methazolamide (10^{-3} mol l^{-1}), to the incubation solution served as a control.

Quantitative PCR (QPCR)

Generation of First-Strand cDNA

Superscript III Reverse Transcriptase kit (Invitrogen) was used to generate cDNA from RNA using manufacturer's instructions. Briefly, the following were combined in a single tube: <5.0 μg total RNA, 1 μl random hexamers (50 ng μl^{-1}), 1.0 μl dNTP mix (10 mmol l^{-1} each dNTP), and DEPC-treated water to 10.0 μl. Reactions were incubated at 65°C for five minutes and then quick cooled on ice for one minute. To each reaction were added the following: 2.0 μl 10x RT buffer, 4.0 μl $MgCl_2$ (25 mmol l^{-1}), 2.0 μl DTT (0.1 mol l^{-1}), 1.0 μl RNaseOUT (40 U/ μl), and SuperScript III RT (200 U/ μl). The reactions were incubated at 25°C for ten minutes, followed by 50°C for 50 minutes, and terminated at 85°C for five minutes. To eliminate residual

RNA, 1.0 µl of RNase H was added to each reaction and incubated at 37°C for 20 minutes. cDNA was stored at 4°C until use.

QPCR Reaction

Primers were designed to both the gene of interest and an 18s ribosomal RNA endogenous control (specific to the species being examined) using ABI primer express software (Applied Biosystems). The quantitative PCR (QPCR) reaction included 0.5 µl cDNA (1-500 ng), 12.5 µl SYBR green dye (Applied Biosystems), forward and reverse primers (50-300 nmol l^{-1} each), and water to a total of 25.0 µl to wells of a 96 well plate (Applied Biosystems). Each reaction was run in triplicate. QPCR was performed using Applied Biosystems 7000 Sequence Detection system and data were analyzed using the method described in Pfaffl, (2001).

In situ Hybridization

Generation of Digoxigenin Labeled Probes

Digoxigenin (DIG)-labeled RNA probes (both sense and antisense) were designed to the full length gene of interest using the DIG RNA labeling kit (Roche; Nutely, NJ, USA). The DNA template was a pCR4-TOPO vector containing the gene of interest. To 1.0 µg of DNA were added 2.0 µl 10x NTP labeling mixture, 2.0 µl 10x transcription buffer, 1.0 µl protector RNase Inhibitor, and 2.0 µl RNA polymerase T3 or T7. The RNA polymerase was chosen based on desired strand of RNA (sense or antisense). The reaction was mixed gently and incubated for two hours at 37°C. To remove template DNA, 2.0 µl DNase I was added and the reaction was incubated for 15.0 minutes at 37°C. The reaction was stopped by adding 2.0 µl 0.2 mo1 l^{-1} EDTA (pH 8.0). Probes were stored at -20°C until use.

Larval Preparation

Ten early fourth-instar *An. gambiae* larvae were dissected to expose the alimentary canal, five for sense and five for antisense detection. The heads of the cold-immobilized larvae were

pinned down using fine stainless-steel pins to a Sylgard layer at the bottom of a Petri dish containing 4% paraformaldehyde in PBS. The anal segment and the saddle papillae were removed using ulta-fine scissors and forceps and an incision was made longitudinally along the thorax. The carcass, including the fat body, central nervous system, trachea, and muscle, was separated from the alimentary canal. RNA was detected according to the *in situ* hybridization protocol outlined in Meleshkevitch et al (2006).

RNA Detection

Preparations were fixed for three hours in 4% paraformaldehyde in PBS and washed three times with PTW (1x PBS, 0.1 % Tween 20) for five minutes each. Preparations were incubated in a 3:1 PTW/MetOH followed by 1:1 PTW/MetOH, 1:3 PTW/MetOH and finally 100% MetOH for ten minutes each to permeablize the tissue. The tissue was rehydrated in 1:3 PTW/MetOH, 1:1 PTW/MetOH, 3:1 PTW/MetOH and finally PTW alone for ten minutes each. The tissue was then incubated with 0.3% TritonX100 in PBS for ten minutes, washed with PTW alone for five minutes and incubated in Proteinase K (10 μg ml^{-1}) in PTW at room temperature for ten minutes. The tissue was fixed a second time in 4% paraformaldehye in PBS at 4°C for 20 minutes and washed twice with each of the following: glycine (2.0 mg ml^{-1}) in PTW, PTW, 0.1 mol l^{-1} triethanolamine hydrochloride pH 8.0 (TEAHCL), and acetic anhydride in TEAHCL (2.5 μl ml^{-1}) for five minutes each. Finally, the tissue was washed three times with PTW and prehybridized in hybridization buffer [50% formamide, 5.0 mmol l^{-1} EDTA, 5x SSC, 1x Denhardt solution (0.02% ficoll, 0.02 % polyvinylpirrolidon, 0.02 % BSA), 0.1% Tween 20, 0.5 mg ml^{-1} yeast tRNA (Gibco BRL)] 6-8 hours at 50°C. The tissue was hybridized with either sense or antisense probe (1.0 μg ml^{-1}) in fresh hybridization buffer at 50°C for 12-14 hours.

After hybridization, the tissue was incubated for 30 minutes each in: 50% formamide/ 5x SSC/ 1% SDS at 60°C, 50% formamide/ 2x SSC/ 1% SDS at 60°C, and twice with 0.2x SSC at

55°C. The tissue was then washed three times in PBT (1x PBS, 0.1% Triton X100, 2.0 mg ml^{-1} BSA) for five minutes each, and incubated in 10% normal goat serum (NGS) in PBT at 4°C for one hour. To detect the probes, the tissue was incubated in a 1:2000 dilution of alkaline phosphatase-conjugated anti-DIG antibodies in 1% NGS in PBT at 4°C and rocked for 24 hours.

The tissue was washed three times with PBT for 20 minutes each and incubated twice in detection buffer (100 mmol l^{-1} NaCl, 50 mmol l^{-1} $MgCl_2$, 0.1% Tween 20, 1 mmol l^{-1} levamisol, 100 mmol l^{-1} Tris-Cl, pH 9.5). Finally, the tissue was incubated in NBT/BCIP (20 µl ml^{-1}) in detection buffer at 4°C in complete darkness until desired color results. The tissue was then washed with 4% paraformaldehyde in methanol at 4°C for one hour, twice with 100% ethanol, and preserved in a 3:1 glycerol: PBS solution.

Antibody Production

CA9 chicken antibody was generated by Aves Labs, Inc. (Tigard, OR, USA) against the *An. gambiae* BSA-conjugated peptide: KEPIEVSHEQLELFREMRC and was affinity-purified using the immunogen peptide (Smith, K. E. et al., 2007).

Na^+K^+-ATPase monoclonal antibodies "α5" that had been raised against the α–subunit of avian Na^+K^+-ATPase in mice were obtained from the Developmental Studies Hybridoma Bank in the form of hybridoma tissue culture supernatant (Lebovitz et al., 1989).

A polyclonal antiserum raised against the B subunit of the V-type H^+-ATPase of *Culex quinquefasciatus* (Filippova et al., 1998) was obtained from Professor Sarjeet Gill at the University of California, Riverside.

For all experiments, the CA9 and V-ATPase antibodies were used at a dilution of 1:1000, and the Na^+K^+-ATPase antibody was used at a dilution of 1:10.

Peptide Blocking Assay

To determine specificity, antibody was pre-incubated with peptide prior to detection of protein. First, the amount of antibody to be used in milligrams (mg) was calculated based on a 1:1000 dilution. Peptide was reconstituted in milli-Q water to 1.0 mg ml^{-1} and was added in 20% excess by weight. This was calculated by multiplying mg of antibody by 0.4. The reconstituted peptide was combined with diluted antibody and incubated for 45 minutes at 37°C prior to use.

Immunolocalization

Paraffin sectioned preparations: Primary fixation was achieved by injection into the larval haemocoel of a 4% formaldehyde solution diluted from ultrapure 16% formaldehyde (PolySciences, Inc., Warrington, PA, USA) with Tris-buffered saline (TBS), and larvae were immersed in 4% formaldehyde overnight at 4°C. Larvae were transferred to Carnoy's solution (60% ethanol, 30% chloroform, 10% glacial acetic acid) for 90 minutes on ice and washed twice for 30 minutes each with 100% ethanol. Larvae were then cleared with aniline: methylsalicylate (1:1) overnight followed by 100% methylsalicylate overnight and embedded in paraffin. Sections were cut six microns thick using a microtome and mounted on gelatin-coated slides. Sections were deparaffinized through successive five minute incubations in 100% xylene (2x) and xylene:ethanol (1:1), rehydrated through a series of five minute washes of graded ethanols: 100% (2x), 95% (2x), 80%, 70%, 50%, and finally washed three times in TBS. The slides were then blocked in pre-incubation buffer (pre-inc: TBS, 1% bovine serum albumin, 1% normal goat serum, 0.1% TritonX100) for 1-2 hours at room temperature and incubated in primary antibodies in pre-inc for one hour at 37°C. The slides were washed three times in TBS and incubated with the appropriate secondary antibodies (Cy5- or FITC-conjugated donkey-anti-chicken [to detect CA9], TRITC-conjugated goat anti-mouse [to detect Na^+K^+-ATPase], or FITC-conjugated goat-anti-rabbit [to detect V-ATPase], Jackson ImmunoResearch, West Grove, PA, USA) at a dilution

of 1:250 in pre-inc for one hour at 37°C. The slides were again rinsed three times in TBS and mounted in 60% glycerol in TBS with phenylenediamine (Sigma-Aldrich Corp.) to diminish fluorescence quenching.

Whole mount preparations: Larvae were dissected to separate the gut from the rest of the larva. The dissected tissue was fixed in a 1:1 solution of hemolymph substitute solution (Clark et al., 1999; in mmol l^{-1}: 42.5 NaCl, 3.0 KCl, 0.6 $MgSO_4$, 5.0 $CaCl_2$, 5.0 $NaHCO_3$, 5.0 succinic acid, 5.0 malic acid, 5.0 L-proline, 9.1 L-glutamine, 8.7 L-histidine, 3.3 L-arginine, 10.0 dextrose, 25.0 Hepes, pH was adjusted to 7.0 with NaOH) and 4% formaldehyde overnight at 4°C. The tissue was then washed twice with TBS for 30 minutes each at room temperature and incubated in pre-inc for 1-2 hours at room temperature. The tissue was incubated with primary antibodies in pre-inc at 4°C overnight. The following day the tissue was washed approximately ten times in pre-inc for 30 minutes each at room temperature. Secondary antibodies (FITC-conjugated donkey-anti-chicken [to detect CA9], TRITC-conjugated goat anti-mouse [to detect Na^+K^+-ATPase], or FITC-conjugated goat-anti-rabbit [to detect V-ATPase]) were diluted 1:250 in pre-inc and incubated with the appropriate tissue(s) overnight at 4°C. The tissue was rinsed twice with pre-inc and once with TBS at room temperature for 30 minutes each, and then mounted in 60% glycerol in TBS with phenylenediamine (Sigma-Aldrich Corp.) to diminish fluorescence quenching.

In all cases, multiple primary or secondary antibodies were added simultaneously rather than sequentially. All secondary antibodies purchased were specifically "ML" grade (multiple label; Jackson ImmunoResearch). This grade is affinity purified and tested for minimal cross-species immunoreactivity. For each image, an n>10 larval sections were observed.

All images were captured using a Leica LSCM SP2 laser scanning confocal microscope (Leica Microsystems, Bannockburn, IL, USA). For each signal in each preparation, laser intensity and detector sensitivity were set to capture the full dynamic range of the fluorescence.

Phylogenetic Analysis

Predicted CA and AE sequences were obtained from the Ensembl database (www.ensembl.org) February 2007 release. Alignments were created using ClustalX and trimmed and visualized using Genedoc. The phylogeny was prepared using MrBayes with the JTT amino acid substitution model and 1.5 million iterations. Trees were visualized using Treeview. All nodes were supported with >.95 posterior probability.

RT-PCR

cDNA was used as a template for PCR reactions with primers specific to the gene of interest (Table 2-3). The PCR mix consisted of 1.0 µl forward primer (10.0 µmol l^{-1}, 1.0 µl reverse primer (10.0 µmol l^{-1}), 1.0 µl cDNA template, and 22.0 µl PCR SuperMix (Invitrogen). This mixture was heated to 95ºC for 2.0 minutes, followed by X cycles of 95ºC for 30 seconds, YºC for 30 seconds and 72ºC for two minutes, and finally one cycle at 72ºC for five minutes for a final extension. The cycles run (X) for each reaction and the annealing temperatures (Y) can be found in Table 2-3. The product was run on a 1% agarose gel, the DNA was extracted (Gel-extraction kit, Qiagen, Valencia, CA, USA), and the product was ligated into the pCR4-TOPO vector (Invitrogen). The product was sequenced using the ABI Prism Big Dye Terminator Cycle Sequencing Kit (Applied Biosystems). The reaction products were analyzed on an ABI Prism 310 Genetic Analyzer (Applied Biosystems).

Transcription of RNA

Transcription was performed in three steps: creation of double stranded (ds)DNA flanked by the T7 promoter sequence on either the 5' or 3' end, transcription of both sense and antisense

strands into single stranded (ss)RNA, and finally, annealing of the two single strands into dsRNA.

Creation of dsDNA Flanked by T7 Promoter

First, primers were designed to amplify either AgCA9 or GFP DNA and to add a T7 promoter sequence at either the 5' or 3' end (Table 2-4). The template used was either AgCA9 cDNA in the pCR4-TOPO vector, or eGFP cDNA in the pGEMTEZ vector (Promega Corporation, Madison, WI). I received the eGFP from Lyric Bartholomay (University of Wisconsin). The reactions were cycled at 95°C for five minutes, followed by X cycles of 95°C for 30 seconds, Y°C for 30 seconds, and 72°C for two minutes, and finally one more cycle at 72°C for five minutes. The cycles run (X) for each reaction and the annealing temperatures (Y) are listed in Table 2-4. Generation of a single DNA product was verified by running the reaction on a 1% agarose gel. The product was purified using the PCR purification kit (Qiagen).

Transcription of Sense and Antisense Strands into ssRNA

Sense and antisense RNA were transcribed using the MEGAscript T7 transcription kit (Applied Biosystems/Ambion). Briefly, the following reagents were combined: 2.0 µl ATP solution, 2.0 µl GTP solution, 2.0 µl CTP solution, 2.0 µl UTP solution, 2.0 µl 10x reaction buffer, 2.0 µl T7 enzyme mix, 1.0 µg DNA, and water to 20.0 µl. The reaction was incubated for four hours at 37°C. To remove template DNA, 1.0 µl TURBO DNase (Applied Biosystems/Ambion) was added and the reaction was incubated 15 minutes more at 37°C. ssRNA was purified using MEGAClear™ Kit (Applied Biosystems/Ambion), eluted in 100 µl, and precipitated with 0.5 mol l^{-1} Ammonium Acetate. RNA was resuspended in DEPC-treated water.

To verify the correct RNA size, 1.0 µl of ssRNA was denatured by adding an equal amount of glyoxyl loading dye (Applied Biosystems/Ambion) and heated to 50°C for 30 minutes. The

RNA was then run next to a 0.5-10 kb RNA ladder (Applied Biosystems/Ambion) on a 1% agarose gel made with sodium phosphate (NaP) running buffer.

Annealing of ssRNA

Each ssRNA strand was then adjusted to equal concentrations for annealing. Equal amounts of sense and antisense ssRNA were combined in a tube and incubated in a water bath heated to 95°C for five minutes. The reaction tubes remained in the water bath while it cooled to room temperature overnight. 1.0 µl of ssRNA was denatured (as described above) and run next to 1.0 µl of native dsRNA on 1% agarose gel in NaP buffer to verify annealing. The dsRNA ran slightly higher than the ssRNA.

RNA Interference

Ag55 cells were grown (see above section on Ag55 cell growth conditions for more information) to 70% confluency in six well plates (Fisher Scientific) for experimental (AgCA9 dsRNA treated) and two control groups (GFP dsRNA treated and untreated). The untreated group did not receive dsRNA, but was subjected to the same conditions as the other two groups. To treat the cells with dsRNA, media was replaced with 800 µl L-15 media lacking FBS and 36.0 µg dsRNA was added (AgCA9 dsRNA or GFP dsRNA). The plate was rocked at room temperature for 30 minutes and then 800 µl L-15 media plus 20% FBS was added. Cells were incubated for 24, 48, 72 or 96 hours after which they were washed twice with two mls L-15 media lacking FBS and resuspended in 0.4 mL Trizol reagent (Molecular Research Center) to extract RNA and protein (see above).

Northern Blot

To generate a radioactive northern probe, a pCR4-TOPO vector containing full length AgCA9 sequence was linearized by restriction enzyme digest. In a PCR tube the following was combined: 1.0 µg linearized plasmid, 2.0 µl 10x reaction buffer, 1.0 µl dATP (10 mmol l^{-1}), 1.0

µl dCTP (2 mmol l^{-1}), 1.0 µl dGTP (10 mmol l^{-1}), 5.0 µl ^{32}P-labeled dUTP (800 Ci (mmol l^{-1})$^{-1}$, 20.0 mCi ml^{-1}; GE Healthcare Bio-Sciences Corp., Piscataway, NJ, USA), 2.0 µl T7 RNA polymerase and water to 20.0 µl. This reaction was incubated at 37°C for one hour. The NorthernMax kit protocol (Applied Biosystems/Ambion) was used to run and analyze the Northern blot (Figure 4-2B). The RNA loaded for all treatment samples within a time point was equivalent, but differed between time points: 48 hours-10.0 µg RNA, 72 hours-6.3 µg RNA and 96 hours-8.0 µg RNA. RNA extracted from cells at the 24 hour time point was too little (less than 1.0 µg) to be visualized on the Northern blot.

Western Blot

Protein samples were prepared and run on a NuPage 4-12% Bis-Tris gel, 1.0 mm x 12 well (Invitrogen). The protein was transferred to nitrocellulose in transfer buffer (5% 20x NuPAGE transfer buffer, 0.1% NuPAGE antioxidant and 10% MetOH in milliQ water) at 24 volts for 4 hours. The nitrocellulose was stained with fast green (40 mls acetic acid, 100mls MetOH, 0.24 grams fast green, 100 mls water) for approximately 15 minutes, destained (5:1:5 MetOH, HOAc, H_2O) for 15 minutes and rinsed with deionized water. The individual lanes were separated and blocked with blotto (400 mls TBS, 10 grams dry milk, 800 µl Tween20) for 1 hour at room temperature. The primary antibody against AgCA9 was added at a 1:1000 dilution in blotto and rocked at 37°C for 1 hour. The blot was washed three times in TBS at room temperature for five minutes each. The secondary antibody (Alkaline phosphatase [AP]-conjugated donkey anti-chicken; Jackson ImmunoResearch) was added at a 1:250 dilution in blotto and incubated at 37°C for one hour. The blot was again washed three times with TBS at room temperature for five minutes each. The labeled bands were detected using an AP conjugate substrate kit (Bio-Rad; Hercules, CA, USA) according to manufacturer's instructions.

Quantification of Protein

The presence of a second protein which cross-reacted with the antibody was used as a loading control for each sample; this protein was distinguishable from AgCA9 by its slightly higher molecular weight. All bands were quantified using Image Quant 5.0 (Molecular Dynamics, Sunnyvale CA, USA) and analyzed using Microsoft Excel. Values for each AgCA9 band were normalized by dividing by the value of the corresponding loading control band. The percent down-regulation of AgCA9 protein was determined at each time point by the following equation:

$$1-\frac{A}{B}*100$$

where A is the normalized AgCA9 band in the AgCA9 dsRNA treated cells lane (lane 1 at each time point) and B is the averaged normalized values from both GFP dsRNA cells lane (lane 2 at each time point) and vehicle treated cells lane (lane 3 at each time point).

Acute Freshwater/Saline Challenges

To determine protein localization in larval rectal cells after acute exposures to fresh or dilute saline water (Figure 5-3), *An. albimanus* larvae were hatched in either fresh water or 25% ASW and reared individually in one ml of fresh water or 25% ASW, respectively, in 24 well plates (Fisher Scientific). Larvae were carefully monitored every 24 hours for molting. Newly molted larvae (within 24 hours) at the second-, third-, or fourth-instar stage were transferred from either fresh water to 25% ASW or from 25% ASW to fresh water. After 24, 48, and 72 hours larvae were removed and prepared for immunohistochemistry. Fourth-instar larvae could not be observed 72 hours post media transfer due to pupation. A minimal concentration of ASW was used which was shown to elicit Na^+/K^+-ATPase shift (25% ASW instead of 50% ASW). N>5 larva for each experimental group. Each experiment was performed in triplicate.

Quantification of Na^+/K^+-ATPase Signal Intensity

Because sources of variability exist in the imaging system as well as in preparation of the samples, I was unable to quantitatively compare rectal Na^+/K^+-ATPase signal intensity between different samples. I was, however, able to compare signal between rectal cell types (dorsal anterior rectal [DAR] and non-DAR, or anterior rectum [AR] and posterior rectum [PR]) in the same sample (Figures 5-1D, H, L and 5-3H). I therefore reported the change in protein distribution as a change in the ratio of peak pixel intensity between the two rectal cell types in each sample. Because rectal cell type distribution of CA and V-ATPase did not change between larvae reared in fresh water and those reared in saline water, I only reported the pixel intensity ratios of Na^+/K^+-ATPase.

To quantitate the immunostaining intensity between DAR and non-DAR cells (or AR and PR), the ROI (region of interest) function of the Leica Confocal "Quantify" software (Leica Microsystems) was used to separately define all cells of either type in a given tissue section. Once I determined that no pixel intensities were beyond the dynamic range of the 8-bit grey scale, the peak pixel intensity of each ROI was calculated and used as the basis of comparison between DAR and non-DAR cells (or AR and PR).

Three representative recta were quantified from each group (including the recta presented in Figure 5-1). For each rectum, the DAR/non-DAR (or AR/PR) peak Na^+/K^+-ATPase pixel intensity ratio was determined by dividing the peak pixel intensity of the DAR cells (or AR) by the peak pixel intensity of the non-DAR cells (or PR). The DAR/non-DAR (AR/PR) ratios of the three recta from each group were then averaged. Finally, the averaged DAR/non-DAR (AR/PR) ratios of the fresh water-reared larvae were plotted next to those of the saline water-reared larvae in each species using Graphpad Prism 3.0 graphing software (La Jolla, CA, USA). Standard deviation between the three recta from each group was indicated. For each graph, a

value of "1" indicates that the peak pixel intensity was equal in the two cell types. A value greater than "1" indicates greater peak pixel intensity in the DAR cells (or AR) whereas a value less than "1" indicates greater peak pixel intensity in the non-DAR cells (or PR). Statistical significance was determined in Microsoft Excel using a paired t-test and reported as two-tailed P-values. Asterisks indicate a significant difference between the DAR/non-DAR (AR/PR) ratios of larvae reared in fresh water and the ratios of those reared in saline water. * P-Value > 0.05; ** P-Value > 0.005.

Physiology

Preparation of samples: Late third-instar *An. albimanus* larvae were anesthetized on ice for 30 minutes prior to dissection in artificial hemolymph solution (modified from Clark et al., 1999; in mmol l^{-1}: 42.5 NaCl, 3.0 KCl, 0.6 $MgSO_4$, 5.0 $CaCl_2$, 5.0 $NaHCO_3$, 5.0 succinic acid, 5.0 malic acid, 5.0 L-proline, 9.1 L-glutamine, 8.7 L-histidine, 3.3 L-arginine, 10.0 dextrose, 5.0 HEPES in milli-Q water, pH 7.1; osmolarity adjusted to 300 mosmol l^{-1} with D-mannitol). Larvae were pinned to a sylgard coated petri dish through the head and the exoskeleton surrounding the ileum, Malpighian tubules and rectum were removed. Exoskeleton surrounding the anterior extreme of the larva was left intact. Malpighian tubules were either removed or pinned away from the rectum. The rectum was immobilized by adhering one side to a poly-lysine-coated coverslip which had been immersed in a 2.0 mg ml^{-1} poly-lysine solution in milli-Q water for 30 minutes.

Measurement of H^+ flux at basal membrane of DAR and non-DAR cells: H^+ gradients were measured at the basal membrane of *An. albimanus* recta using the self-referencing, ion-selective microelectrodes technique (SIET; Smith et al., 1999; reviewed in Messerli et al., 2006; Smith, P. J. et al., 2007). Microelectrodes were pulled to a tip diameter of approximately 2-3 μm from 1.5 mm diameter borosilicate thin-wall glass capillary tubes (TW150- 6, WPI, Sarasota, FL,

USA) using a Sutter P-97 micropipette puller (Sutter instruments Inc., Novato, CA, USA) and salinized prior to use as described in Smith et al (1999). Microelectrodes were backfilled with 100 mmol l^{-1} KCl, 10.0 mmol l^{-1} HEPES, pH 7.4 and tip filled with a 50-200 μm column of H^+ ionophore B (Fluka, Buchs SG, Switzerland).

H^+ flux was measured at a distance approximately 5-10 μm from the membrane beginning at the rectum-ileum junction and stopping when the end of the rectum was reached. Measurements were taken in 50 μm increments at distinct positions along the anterior-posterior axis of the rectum. Reported values for each position reflect an average of recordings taken over five minutes at 1000 samples per second with the first 30% sampled before and after probe excursion being discarded (Figure 6-1B). H^+ flux was considered outwardly directed, or an efflux, if the probe detected higher H^+ activity closest to the membrane. By contrast, an inwardly directed H^+ flux, or influx, was considered if the probe detected higher H^+ activity furthest from the membrane. Seven biological replicates were performed.

Because the DAR cells are not visibly discernable from non-DAR cells using a dissecting microscope, preparations were post-stained with rhodamine 123 (Molecular Probes®, Invitrogen, Carlsbad, California, USA) following H^+ flux measurements and imaged using an Axio Observer Z1 microscope (Carl Zeiss Inc., Thornwood, NY, USA) and an AxioCam MRc camera (Carl Zeiss Inc.). The fluorescent staining allowed for the identification of the DAR/non-DAR boundary (Figure 6-1A).

Data was analyzed in Microsoft Excel and graphs were generated using Graphpad Prism 3.0 graphing software. To determine the average DAR and non-DAR H^+ fluxes (Figure 6-1C), all flux measurements taken from the DAR cells or non-DAR cells of a single prep were first averaged. Averaged values for all like measurements were then averaged (all DAR cell

measurements or all non-DAR cell measurements) and used as raw data for statistical analysis. Statistical significance was determined for all data in Microsoft Excel using a paired t-test and reported as two-tailed P-values.

Pharmacology: To determine the effects of pharmacological inhibitors on H^+ flux, a single point of stable H^+ efflux in the DAR cells, or influx in the non-DAR cells, was chosen for each preparation. The flux was considered stable if it did not significantly vary over a ten minute period. Measurements were recorded as described above for a period of ten minutes prior to, and ten minutes following addition of a pharmacological inhibitor.

Concanamycin A (10^{-3} mol l^{-1}; A.G. Scientific Inc., San Diego, CA, USA) and DIDS (10^{-3} mol l^{-1}; Sigma-Aldrich Corp.) were prepared in DMSO and added to the preparation at a final concentration of 10^{-6} mol l^{-1}. Methazolamide (0.1 mol l^{-1} Sigma-Aldrich Corp.) was prepared in DMSO, diluted with artificial hemolymph to 10^{-3} mol l^{-1}, and added to the preparation at a final concentration of 10^{-4} mol l^{-1}. All reported results were an average of $n \geq 5$ preparations. Results were reported as a ratio of flux after treatment, to flux before treatment with a pharmacological inhibitor (Figure 6-2).

Data was analyzed in Microsoft Excel and graphs were generated using Graphpad Prism 3.0 graphing software. For each graph, a value of "1", for DAR cell flux, or "-1", for non-DAR cell flux, indicates no change in H^+ flux following addition of inhibitor. A value greater than "1" for DAR cell flux indicates an increase in H^+ efflux, whereas a value less than "-1" for non-DAR cell flux indicates an increase in H^+ influx. A value less than "1" for DAR cell flux indicates a decrease in H^+ efflux, whereas a value greater than "-1" for non-DAR cell flux indicates a decrease in H^+ influx. Statistical significance was determined for all data in Microsoft Excel using a paired t-test and reported as two-tailed P-values.

Flux (J) Calculations: Ion fluxes (J) were calculated using the following equation:

$$J = D * \frac{C_{av} * 10^{\frac{dV}{slope}} - C_{av}}{\Delta x}$$

Where 'D' is the H^+ diffusion coefficient ($9.31*10^{-5}$ cm^2 s^{-1}), 'C_{av}' is the background hemolymph [H^+] concentration (mol cm^{-2}), 'dV' is the voltage difference between the near and far positions (mV), 'Δx' is the probe excursion distance ($2*10^{-3}$ cm_2), and 'slope' is the experimentally determined slope for each probe.

To correct for the buffering capacity of water, bicarbonate, and histidine found in the artificial hemolymph, the following equation was used:

$$J_{Htotal} = J_{Hmeasured} * (1 + x_i + ... + x_n)$$

The correction factor, 'x_i', is the ratio of H^+ bound buffer flux to free H^+ flux and is calculated using the following equation for each buffer (B) present:

$$x_i = \frac{D_B}{D_{H+}} * [B] * \frac{Ka}{(Ka + [H^+])^2}$$

Where '[B]' is the buffer concentration, '[H^+]' is the H^+ concentration, and 'Ka' is the acid constant of the buffer.

Table 2-1. Sequences of primers used in the generation of cDNA collections and RACE reactions.

Primer	Sequence
TRSa	CGCAGTCGGTAC (T)13
TS-PCR	AAGCAGTGGTATCAACGCAGAGT
TS-oligo	AAGCAGTGGTATCAACGCAGAGTACGCrGrGrG
AgCA-RP2 3_1	GGTACCAGTTCGAGGAGATCT
AgCA-RP2 3_2	GCACGGTCTGGATTATCCTCAATA
AgCA-RP2 5_1	AGAAGATCCTTTGTACAGGACTTT
AgCA-RP2 5_2	GTAGGGATCGAACAGTAGCTTCT
AgCA6 3_1	TTTCACTGGGGCGACAAAAA
AgCA6 3_2	GGATCGATCTGACGCGCTTCT
AgCA6 5_1	TCGCCGACGGATTTGTACTTT
AgCA6 5_2	GGGCCCGGAAGGAGATTGTT
AgCA9 3_1	AGCATACGGTGGATGGTGAAT
AgCA9 3_2	CGGCAAGGTCATTAACAACTTT
AgCA9 5_1	GGAAGCAAACGAGCGATAATAT
AgCA9 5_2	CTTCTGGGGTCCGTTCATTT
AgCAb 3_1	GTCGTGAACAACATCAAGCATAT
AgCAb 3_2	TAAGCCGCTCATCTTCTCGTCCGAAA
AgAE3 3_1	GTGCGCTTTCTGTTTCTTCT
AgAE3 3_2	ACTACTTCGATTGGATTGCTAGAA
AgAE3 5_1	CCGTGTTGAGTCCATCCATAA
AgAE3 5_2	GGTGTAGGATTCGTCGTTGAT
5_prox	CGACGTGGACTATCCATGAACGCAAAGCAGTGGTATCAACGCAGAGT
3_prox	CGACGTGGACTATCCATGAACGCACGCAGTCGGTAC
Udist	TCGAGCGGCCGCCCGGGCAGGTCGACGTGGACTATCCATGAACGCA

Table 2-2. Sequences of forward and reverse primers used to amplify CA and AE full-length gene products.

CA	Forward primer	Reverse primer
AgCA-RP2	CGAGCCATGTCAGTCAT	CTATGGAAGCGAATGGAAC
AgCA6	ATGCAGTTGTCGATTGGATC	CTAGTACACCCAGTCCCATTTG
AgCA9	TTAGTAGCTATCGACTTCACGCAG	ATGTCTGTCACTTGGGGATACAC
AgCAb	TCACGAATAGTATCGCCGTAC	ATGGAGCGTATATTGCGAG
AeCA4	ATGTCGACCTCTTGGGGATAC	TCAGTGTCCTCCGAATTCGC
AgAE3	ATGGCTCATTTCCTCGATATTC	TTAGGCAGGAATGGGAGCTT

Table 2-3. Specifics of the primers used to amplify full-length and partial AgAGO2 and CA sequences including primer sequences, annealing temperatures, PCR cycles run, and expected length of products for each primer set.

CA	ENSEMBL ID	Forward primer	Reverse primer	Length (bp)	Annealing temp (°C)	# cycles
AgCA1	AGAP002360	ATGAGTGCGCTGTGTTTG	ATCCAGTTGACCGTCTCC	800	57	35
AgCA-RP2	AGAP000715	CGAGCCATGTCAGTCAT	CTATGGAAGCGAATGGAAC	1032	55	35
AgCA3	AGAP000401	CACTACGTGGGCCACTGGGAC	CTAAAGTTTGGCGCGCCG	750	55	35
AgCA4	AGAP007550	AATAGCTTCAACCACCAAACC	GTGTCAGTGGGTGTCCTTC	913	57	35
AgCA-RP5	AGAP000688	CCGACAGTCACCCGTCA	GGACCACCCTGCATTAAC	657	63	40
AgCA6	AGAP003289	ATGCAGTTGTCGATTGGATC	CTAGTACACCCAGTCCCATTTG	957	60	35
AgCA7	AGAP002359	AGTTCACTTACCGCATCTCG	TGGAACTGATCGAACAGGTAC	904	57	40
AgCA8	AGAP010844	TCGTATGGTCACTGGCAC	GACACTGCACTTCGTCCTC	930	58	35
AgCA9	AGAP010052	ATGTCTGTCACTTGGGGATACAC	TTAGTAGCTATCGACTTCACGCAG	831	60	35
AgCA10	AGAP004895	ATGAAAAGTTTCACTTTATTGCTCTG	TCAGTGGTAACTCAATCTGGATG	960	60	35
AgCA11	AGAP005066	ATGGCATCAAAAACAACAAAGAAC	TTACAGCTTCGAAAGCACAACGG	774	63	40
AgCAb	AGAP002992	ATGGAGCGTATATTGCGAG	TCACGAATAGTATCGCCGTAC	768	60	35
AgAGO2	AGAP011537	CGCCCATACCTAAACGTG	GGCACTTGTTGTACTGGATC	646	57	30

Table 2-4. Specifics of the primers used to generate AgCA9 or GFP dsDNA flanked by the T7 primer sequence on either the 5' or 3' extreme.

Gene	T7 position	Forward primer	Reverse primer	Annealing temp (°C)	Cycles run	Length (bp)
AgCA9	5'	TAATACGACTCACTATAGG GATGTCTGTCACTTGGGGA TACAC	TTAGTAGCTATCGAC TTCACGCAG	60	30	871
AgCA9	3'	ATGTCTGTCACTTGGGGAT ACAC	TAATACGACTCACTA TAGGGTTAGTAGCTA TCGACTTCACGCAG	60	30	871
GFP	5'	TAATACGACTCACTATAGG GGAGGTGAAGTTCGAGGGC	TCCATGCCGAGAGTG ATC	55	30	411
GFP	3'	GAGGTGAAGTTCGAGGGC	TAATACGACTCACTA TAGGGTCCATGCCGA GAGTGATC	55	30	411

Table 2-5. Sequences of forward and reverse primers used to detect CA and AE mRNA in q-PCR reactions.

Gene	Forward primer	Reverse primer
18s	GCGACCTCGTCGGTCAAG	AGAGTTCCCGGGCACCAT
AgCA6	TCC ATTACACAACACCCCATGT	CGCGATGTTCCCTTCTCAAC
AgCA9	CAACGGTAGGAGTATGGTCGATCT	ACGTACCGCGCTTTGCA
AgCAb	AGCCTGGCCAAGTTTCAAA	GACGAGAAGATGAGCGGCTTA
AgAE2	CTGCGCGCCTGATTGTC	ACACGCGCTCGATTTCG
AgAE3	GTGTGTACGTGCGAATGTTCACT	GCGTGATTAGGGCGGAAA

CHAPTER 3
CLONING AND CHARACTERIZATION OF CARBONIC ANHYDRASE FROM *ANOPHELES GAMBIAE* GILES SENSU STRICTO LARVAE

Introduction

Members of the CA family have been implicated in the generation and maintenance of the larval mosquito AMG alkalization (Corena et al., 2002; Seron et al., 2004; T. J. Seron, personal communication). A current view of larval AMG alkalization proposes that CA in the epithelial cells of the alimentary canal catalyzes the formation of HCO_3^-. HCO_3^- is then translocated into the lumen by a HCO_3^- transporter and deprotonated to CO_3^{2-} (pKa_2 10.32) (Dow, 1984). Together with a strong cation such as K^+ or Na^+, CO_3^{2-} could serve as the buffer in the highly alkaline AMG lumen. Although there are still unanswered questions regarding this model, it is clear that CA is a major player in the regulation of pH gradients within the larval mosquito alimentary canal (Corena et al., 2002; Seron et al., 2004; Strange and Phillips, 1984; T. J. Seron, personal communication).

Multiple CAs have been cloned from, and immunolocalized to, the *An. gambiae* (Seron et al., 2004; Smith, K. E. et al., 2007; T. J. Seron, personal communication; K. E. Smith, unpublished data) and *Ae. aegypti* (Corena et al., 2002; Seron et al., 2004; K. E. Smith, unpublished data) alimentary canals and it has been shown that inhibition of CA in mosquito larvae blocks AMG alkalization (Boudko et al., 2001a; Corena et al., 2002). CA catalyzes the reversible reaction:

$$H_2O + CO_2 \xleftrightarrow{CA} H^+ + HCO_3^-$$

and can generate HCO_3^- within alimentary canal epithelial cells. Living larvae are thought to actively excrete HCO_3^-, resulting in a net alkalization of their surrounding media (Stobbart,

1971). Moreover, addition of the global CA inhibitor, methazolamide, inhibits this alkalization (Corena et al., 2002). These data implicate CA as a key player in AMG alkalization.

There are at least five genetically unrelated families of CA isoforms, α, β, γ, δ, and ε (Alber and Ferry, 1996; Cronk et al., 2001; So et al., 2004; Lane et al., 2005). Presently, members of the γ, δ, and ε families are not predicted to be present in any mosquito genome, and therefore they will not be discussed in this manuscript. Both α- and β-CAs are found in invertebrates, while only the α-CAs are present in vertebrates. α-CAs are zinc metalloenzymes approximately 29 kDa in molecular weight. The active site of these CAs includes three histidines which are essential for coordinating the zinc ion (Liljas et al., 1972). α-CA activity is specifically inhibited by certain sulfonamide compounds (Mann and Keilin, 1940) including acetazolamide and methazolamide. The structures of several members of the β-CA have been determined (Cronk et al., 2000; Kimber and Pai, 2000; Mitsuhashi et al., 2000). Although this class can hydrate CO_2 with comparable efficiency to α-CAs, the β-CA active site differs in conserved amino acid residues from that of α-CAs, and they are much less sensitive to the classic sulfonamide CA inhibitors. β-CAs are predominant in the leaf tissues of vascular plants, as well as in bacteria and algae (Chegwidden and Carter, 2000); however, at least one β-CA gene is predicted to be present in both the *An. gambiae* and *Ae. aegypti* genomes (AGAP002992 and AAEL000816, respectively), as well as in the *Drosophila melanogaster* genome (FBgn0037646; www. ensembl.org).

In *Homo sapiens,* there are at least 14 α-CAs which can be placed into five distinct groups based on their subcellular localization: (1) cytoplasmic CAs; (2) membrane-bound CAs, which are attached to the membrane via a glycosylphosphatidylinositol (GPI) anchor; (3) mitochondrial CAs; (4) secreted CAs; and (5) transmembrane CAs, which span the membrane once and have an

extracellular N-terminal region and an intracellular C-terminal region (Chegwidden and Carter, 2000; Tashian et al., 2000). Additionally, three of the 14 *H. sapiens* CAs are CA-related proteins (CA-RPs), which have lost at least one essential histidine and are no longer active (Tashian et al., 2000).

There are eleven α–CAs, and one β–CA predicted to be present in the *An. gambiae* genome (www.ensembl.org), including cytoplasmic, membrane-bound, secreted, and transmembrane forms. Here I report the cloning and characterization of a cytosolic-like α-CA (GenBank accession # DQ518576), henceforth referred to as AgCA9, from the alimentary canal of *An. gambiae* mosquito larvae. I also report the cloning of a CA-RP (AgCA-RP2; GenBank accession # FJ612599), a secreted-like α–CA (AgCA6; GenBank accession # DQ518577) and a β–CA (AgCAb; GenBank accession # EF065522) from the *An. gambiae* alimentary canal, as well as the mRNA characterization of AgCA6 and AgCAb. I report the phylogenetic analysis of members of the α–CA family from the *H. sapiens*, *D. melanogaster*, *Ae. aegypti*, and *An. gambiae* genomes and show that AgCA9 clusters with *H. sapiens* cytoplasmic CAs. I also suggest a uniform naming system for newly cloned *An. gambiae* CAs which does not currently exist.

Results

Uniform CA Naming System

Table 3-1 lists the ensembl (www.ensembl.org) protein (ENSANGP) identifiers based on the July 2008 release, as well as the new suggested name convention of the twelve *An. gambiae* CAs (Smith, K. E. et al., 2007). Each name begins with a species identifier, 'Ag', followed by a protein abbreviation, CA, or CA-RP in the case of the CA-related proteins (CA-RPs). ENSANGP numbers were listed in ascending numerical order and α-CAs were named sequentially beginning with AgCA1. The β–CA was named AgCAb. Also recorded are the

accession numbers of those CAs which members of the Linser laboratory have fully cloned and sequence confirmed.

Detection of CA Activity in the Alimentary Canal of *An. gambiae*

Hansson's histochemical stain was used to detect CA activity in freshly cut frozen sections of early fourth-instar *An. gambiae* larvae (Figure 3-1). CA activity was detected in the ventral nerve cord (Figure 3-1B) and in the cells of the GC and AMG (Figure 3-1C), the MTs (Figure 3-1D, E), and the dorsal anterior rectal (DAR) region of the rectum (Figure 3-1D, E). CA activity was inhibited by the addition of methazolamide to the incubation solution in all regions except the MTs.

Cloning of Full-Length AgCAs from the Alimentary Canal of *An. gambiae*

Internal fragments of AgCA-RP2, AgCA6, AgCA9 and AgCAb were cloned from the *An. gambiae* larval alimentary canal using primers designed according to the partial cDNA sequence predicted by ensembl. Using gene-specific sequences from these fragments (Table 2-1), rapid amplification of cDNA ends (RACE) was used to amplify and sequence the 3' and 5' ends. The cDNA sequences spanned both the start and stop codons of each gene and were determined to be full length by the presence of a stop codon in the 5' UTR and the presence of a 3' stop codon followed by a poly-A tail in the 3' UTR. An alignment of the full length protein sequences of the α-CAs AgCA-RP2, AgCA6, and AgCA9, along with *H. sapiens* CAII (HCAII) and *D. melanogaster* CAI (DrosCAI) demonstrated their relative homology (Figure 3-2). The three histidines essential for α–CA catalytic activity, His-94, His-96, and His-119 (numbering is relative to HCAII), are indicated with asterisks. An alignment of the full length protein sequence of the β–CA, AgCAb, along with β–CA sequences from *Caenorhabditis elegans* (GenBank accession# NP_741809.1) and *Escherichia coli* (GenBank accession# AAC73237) indicated the relative homology of AgCAb to other β–CA sequences (Figure 3-3). The four amino acid

residues which are conserved in all β–CA sequences and thought to coordinate the active-site zinc, Cys-42, Asp-44, His-98, and Cys-101 (numbering is relative to *E. coli*; Cronk et al., 2001), are indicated with asterisks.

AgCA-RP2

The full length AgCA-RP2 transcript was determined to be 1,026 basepairs, corresponding to a protein product of 341 amino acids, with a molecular mass of 39.22 kDa as determined by The Sequence Manipulation Suite (Stothard, 2000). The sequence was submitted to the NCBI database and allocated the accession number FJ612599. The 5' extreme of the transcript encoded two in-frame methionine residues which were separated by only two amino acid residues. I currently do not know which methionine acts as the start codon in AgCA-RP2 translation. AgCA-RP2 is a predicted CA-RP and lacks two of the essential histidines for CA activity (Figure 3-2). The gene for AgCA-RP2 is located on chromosome X (www.vectorbase.org).

AgCA6

The full length AgCA6 transcript was determined to be 957 basepairs, corresponding to a protein product of 318 amino acids, with a molecular mass of 36.02 kDa. The sequence was submitted to the NCBI database and allocated the accession number DQ518577. AgCA6 belongs to the α–CA family and is located on chromosome 2R (www.vectorbase.org). AgCA6 is predicted to be a secreted protein by the presence of a 32 amino acid signal peptide at the 5' extreme of the protein (Figure 3-2).

AgCA9

The full length AgCA9 transcript was determined to be 831 basepairs, corresponding to a protein product of 276 amino acids, with a molecular mass of 31.5 kDa. The sequence was submitted to the NCBI database and allocated the accession number DQ518576. AgCA9

belongs to the α-CA family and is located on chromosome 3R (www.vectorbase.org). The protein is predicted to be cytoplasmically distributed based on the lack of signal peptide or transmembrane sequences.

AgCAb

The full length AgCAb transcript was determined to be 768 basepairs, corresponding to a protein product of 255 amino acids, with a molecular mass of 29.92 kDa. The gene is located on chromosome 2R (www.vectorbase.org). The AgCAb sequence was submitted to the NCBI database and allocated the accession number EF065522. AgCAb belongs to the β–CA family and shows poor homology with α–CAs (K. E. Smith, unpublished data), but shows high homology with other β–CA proteins (Figure 3-3). Specifically, AgCAb contains the four amino acid residues which are thought to be required for β–CA catalytic activity (Figure 3-3 asterisks).

Detection of RNA Expression in Alimentary Canal Regions

Quantitative PCR (qPCR) and *in situ* hybridization were used to detect CA mRNA within the mosquito larval alimentary canal. AgCA6, AgCA9, and AgCAb mRNA expression was evaluated using qPCR from cDNA derived from either the whole larval alimentary canal, GC, AMG, PMG, MT or rectum. The results were normalized to the *An. gambiae* 18s ribosomal RNA gene and reported relative to whole larval alimentary canal (Figure 3-4). qPCR detected mRNA expression of all three genes in every region tested; however, each CA was expressed at a different level in each region. A specific CA was considered to be expressed significantly in a particular region if it was expressed at a statistically significant level (P-Value > 0.01) above that of whole larval alimentary canal samples. AgCA6 and AgCA9 were expressed significantly in the rectum, and AgCAb was expressed significantly in the AMG and rectum.

In situ hybridization was performed using full length DIG-labeled RNA probes to detect AgCA9 RNA in early fourth-instar whole-mounted *An. gambiae* larval alimentary canals and

carcasses (Figure 3-5). The most intense AgCA9 specific staining of the alimentary canal was seen throughout the cytoplasm of the cells of the GC, transitional region between the AMG and PMG (TR), and rectum, with weaker staining seen in the cells of the PMG. Currently, there is no method of morphologically discriminating the TR in the dissection of alimentary canal regions without electron microscopy or immunohistochemistry. Therefore, RNA from this region cannot be distinguished using qPCR. The most abundant staining of the carcass was seen in the fat body and muscle. No staining was seen in the alimentary canal or carcass using the sense probe.

Verification of AgCA9 Antibody Specificity

Two antibodies were generated by Aves Labs, Inc (Tigard, OR, USA) for use in Western blotting and immunohistochemistry. The first antibody (from hen 5340), was generated against the BSA-conjugated peptide: CZELGNRQLREVDSY. The second antibody (from hen 5563) was generated against the BSA-conjugated peptide: KEPIEVSHEQLELFREMRC and affinity purified. Figure 3-2 illustrates the antigenic sites on the AgCA9 protein against which these antibodies were generated. Both antibodies specifically recognized AgCA9 on a western blot (e.g. Figure 3-6A); however, the antibody from hen 5340 recognized a second protein as well (see Figure 4-3A). Only results that were consistent between the two antibodies were reported here. Western blot results for antibody 5563 are shown in Figure 3-6A. The blot was performed using protein extracted from whole *An. gambiae* fourth-instar larvae. The antibody detected a single specific band at 31.5 kDa representing AgCA9. The identity of the band was then verified by blocking the antibody with reconstituted peptide. When blocked, the antibody failed to detect any bands, further confirming that the antibody recognized AgCA9 in a specific manner. Specificity of protein localization seen in longitudinal sections (as discussed in the next section) was also verified using a preadsorption blocking assay. When the antibody was blocked with reconstituted peptide, it failed to detect AgCA9 protein (Figure 3-6B-D; compare 3-8A with 3-

6B and C, and 3-6D with 3-6E). Apparent expression in the exoskeleton is nonspecific (Figure 3-6B and C).

Detection of AgCA9 Protein in *An. gambiae* Larvae

Once the specificity of the affinity purified antibody 5563 was verified, a Western blot was used to determine the presence of AgCA9 protein in the individual regions of the alimentary canal including GC, AMG, PMG, MT, and rectum (Figure 3-7). AgCA9 protein was most abundant in the GC and rectum, followed by the MT. AgCA9 detection in the AMG and PMG was relatively weak.

Both whole mount larval preparations and longitudinal sections of whole larvae embedded in paraffin were used to detect AgCA9 protein with antibodies 5563 and 5340. Specific protein was detected in the GC, ectoperitrophic fluid and in the cells of the TR, MT, and rectum as will be discussed in more detail below (Figure 3-8A) (Smith, K. E. et al., 2007).

Ectoperitrophic fluid

While detection of AgCA9 protein on a Western blot indicated significant protein levels in the GC, immunohistochemical results within the cells of the GC were variable. In most preparations AgCA9 was detected in the proteinaceous matrix that occupied the lumen of the GC and lined the alimentary canal (from the GC through the PMG) within the ectoperitrophic space but was not detected in the food bolus (Figure 3-8A). AgCA9 protein is indeed within the ectoperitrophic space and not in the peritrophic matrix (PM). The proteinaceous matrix expressing AgCA9 was measured to be 10-27 μm thick in both longitudinal and cross-sections of whole larvae embedded in paraffin (e.g. Figure 3-8A), making it 10-30 times thicker than the PM in *Ae. aegypti* (Clements, 1992). This proteinaceous matrix is clearly non-cellular and most likely comprises the ectoperitrophic fluid, which is known to have an important role in insect digestion (Terra and Ferreira, 1981; Terra et al., 1979). Both vitally and as a result of fixation,

there are areas along the alimentary canal where the PM lies very close to the epithelial cells. This results in a very thin ectoperitrophic space where the ectoperitrophic fluid is immediately adjacent to the apical membrane of the epithelial cells. Based on numerous immunolocalization experiments I do not believe that AgCA9 protein is located on the apical membrane of any alimentary canal epithelial cells, but is confined to the ectoperitrophic fluid.

Transitional region

The cells of the TR clearly express AgCA9 mRNA as demonstrated by *in situ* hybridization; however, protein detection was variable. In many preparations AgCA9 protein was observed in association with the periphery of the nucleus (Figure 3-8B). Another protein, Na^+K^+-ATPase, was found by others to have regionally specific membrane distribution in *Ae. aegypti* with a switch in polarity from the apical membrane in the AMG to the basal membrane in the PMG (Patrick et al., 2006). This polarity switch is also evident in *An. gambiae* and can be used to identify the AMG and PMG regions. The beginning of the TR is marked by the switch in localization of Na^+K^+-ATPase to the basal membrane (Figure 3-8C, arrowhead). The AgCA9 protein was restricted to the nuclei of the cells of the TR and did not extend into the AMG. No biochemical marker for the end of the TR and beginning of the PMG is known at this time. Counterstaining with the nuclear stain DRAQ-5 confirmed that CA protein was confined to the periphery of the nucleus, but was absent from the center region of the structure (Figure 3-8D).

Malpighian tubules

AgCA9 protein was detected in a punctate pattern within the principal cells of the MT, with stellate cells appearing devoid of protein (Figure 3-9). The protein appeared to associate with cytoplasmic inclusions throughout the MT and did not localize to either the membrane or nucleus.

Rectum

A patch of epithelial cells covering roughly one quarter of the rectum and positioned on the dorsal side of the apical extreme of this alimentary canal region showed very intense and specific AgCA9 staining. These cells will henceforth be referred to as "dorsal anterior rectal cells", or DAR cells, whereas the cells of the remainder of the rectum will be referred to as non-DAR cells. This localization pattern was recognized first by the antibody 5340 in whole mount larval alimentary canal preparations (Figure 3-10A), and specificity to AgCA9 was verified using affinity purified antibody 5563 in paraffin sections (Figure 3-10B). To compare and contrast this staining pattern a monoclonal antibody to Na^+K^+-ATPase was used, which was found by others working in parallel to produce a negative staining pattern in this region relative to the AgCA9 in whole mount larval preparations (Rheault et al., 2007). Indeed, this basal membrane protein produced a reversed image of the AgCA9 pattern (Figure 3-10C), localizing solely to the non-DAR cells. Localization in paraffin sections of the rectum showed AgCA9 protein to be clearly cytoplasmic whereas the Na^+K^+-ATPase localized to the extensive basal infoldings as described by Patrick et al., (2006). The unusual banding pattern seen in the DAR cells was investigated by counterstaining with TRITC-Phalloidin to reveal circumferential muscles surrounding the rectum (Figure 3-10D).

Phylogenetic Analysis

A phylogenetic tree comparing predicted and cloned CA transcripts from *H. sapiens*, *D. melanogaster*, *Ae. aegypti*, and *An. gambiae* showed a general segregation of human and insect CAs (Figure 3-11). This separation was not seen in the case of the CA-RPs. Interestingly, AgCA9 was the sole *An. gambiae* CA that clustered with *H. sapiens* CAs, along with its *D. melanogaster* and *Ae. aegypti* orthologues. Within the *H. sapiens* CAs, clustering occured between proteins with the same or similar subcellular localizations. There was a distinct

separation between the secreted, membrane-bound, and transmembrane CAs. Cytosolic and mitochondrial CAs formed a fourth cluster.

Discussion

The ensembl database predicts a total of eleven α-CA (two of which are CA-RPs), and one β–CA genes to be present in the *An. gambiae* genome, six of which have been fully cloned by the members of the Linser laboratory (e.g. Table 3-1) (Linser et al., 2003; Smith, K. E. et al., 2007; T. J. Seron, personal communication; K. E. Smith, unpublished data). Here I report the cloning of four of these six CAs: AgCA-RP2, a CA-RP, AgCA6, a secreted-like α–CA, AgCA9, a cytoplasmic α-like CA, and AgCAb, a β–CA from the alimentary canal of the larval malaria mosquito, *An. gambiae.* Additionally, I report the mRNA characterization of AgCA6, AgCA9, and AgCAb, and protein characterization of AgCA9.

CA Activity in *An. gambiae* Larvae

CA activity was detected by Hansson's histochemical method in the ventral nerve cord and in the cells of the GC, AMG, MT, and rectum. All staining except that in the MT was inhibitable by the α-CA inhibitor, methazolamide. These results differ from those reported by Corena et al., (2002) who reported CA activity only in the cells of the GC and PMG of *Ae. aegypti* using a similar method. This discrepancy could be attributed to a difference in preparations; besides using a different mosquito species, Corena et al., (2002) detected CA activity in whole mount preparations compared to frozen sections which were used in this study. Hansson's method involves incubating tissue in media containing HCO_3^-, PO_4^{2-} and cobalt at pH 6–8. As described by Maren (1979), the method depends on the loss of CO_2 from the surface of the tissue which displaces the CA reaction equilibria towards the production of OH^-. The resulting increase in alkalization near sites of enzymatic activity produces a cobalt precipitate. The use of whole mount preparations may have prevented proper CO_2 loss from within the cells and resulted in

false negative results. Additionally, Corena et al., (2002) did not report the pharmacological inhibition of CA to verify specificity of the staining. The CA staining patterns observed in this study support the mRNA localization patterns identified for the three characterized CAs which will be discussed below.

Inability to inhibit CA staining in the MTs has been previously reported (Palatroni et al., 1981) and could be due to several causes. It is possible that a non-specific precipitate is being formed in the concretion bodies of the MT (described in later text), and that this precipitate is independent of CA activity. Alternatively, residual staining could be due to an extraordinarily high concentration of the CA enzyme, in which case, a higher concentration of inhibitor may eliminate staining. However, increased inhibitor could result in the formation of an inhibitor-cobalt complex rather than in the inhibition of CA directly (Muther, 1966). Finally, MT CA activity could be mediated by AgCAb, a β –CA, which would be resistant to methazolamide inhibition. However, qPCR results indicated a lower level of AgCAb in the MT than most other regions of the alimentary canal.

AgCA6, AgCA9, and AgCAb mRNA Localization

AgCA6, AgCA9, and AgCAb displayed unique expression profiles when regional mRNA levels were compared to those in the whole alimentary canal, suggesting that individual cell types may employ specific CAs over others. The GC, PMG and MT did not significantly express AgCA6, AgCA9 or AgCAb, whereas the AMG significantly expressed only AgCAb when compared to whole alimentary canal. The rectum was the single region tested which showed a significant abundance of all three AgCAs above whole alimentary canal levels. This suggests that the rectum is heavily involved in pH regulation. Indeed, CA in the rectum is implicated in both pH- and ion-regulation, as discussed in more detail in Chapter 5, and consequently, multiple isoforms of the enzyme may be required by this region. The CA mRNA

localization patterns were supported by microarray analysis performed using mRNA from the various regions of the *An. gambiae* alimentary canal (GC, AMG, PMG, hindgut (HG)) (Neira et al., 2008). Separate data were not available for MT and rectum, but were combined into one sample labeled "HG". The microarray compared expression levels of approximately 14,000 *An. gambiae* genes (Affymetrix GeneChip® *Plasmodium*/*Anopheles* Genome Array, Affymetrix Inc; Santa Clara, CA, USA) in each region of the alimentary canal as compared to whole insect.

AgCA9 Protein Distribution

Antibody probes against AgCA9 were used to determine protein distribution within the alimentary canal. AgCA9 was detected in the proteinaceous matrix that occupies the GC lumina as well as the length of the alimentary canal in the ectoperitrophic space. Additionally, AgCA9 protein was found in the cells of the TR, MT and in the cytoplasm of the DAR cells within the rectum.

There are obvious discrepancies between the measured AgCA9 mRNA and protein distribution. These can be explained simply by recalling that protein localization does not necessarily mirror mRNA transcription. For example, MT were found to have very little AgCA9 mRNA; however, I consistently saw protein in MTs of larval paraffin sections. A developmental shift in mRNA and protein production could account for these differences. All experiments were performed using early fourth-instar larvae. It is possible that AgCA9 mRNA is expressed in the MT of earlier larval stages and then wanes as the larvae nears pupation; if AgCA9 has a slow protein turnover rate, this would lead to the presence of protein in the absence of mRNA expression.

Ectoperitrophic fluid

According to the current model of pH regulation in the mosquito alimentary canal, CA catalyzes the production of HCO_3^- in the cells of the alimentary canal which is then translocated

into the lumen by a plasma membrane anion exchanger. Our failure to localize an anion exchanger protein in the alimentary canal led members of the Linser laboratory to seek other possible means for HCO_3^- transport into the lumen. The detection of AgCA9 protein in the ectoperitrophic space obviated the need for an anion exchanger and offered an alternative mechanism for the production of HCO_3^- in the lumen (Figure 3-12).

Mosquito alimentary canal epithelial cells are metabolically active, producing CO_2. CO_2 can diffuse freely across the cellular membrane and into the ectoperitrophic space where AgCA9 can catalyze its conversion to HCO_3^-. HCO_3^- can buffer the lumina of the GC and PMG to a pH around 8.0. In the AMG epithelium, a basally located V-ATPase is positioned to move H^+ vectorally out of the cells (Zhuang et al., 1999), resulting in a transepithelial potential that is lumen-negative (Clark et al., 1999). This likely results from the combined activities of the V-ATPase and a $K^+/2H^+$ antiporter (Lepier et al., 1994) that produce a net movement of protons into the hemolymph in the AMG. A $K^+/2H^+$ antiporter has yet to be localized to the AMG, therefore this protein has been left out of the putative model (Figure 3-12). This loss of luminal H^+ should result in the deprotonation of HCO_3^-, forming CO_3^{2-}. This, combined with a strong cation such as K^+ or Na^+, would then provide the basis for buffering at a pH near 10.5. In caterpillars, the ectoperitrophic space was found by Gringorten et al., (1993) to be equal in pH to the endoperitrophic space. Thus, the same pH gradient exists in both compartments of the lumen and HCO_3^-/ CO_3^{2-} in the ectoperitrophic space could lead to a buffering of the entire lumen.

How does a cytoplasmic-like protein, one that is not predicted to have a signal sequence, end up in the extracellular ectoperitrophic fluid? I suggest that AgCA9 protein is produced in the cells of the GC (recall that the GC was found to be enriched in AgCA9 mRNA) and secreted into the ectoperitrophic space by a type of exocytosis. There are several methods of secretion that do

not require a signal sequence and are often utilized to export digestive enzymes in the cells of insect alimentary canals. Merocrine secretion is a classic form of exocytosis, occurring when membrane bound vesicles containing soluble proteins open onto the surface of the cell, allowing the proteins to be secreted into the lumen (Hung et al., 2000). Alternatively, apocrine release occurs when a portion of the plasma membrane buds off the cell, containing the proteins (*ibid*).

Notably, there was an unexpected lack of accumulation of AgCA9 protein within the food bolus. The peritrophic matrix of *An. gambiae* larvae is permeable to 148 kDa particles (Edwards and Jacobs-Lorena, 2000) and would be expected to allow 31.5 kDa AgCA9 to freely diffuse into the food bolus. However, the native enzyme conformation of AgCA9 is unknown at this time and could be oligomeric. Additionally, the enzyme may be complexed with other enzymes, making it larger, or may associate with the PM and accumulate at this junction without passing through to the food bolus.

Transitional region

AgCA9 mRNA clearly localized to the TR using *in situ* hybridization; however, the protein localization was not as clear, appearing to localize to the periphery of the nuclei of the cells in this area. The unusual localization of AgCA9 to the nuclei is not unprecedented. There are many manuscripts that have noted CA in the nucleus using both immuno- and enzyme-histochemical methods (Hansson, 1967; Lutjen-Drecoll and Lonnerholm, 1981; Anderson et al., 1982; Brown et al., 1983; Brown and Kumpulainen, 1985; Toyosawa et al., 1996). These papers make no claims as to the validity of these findings and most relate enzyme histochemical detection to the fact that the nuclei act as crystallization centers for the reaction products of Hansson's cobalt precipitation method (Ridderstråle, 1991). I observed AgCA9 nuclear localization using immunohistochemical analyses which are not based on enzymatic activity and hence nuclear CA remains a physiological mystery.

The TR is described as a unique region in the alimentary canal which was previously thought to be a part of the PMG. This region is described as having a continuous morphological change between the AMG and PMG in contrast to a mixture of cells from each region (Clark et al., 2005). Clark et al., (2005) found the cells of this region to have long microvilli and a high density of mitochondria, suggesting a transport role involving a high rate of ATPase activity in *Ae*. *aegypti*. A distinct band of GPI-linked CA mRNA has previously been described in the anterior end of the PMG as well as an increased mRNA expression of an anion exchanger, AgAE1, in this region (Seron et al., 2004; T. J. Seron, personal communication). This localization to the nuclei of the TR identifies a differential quality of these cells compared to the rest of the alimentary canal. The beginning of the TR demarks the area at which the highly alkaline pH of the AMG drops to near neutral values within the lumen of the alimentary canal. I predict that these cells have an important role in the de-alkalization of the alimentary canal. At this time, no explanation is evident for the association of AgCA9 with the nuclei of these cells.

Malpighian tubules

MTs are important components of the mosquito osmoregulatory system, maintaining hemolymph volume and composition (Bradley, 1987b). *An. gambiae* larvae are equipped with five MT which are composed of two cell types: principal cells and stellate cells. The larger principal cells contained AgCA9 protein associated with membranes of vesicular cytoplasmic inclusions, while no such protein was detected in the smaller stellate cells. Palatroni et al. (1981) localized CA activity to vesicular cytoplasmic inclusions within the MT of *Culex pipiens* using Hansson's method for histochemical localization. The authors noted that CA activity was only evident at the level of the membranes of these inclusions and was lacking on the cellular membrane, nucleus and other cytoplasmic structures. The cytoplasm of principal cells is densely packed with membrane-limited vesicles containing concretion bodies, metallo-organic

aggregates of Ca^{2+}, Mg^{2+} and K^{+} that have roles in metal ion storage as well as transepithelial transport. Stellate cells notably lack these concretion bodies (Beyenbach, 2003; Clements, 1992). AgCA9 protein detection mirrored the enzymatic pattern shown by Palatroni et al., (1981), and possibly represents association with concretion bodies. I suggest AgCA9 may play a role in concretion formation and ion transport within the MT. In support of this, HCO_3^- formed by the CA-catalyzed reaction is an essential component of concretion bodies in *D. melanogaster*, and inhibition of CA inhibits concretion formation (Wessing and Zierold, 1997). Additionally, intracellular CA has an important role in providing H^+ and HCO_3^- to transport systems within *D. melanogaster* MTs (Wessing et al., 1999).

DAR cells

Meredith and Phillips analyzed the ultrastructure of freshwater vs. saltwater mosquito larvae, using *Ae. aegypti* and *Aedes campestris* respectively, as representative mosquitoes. They noted that whereas salt water mosquito larvae possess recta that are divided into two regions, the recta of freshwater mosquito larvae is uniform in structure and function, similar to the anterior rectum of salt water breeders (Meredith and Phillips, 1973). This has been supported by light microscopy of two other species of mosquito, *Aedes albopictus* (Asakura, 1970) and *Aedes detritus* (Ramsay, 1950) as well as with hemipteran larvae, *Hydrometra stagnorum* and *Halosalada lateralis* (Goodchild, 1969). Meredith and Phillips hypothesized that the posterior region of the rectum is unique to saltwater breeders and generates a hyperosmotic urine as a way of regulating the high salt intake. The anterior portion of the rectum is thought to selectively resorb ions, water and metabolites produced by the MTs (Meredith and Phillips, 1973). As primarily a fresh water breeder, *An. gambiae* larvae would be expected to have a uniform rectum. However, AgCA9 clearly localized solely to a subset of cells in the anterior region of the rectum,

suggesting distinctive functions of these cells within the rectum. The protein was not detected in the entire anterior rectum, but localized to cells on the dorsal side (DAR cells).

The DAR cells also differentially expressed other pH- and ion- regulatory proteins such as Na^+/K^+-ATPase, V-ATPase (Okech et al, 2008; Smith et al., 2008), and an *An. gambiae* cytoplasmic CA (AgCA11, accession # AY280613) (T. J. Seron, personal communication). This suggests a highly regulated system of pH and ion regulation within the rectum. Clearly the rectum of this particular freshwater breeder is not uniform as originally thought; however the specific roles of the DAR cells remain to be determined. Most of the research regarding the larval mosquito rectum has been performed on members of the subfamily Culicinae, with no information available on the rectum of Anophelinae larvae, including *An. gambiae*. The DAR cells are likely unique to the larvae of anopheline mosquitoes, as further investigated and discussed in Chapter 5.

My data suggests that the DAR cells of the *An. gambiae* rectum may have a role similar to the anterior rectum of salt water culicines. The rectum is an important site of pH and HCO_3^- regulation in the larvae of *Aedes dorsalis*, a salt-water mosquito capable of inhabiting hypersaline lakes (HCO_3^- and CO_3^{2-} concentrations as high as 1.0 - 2.4 mol^{-1} and pH values exceeding 10.0) (Strange et al., 1982). Using microperfused recta preparations, it was reported that the anterior rectum is a site of CO_2 secretion in the form of a Cl^--HCO_3^- exchange. Additionally, the authors predicted the involvement of a basolateral 1:1 Cl^--HCO_3^- exchanger and a CA, based on data obtained using inhibitory compounds (Strange et al., 1984). My data suggests that the DAR cells of *An. gambiae* may behave in a similar manner. AgCA9 within these cells can catalyze the conversion of CO_2 to HCO_3^- which can then be transported into the lumen by an anion exchanger and excreted. Supporting this hypothesis, it is known that

mosquito larvae alkalize their rearing media by excreting bicarbonate (Stobbart, 1971) and it has been shown that this alkalization can be blocked using global CA inhibitors (Corena et al., 2002). Possible functions of both DAR and non-DAR cells will be discussed further in Chapters 5 and 6.

Phylogeny

A phylogenetic analysis was performed to examine the relationship between CAs in the *H. sapiens*, *D. melanogaster*, *Ae. aegypti*, and *An. gambiae* genomes. Alignments were made between known and predicted protein sequences as reported by the Ensembl February 2007 release and a tree was generated. A distinct separation was seen between insect and human CAs. However, CA-RPs showed no such distinction and clustered together. This suggests that the CA-RPs are conserved between protostomes and deuterostomes and that active CA amplification took place after their divergence. Although CA-RPs lack CA activity, they are highly conserved proteins, indicating that they serve a critical cellular function (Tashian et al., 2000). Interestingly, AgCA9 and its *Drosophila* and *Aedes* orthologs were the sole insect CAs that clustered with *H. sapiens* CAs. This association suggests that AgCA9 is closer to the primal protein from which other CAs branched. In fact, AgCA9 was closely associated with CAVII, the *H. sapiens* CA which is the most highly conserved of the active CA isozymes and thought to most closely resemble the ancestral state (Hewett-Emmett and Tashian, 1996; Chegwidden and Carter, 2000). This implies that AgCA9 is a highly conserved protein and likely to play a role in similarly conserved functionalities.

Conclusions: Histochemical detection of CA activity in the larval alimentary canal challenges previous data and, along with the cloning and characterization of several CAs, suggests an alternative model for CA expression and activity in larval mosquitoes. The cloning of AgCA-RP2, and the cloning and characterization of secreted-like AgCA6, cytoplasmic-like

AgCA9, and AgCAb, expands the current knowledge of AgCAs distribution in the alimentary canal of *An. gambiae*. These data suggest that each region of the alimentary canal expresses a different set of AgCAs, and that certain AgCAs may be optimally suited for certain cell types. Additionally, the detection of significant and abundant levels of AgCA6, AgCA9 and AgCAb in the rectum supports current literature that reports heavy involvement of the larval rectum in pH- and ion-regulation.

The protein localization of the cytosolic-like α-CA, AgCA9, to the ectoperitrophic fluid suggests that HCO_3^- production in the lumen is mediated by CO_2 diffusion followed by the action of an extracellular CA. If AgCA9 actively catalyzes the production of HCO_3^- within the alimentary canal lumen, it would suggest that this CA is a key player in AMG alkalization, and therefore in larval survival. The protein was also detected in the cells of the TR, MT and DAR, a previously undescribed region of the rectum. I have shown differential localization of the ion-regulatory protein Na^+K^+-ATPase in addition to AgCA9 in this region. The fact that DAR cells differentially express a number of pH- and ion-regulatory proteins suggests an overlooked and important role for these cells in larval pH regulation in anopheline mosquitoes.

Finally, a phylogenetic analysis revealed AgCA9 to cluster with *H. sapiens* CAs and in close association with CAVII, the most basal *H. sapiens* CA, implying a highly conserved, and thus important physiological role. Further studies should be performed to investigate the function of AgCA9, as well as the functions of AgCA-RP2, AgCA6, and AgCAb, specifically focusing on their role in pH- and ion-regulation in each region of the alimentary canal.

Table 3-1. *An. gambiae* carbonic anhydrase (CA) new naming convention. Table 3-1 lists the CA family (column 1), ensembl identifier (AGAP; column 2), and the suggested naming convention (column 3) for the 11 predicted α-CAs, including the two predicted CA-related proteins (CA-RPs), and the single β-CA encoded in the genome. Also noted are the accession numbers of those CAs which members of the Linser laboratory have fully cloned and sequence confirmed. The ensembl identifiers are based on the July 2008 release.

CA family	AGAP0	New convention	Accession #
α-CA	02360	AgCA1	
α-CA-RP	00715	AgCA-RP2	FJ612599
α-CA	00401	AgCA3	
α-CA	07550	AgCA4	
α-CA-RP	00688	AgCA-RP5	
α-CA	03289	AgCA6	DQ518577
α-CA	02359	AgCA7	
α-CA	10844	AgCA8	
α-CA	10052	AgCA9	DQ518576
α-CA	04895	AgCA10	AY280612
α-CA	05066	AgCA11	AY280613
β-CA	02992	AgCAb	EF065522

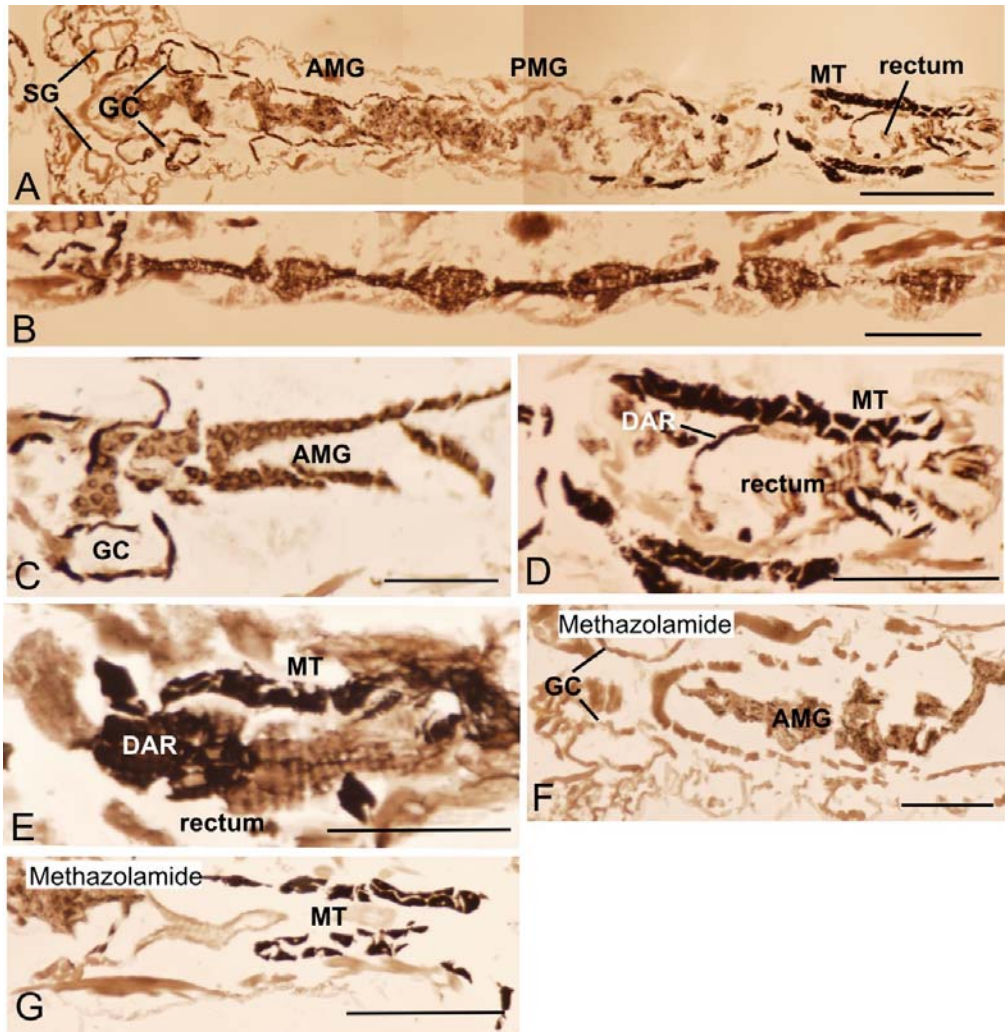

Figure 3-1. Hansson's histochemical detection of CA activity in newly cut frozen sections of fourth-instar *An. gambiae* larvae. A) Whole larval alimentary canal. Activity was detected in B) the ventral nerve cord, C) within the cells of the GC and AMG, and D, E) within the cells of the MT and rectum. F, G) Treatment of incubation media with methazolamide inhibited CA activity in all regions except for the MT. Abbreviations: AMG, anterior midgut; DAR, dorsal anterior rectum; GC, gastric ceaca; MT, Malpighian tubules; PMG, posterior midgut; SG, salivary glands. Scale bars: 250µm (A), 125µm (B, D, F), 200µm (C, E, G).

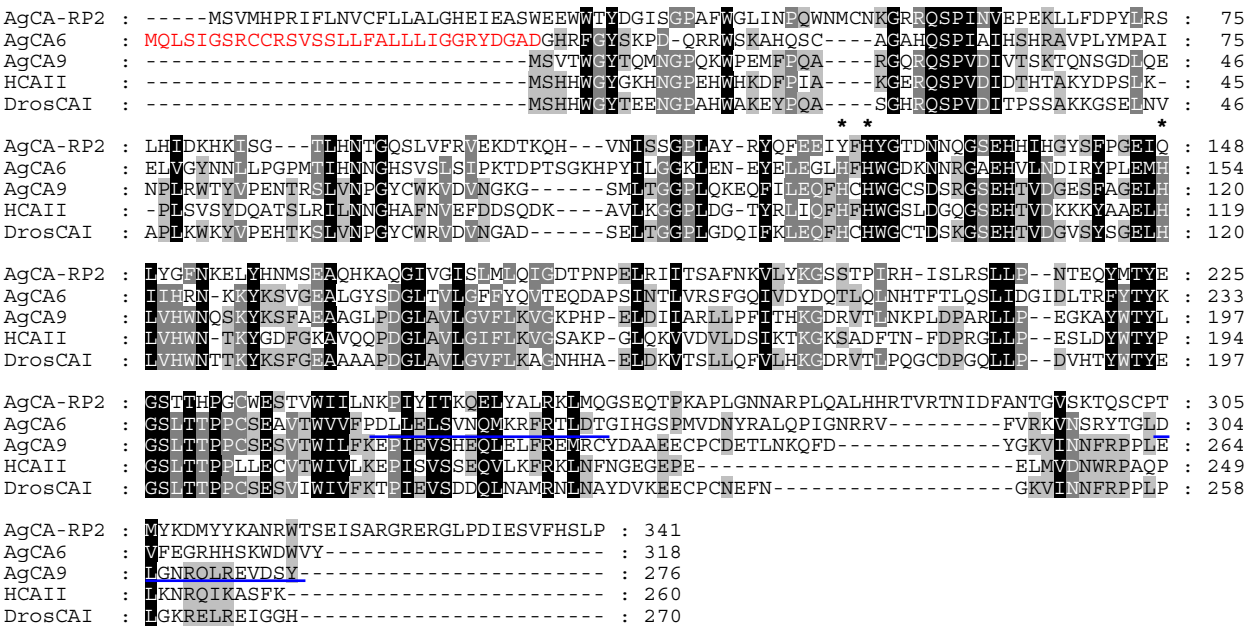

Figure 3-2. Alignment of cloned *An. gambiae* α–CAs AgCA-RP2, AgCA6, and AgCA9 with *H. sapiens* CAII (HCAII) and *D. melanogastor* CAI (DrosCAI). Regions with high similarity are highlighted in black (100%). Regions of lesser similarity are highlighted in dark grey (>80%) and light grey (>60%). The three histidines essential for α–CA activity (HCAII his-94, his-96, his-119) are indicted with asterisks. The signal peptide in AgCA6 is highlighted in red, and the antigenic sites against which the AgCA9 antibodies (5340 and 5563) were generated are identified by blue bars.

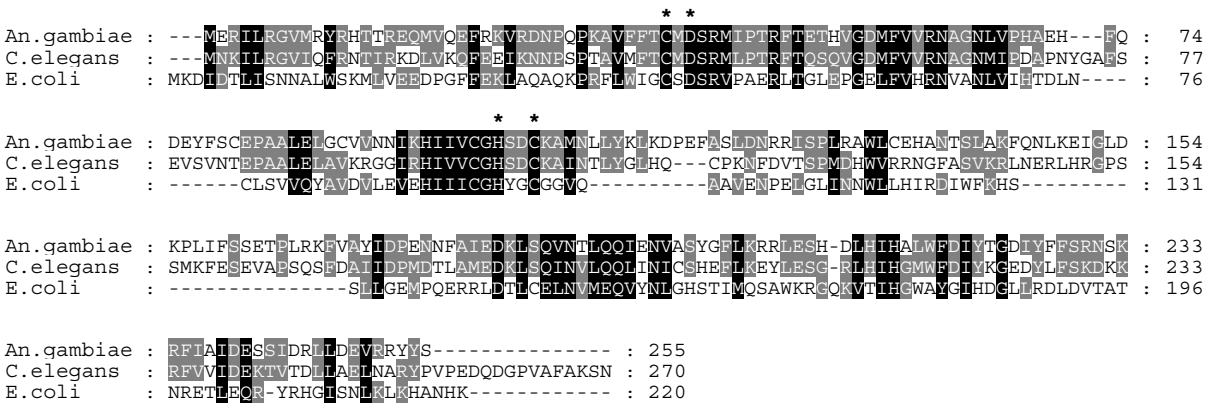

Figure 3-3. Alignment of the predicted *An. gambiae* β–CA (AgCAb) with β–CAs from *C. elegans* and *E. coli*. Regions with high similarity are highlighted in black (100%). Regions of lesser similarity are highlighted in dark grey (>80%) and light grey (>60%). The four amino acid residues essential for β–CA activity (E. coli cys-42, asp-44, his-98, and cys-101) are indicted with asterisks.

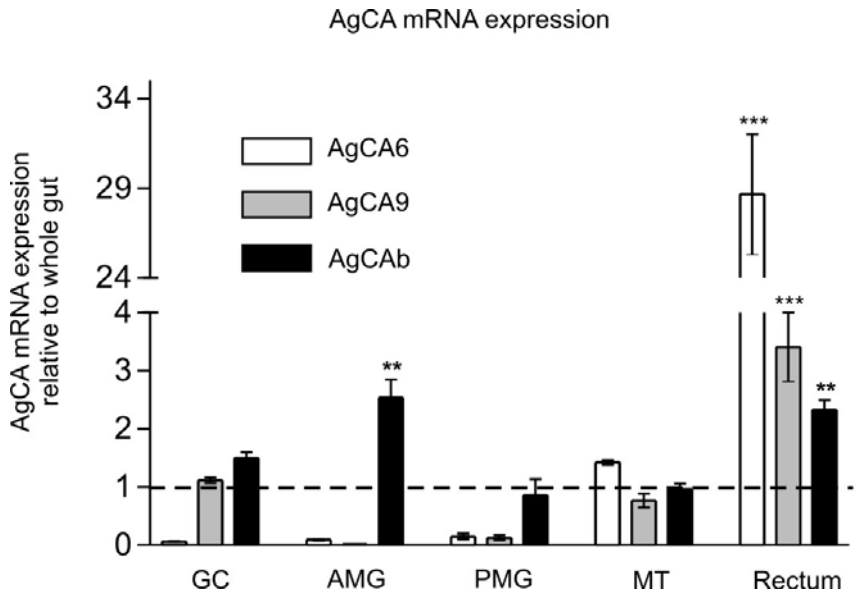

Figure 3-4. mRNA expression of cloned AgCAs in the alimentary canal of *An. gambiae* larvae as determined by qPCR. qPCR was used to measure expression of AgCA6, AgCA9 and AgCAb mRNA in alimentary canal regions, gastric caeca (GC), anterior midgut (AMG), posterior midgut (PMG), Malpighian tubules (MT) and rectum, relative to whole alimentary canal. All values were normalized to an 18s RNA endogenous control. 'Whole alimentary canal' sample was normalized to a value of "1" and is indicated by a dashed line. Error bars indicate standard deviation between three biological replicates. **: P-Value < 0.01; ***: P-Value < 0.001.

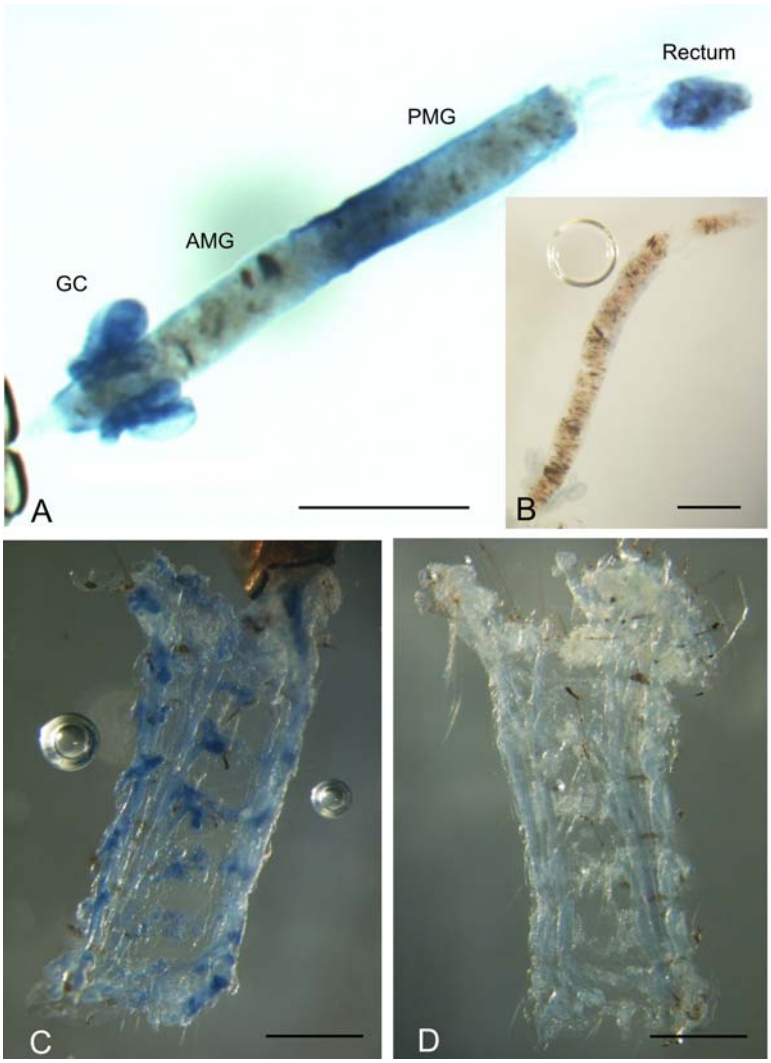

Figure 3-5. mRNA expression of AgCA9 in *An. gambiae* larvae as determined by *in situ* hybridization. *In situ* hybridization was used to detect AgCA9 mRNA in whole larval alimentary canals and carcass. Antisense probe generated intense staining in the A) GC, transitional region between the anterior and posterior midguts (indicated by arrow), and rectum of the larval alimentary canal with weaker staining seen in the cells of the PMG. C) Carcass showed the most intense staining in the muscle fibers and fat body. Sense probe did not significantly stain any areas of the B) alimentary canal or D) carcass. For abbreviations see Figure 3-1 legend. Scale bars: 400 μm.

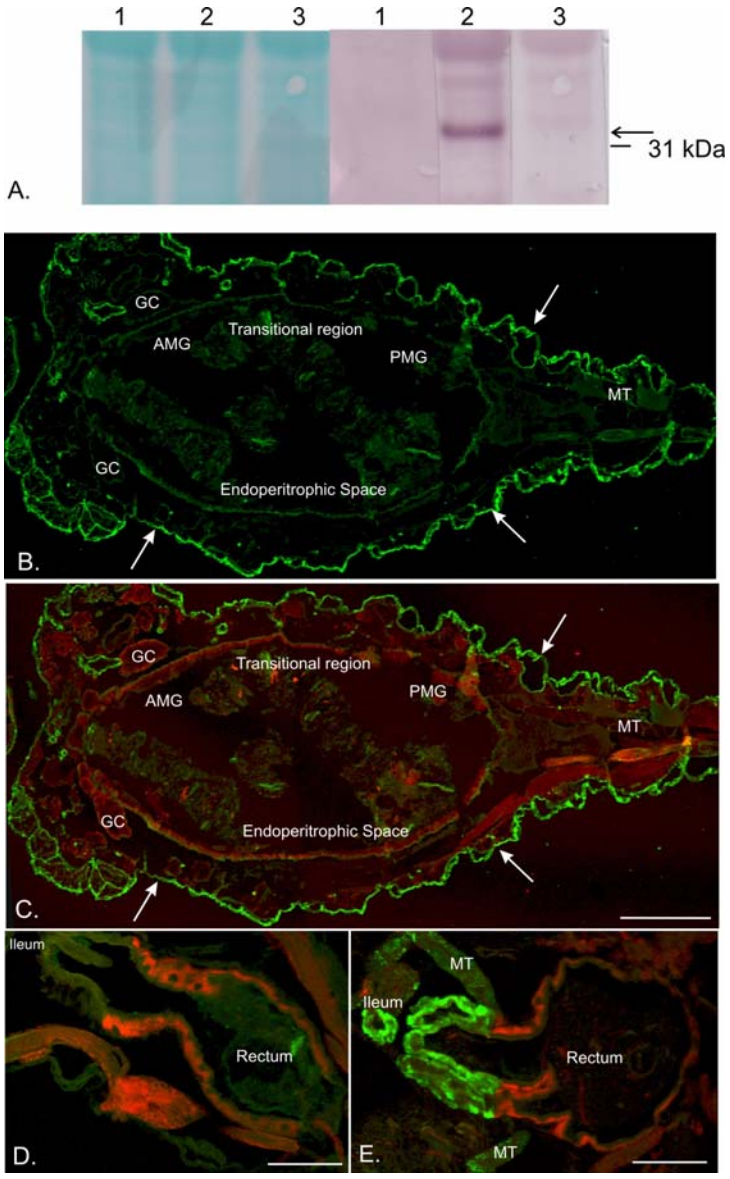

Figure 3-6. Verification of the specificity of antibody 5563 in longitudinal sections of *An. gambiae* larvae. The specificity of the affinity purified antibody 5563 was verified using a A) Western blot and B-E) immunohistochemistry. Image A shows the results of an antibody adsorption assay. The left panel of the image is the fast green staining of total protein to ensure equal loading. Antibody was pre-incubated with peptide prior to detection of protein. The Western blot (right panel) illustrates the detection of AgCA9 protein with pre-immune IgY (lane 1), affinity purified antibody 5563 IgY (lane 2), and peptide blocked IgY (lane 3) (A). Images B-E illustrate immunohistochemistry results obtained using affinity purified antibody 5563 IgY (E) and peptide blocked IgY (B, C, D) in longitudinal sections of whole larvae embedded in paraffin. The images were generated on a laser confocal microscope (Leica SP2). B and C are images of the same section of larval alimentary canal (without the rectum) with two different fluorochromes (FITC = green = AgCA9; TRITC = red =

Na^+K^+-ATPase). D and E are images of the rectum positioned such that the anterior end is to the left. Na^+K^+-ATPase immunostaining was used as a counter stain to better visualize the regions of the alimentary canal in images C, D and E. The pre-adsorbed antibody (B, C, D) failed to detect AgCA9 protein compared with antibody not treated with peptide (E, also compare with Figure 3-8). Apparent exoskeleton staining is non-specific (B, C; arrows). For abbreviations see Figure 3-1 legend. Scale bars: 150 μm (B, C); 75 μm (D, E).

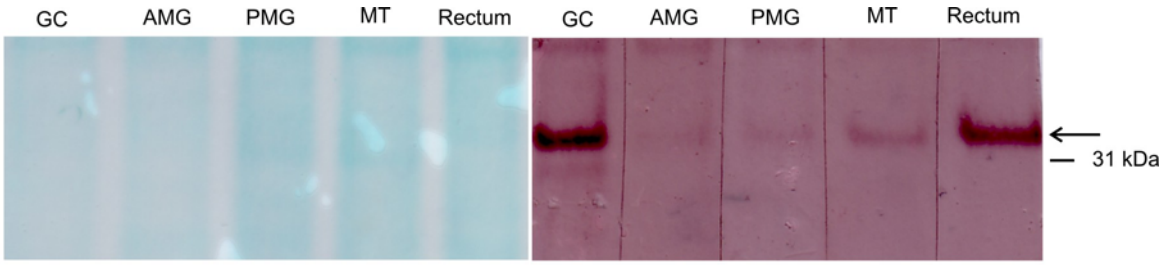

Figure 3-7. Western blot used to determine AgCA9 protein localization in *An. gambiae* larval alimentary canal regions including GC, AMG, PMG, MT, and rectum. The left panel of Figure 3-7 is the fast green staining of total protein to ensure equal loading. The right panel shows protein detection using an AgCA9 specific antibody, 5563. AgCA9 protein band is indicated by an arrow. For abbreviations see Figure 3-1 legend.

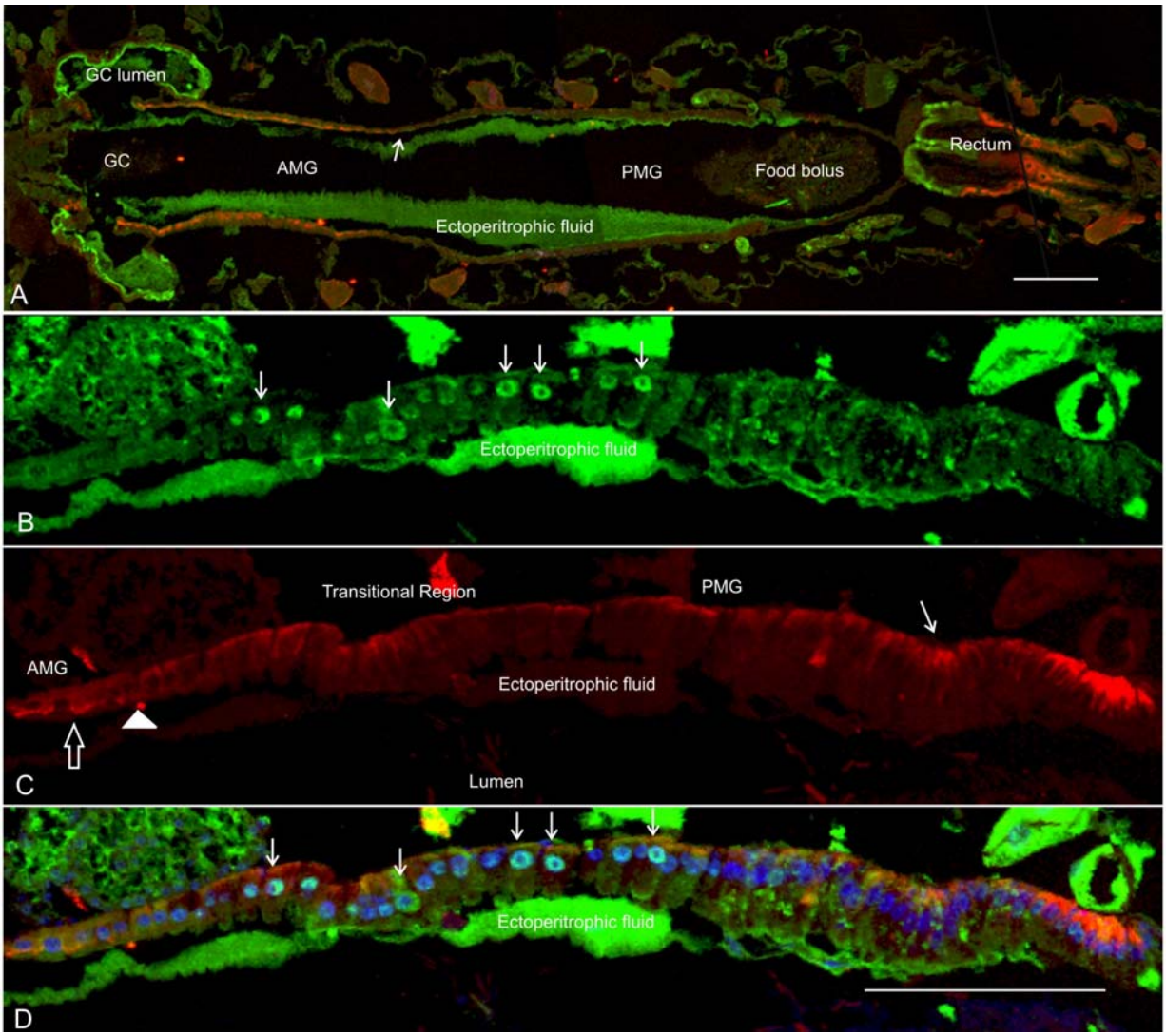

Figure 3-8. Immunohistochemistry to detect AgCA9 and Na^+K^+-ATPase protein in longitudinal sections of whole *An. gambiae* larvae. A) Whole alimentary canal; B, C, D) higher magnification of AMG, TR, and PMG. The images were generated on a laser confocal microscope (Leica SP2). The anterior end of the larvae is towards the left. B, C, and D are images of the same section with the three different fluorochromes (FITC = green = AgCA9; TRITC = red = Na^+K^+-ATPase; Cy5 = blue= DRAQ-5 nuclear stain). AgCA9 protein detection was variable in the epithelial cells of the GC but was consistently seen in the proteinaceous matrix that fills the GC lumen and lines the alimentary canal within the ectoperitrophic space (ectoperitrophic fluid) (A). Na^+K^+-ATPase was used as a counter stain to identify the regions of the alimentary canal (A, C, D). Na^+K^+-ATPase is localized to the apical membrane in the cells of the AMG (C, hollow arrow) and to the basal membrane in the cells of the PMG (C, arrow). In the vicinity of the switch from apical to basal localization is the beginning of the TR (A, arrow; C, arrowhead). AgCA9 detection in the transitional region reveals an association with the periphery of the nucleus (B, D; e.g. arrows). Nuclear

localization was confirmed by counterstaining with the nuclear stain DRAQ-5 (D, blue). For abbreviations see Figure 3-1 legend. Scale bars: 150 μm (A); 172.2 μm (B, C, D).

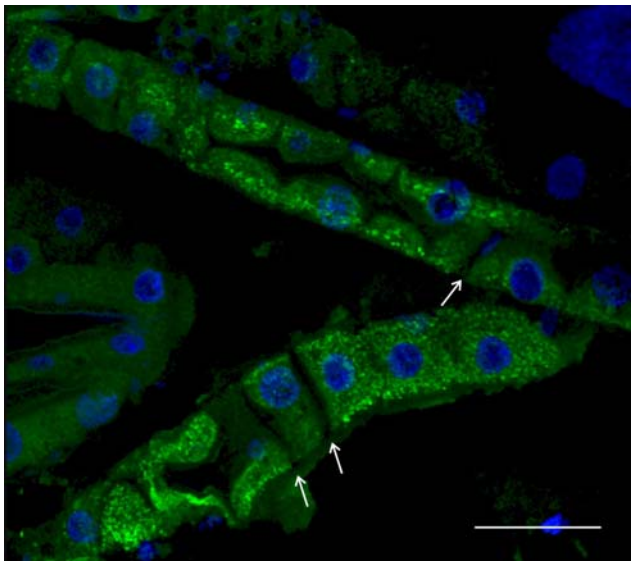

Figure 3-9. Immunohistochemistry of AgCA9 in *An. gambiae* Malpighian tubule sections. The confocal image demonstrates punctate AgCA9 protein localization within the principal cells of the MT (green). Stellate cells (e.g. arrows) do not appear to contain AgCA9 protein. The nuclei were detected using nuclear stain DRAQ-5 (blue). For abbreviation see Figure 3-1 legend. Scale bar: 47.62 μm.

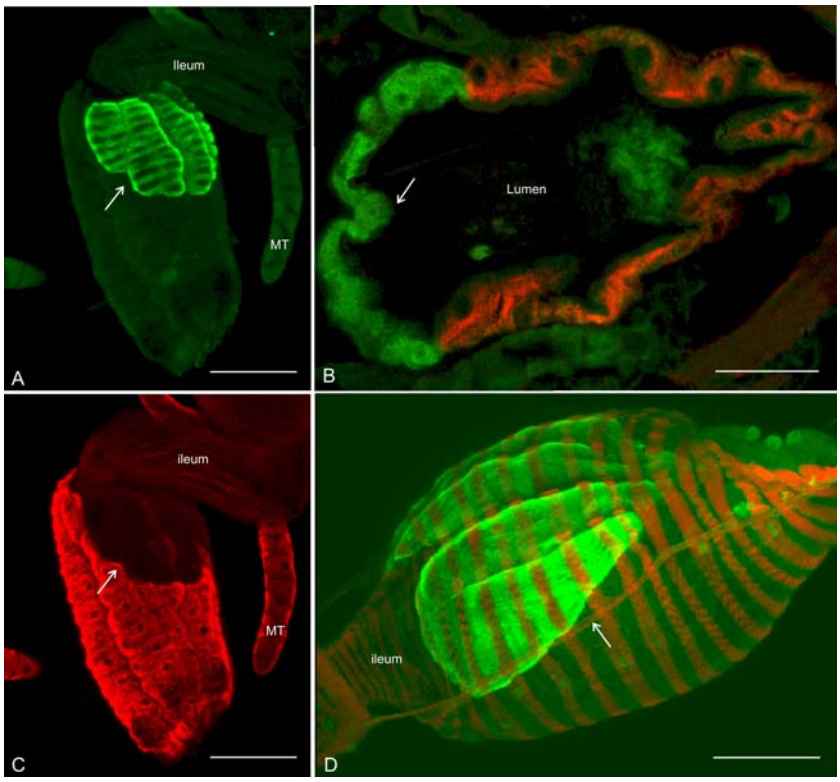

Figure 3-10. AgCA9 and Na^+K^+-ATPase distribution in *An. gambiae* recta. A, C, D) AgCA9 protein distribution in whole mount larvae and B) longitudinal paraffin sections of larvae. The Figure 3-10 shows laser confocal microscope images of *An. gambiae* larval rectum immuno-stained with chicken antibodies 5340 (green; A, D) and 5563 (green; B), and mouse monoclonal antibodies against Na^+K^+-ATPase (red; B, C). The ileum is indicated at the anterior end of the rectum (A, C, D). AgCA9 protein localized to the DAR cells exclusively (A, B, D arrow). The banding pattern seen in the DAR cells of whole mounts of the rectum is due to the circumferential muscles of the rectum. This is better seen in (D) which shows muscle stained with TRITC-Phalloidin (red). Na^+K^+-ATPase localized to the non-DAR cells (B, C). DAR cells are indicated with an arrow in each image. Scale bars: 150 μm (A, C); 75 μm (B, D).

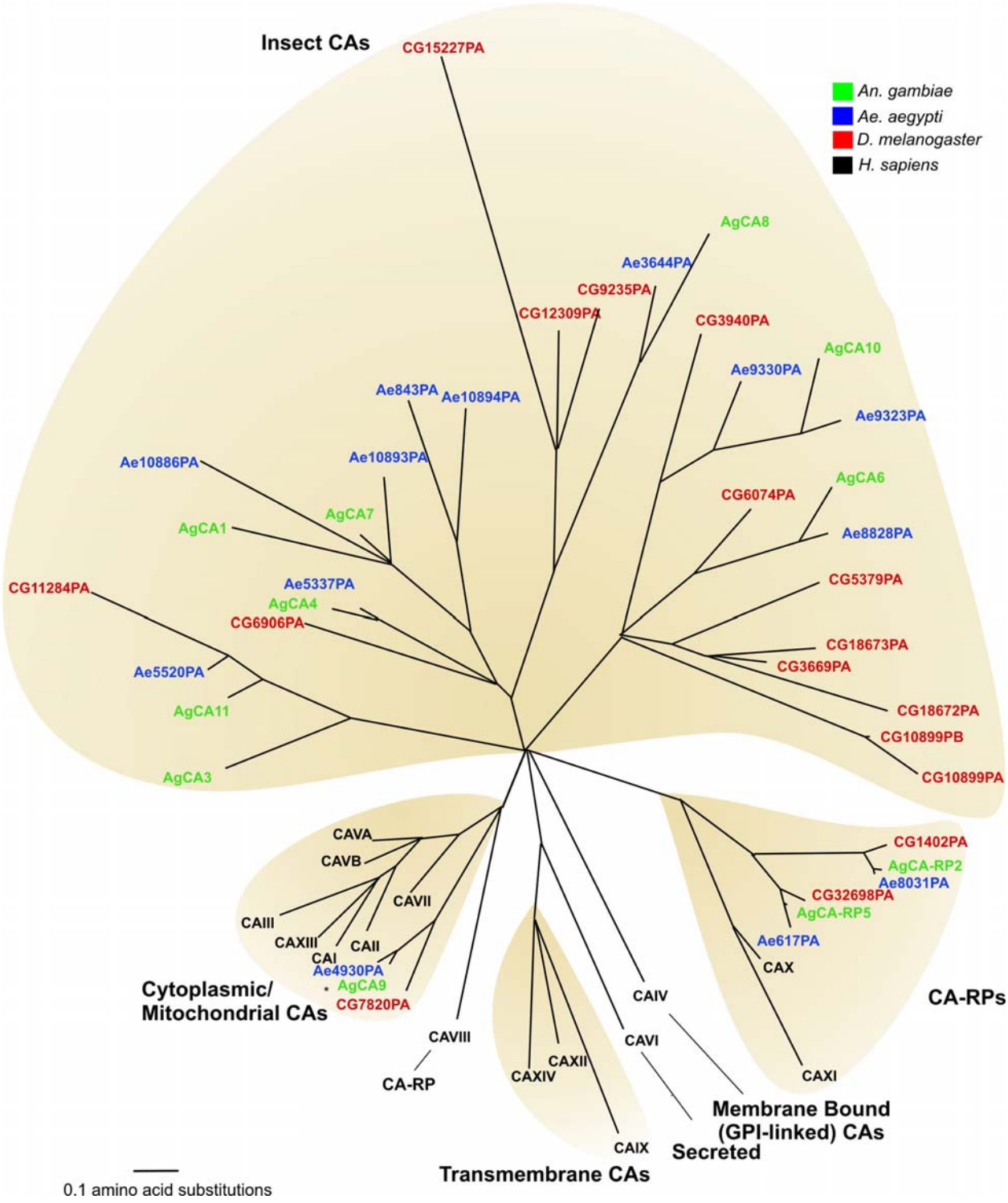

Figure 3-11. Phylogenetic analysis of members of the α-CA family in *H. sapiens* (black), *D. melanogaster* (red), *Ae. aegypti* (blue), and *An. gambiae* (green) genomes. Phylogeny was prepared using MrBayes with the JTT amino acid substitution model and 1.5 million iterations. Interestingly, AgCA9 (starred) and its *Drosophila* and *Aedes*

orthologs were the sole insect CA that clusters with human CAs, indicating that it most closely resembles the primal CA from which other CAs branched.

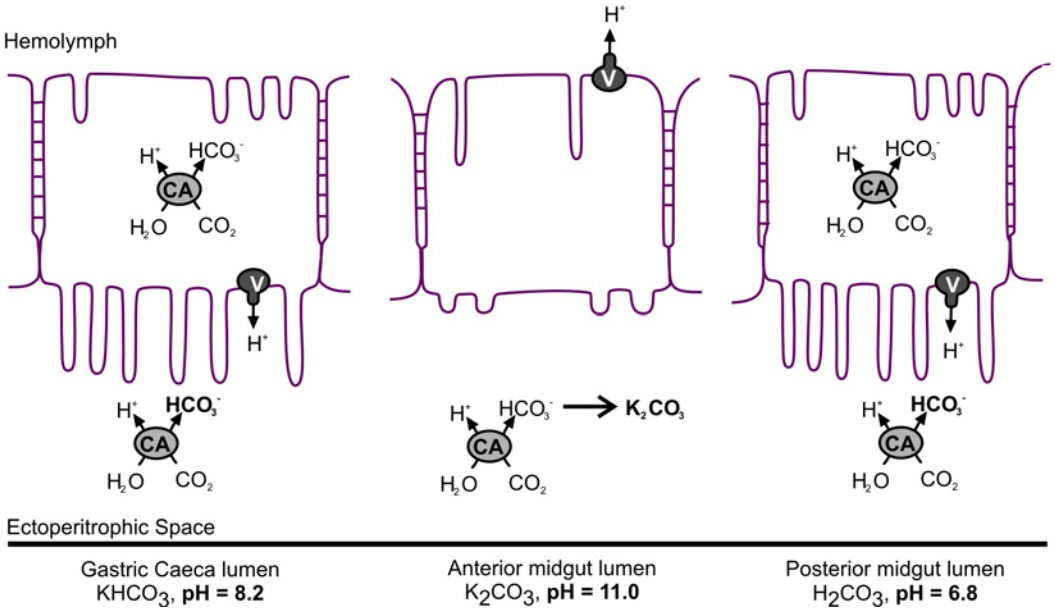

Figure 3-12. Simplified model for the role of CA in larval alimentary canal pH regulation. Metabolic CO_2 can be converted to H^+ and HCO_3^- either intracellularly, for use in ion transport processes, or extracellularly, by diffusing into the lumen. Whereas the gastric caeca and posterior midgut express an apical V-ATPase, translocating protons into the lumen, the anterior midgut expresses a basal V-ATPase, vectorally translocating protons out of the lumen. This results in the formation of luminal CO_3^{2-}. HCO_3^- and CO_3^{2-} in the lumen can buffer the highly alkaline anterior midgut and the more neutral gastric caecae and posterior midguts, respectively.

CHAPTER 4
SILENCING OF AGCA9 IN AN *AN. GAMBIAE* LARVAL CELL LINE, AG55

Introduction

Mosquito larvae can generate a highly alkaline pH (~10.5) in a restricted area of their alimentary canal (the AMG) (Dadd, 1975), despite the absence of morphological barriers between the AMG and adjacent, more neutral, regions of the alimentary canal. The alkaline environment is thought to aid in digestion and is crucial for larval survival (Corena et al., 2004). However, little is known about the mechanisms responsible for the generation and maintenance of the pH gradient. If well understood, these mechanisms could be exploited for the discovery of novel targets for new and improved larvacides.

One group of proteins with a role in AMG alkalization is the CA family (Boudko et al., 2001a; Corena et al., 2002). There are a predicted twelve genes belonging to the *An. gambiae* CA family (www.ensembl.org, February 2007 release), six of which have been cloned by members of the Linser laboratory (see Table 3-1 for accession numbers). The enzymes catalyze the conversion of H_2O and CO_2 to H^+ and HCO_3^- and can generate HCO_3^- within alimentary canal epithelial cells. Larvae are thought to actively excrete HCO_3^-, resulting in a net alkalization of their surrounding media (Stobbart, 1971). Moreover, addition of the global CA inhibitor, methazolamide, inhibits this alkalization (Corena et al., 2002). These data implicate CA as a driving force for AMG alkalization. HCO_3^- generated by CA can be deprotonated to CO_3^{2-} which has a pKa in excess of 10.0. Together with a strong cation such as a K^+ or Na^+, CO_3^{2-} could serve as a buffer in the AMG lumen.

The Linser research group has demonstrated the presence of CA within the epithelial cells of the mosquito larval alimentary canal (in both *An. gambiae* and *Ae. aegypti*) using various

methods. We have detected numerous CA mRNA transcripts using qPCR (Seron et al., 2004; Smith, K. E. et al., 2007; K. E. Smith, unpublished data), microarray analysis (Neira et al., 2008), and *in situ* hybridization (Corena et al., 2002; Seron et al., 2004; Smith, K. E. et al., 2007). We have shown the presence of CA proteins using immunohistochemistry (Seron et al., 2004; Smith, K. E. et al., 2007), and demonstrated CA protein activity in various mosquito species (Corena et al, 2002; Corena et al, 2004; K. E. Smith, unpublished data). In addition, we established that CA is a necessary enzyme for larval mosquito alimentary canal alkalization and survival (Corena et al, 2004).

Although we have shown the CA family to be crucial for AMG alkalization, the specific roles of each member are unknown. A first step in determining if any one CA or combination of CAs is responsible for pH regulation is to silence them either individually or in concert. RNA interference (RNAi) is a powerful tool to manipulate mRNA levels in many organisms. This technique has recently been adapted for use in adult mosquitoes (Blandin et al., 2002) but is not well established for mosquito larvae. Therefore, I seek to first demonstrate the silencing of a CA in an *An. gambiae* larval cell line, Ag55, prior to attempting RNAi in live larvae. Here I report the mRNA silencing of an abundant alimentary canal CA, AgCA9 (GenBank accession # DQ518576), in Ag55 cells and the resulting down-regulation of the protein product.

Results

AgAGO2 in Ag55

One protein crucial for the RNAi pathway is argonaut, and the presence of this gene has been used to indicate active RNAi machinery (Hoa et al., 2003; Keene et al., 2004). To verify that argonaut was expressed in Ag55 cells, I performed PCR using Ag55 cDNA as a template and primers specific to a 646 basepair region of AgAGO2, the *An. gambiae* argonaute 2 gene (Table 2-3). The cDNA product (Figure 4-1A, arrow) showed 100% sequence identity to the

AgAGO2 sequence, indicating that argonaut was present in the Ag55 cell line and that this cell line would be appropriate for RNAi experiments.

CA Isoforms in Ag55 Cells

To determine which CA genes were expressed in the Ag55 cell line, I used primers to the twelve CA sequences (11 α–CAs and one β–CA; Table 2-3) in individual PCR reactions. Primers were designed to amplify either the full length mRNA, in the case of those fully cloned and sequenced genes, or a portion of the mRNA predicted by the *An. gambiae* genome (www.ensembl.org). I determined the expression of CA genes in the Ag55 cell line as well as in whole larvae cDNA (Figure 4-1B). Whole larvae cDNA was used as a control to ensure that the primers detected the CA against which they were designed. I detected all but AgCA1 and AgCA7 in the whole larvae controls using the primers indicated. In the Ag55 cells, I found only AgCA3, AgCA9 and AgCAb. AgCA9 is abundant in the alimentary canal and thought to have a role in pH regulation (Smith, K. E. et al., 2007); therefore I chose to test if this CA could be silenced in an *An. gambiae* cell line using RNAi.

AgCA9 mRNA Silencing

Ag55 cells were treated with either full length AgCA9 double-stranded (ds) RNA or GFP dsRNA (negative control). A second negative control group was exposed to the same conditions as the other two groups, but received no dsRNA. RNA was isolated from cells 24, 48, 72, or 96 hours after treatment and reverse transcribed into cDNA for use in qPCR assays to measure the expression of endogenous AgCA9 mRNA in each sample. Primers used to detect AgCA9 were gene specific and designed against the 3' UTR to eliminate detection of exogenous RNA (dsRNA which was added to each culture). Three biological replicates of this experiment were performed and each resulted in a consistent knock-down of AgCA9 mRNA in the AgCA9 dsRNA treated cells compared to the GFP dsRNA or untreated cells. Statistically significant

down regulation (P-Value < 0.05) of AgCA9 mRNA was seen after 24 hours and persisted throughout 96 hours, resulting in a down regulation of 88% after 96 hours (Figure 4-2A).

In addition to qPCR, a Northern blot was performed using RNA extracted from untreated cells, or those treated with AgCA9 dsRNA or GFP dsRNA for 48, 72, or 96 hours (Figure 4-2B). An equal amount of RNA was loaded for all treatment groups within a time point, but differed between the four time points. AgCA9 mRNA was detected using a full length radioactive P^{32} RNA probe. The Northern blot showed a distinct AgCA9 mRNA band at the approximate expected size (~ 1.5 kb with untranslated regions) in the control lanes (Figure 4-2B, lanes 2 and 3 at each time point, arrow) which is absent in the lanes corresponding to cells treated with AgCA9 dsRNA (lane 1 at each time point). Furthermore, siRNAs and cleaved endogenous AgCA9 mRNA were visible as a lower molecular weight smear in the AgCA9 dsRNA treated lanes (Figure 4-2B, arrowheads).

AgCA9 Protein Down-Regulation

Antibody specificity: The antibody 5340 recognized AgCA9 on a western blot at the predicted molecular weight of 31.5 kDa as well as a second protein of a slightly higher molecular weight (Smith, K. E. et al., 2007). When antibody was incubated with the peptide antigen, neither band was recognized (Figure 4-3A).

Western blot analysis: A Western blot was used to determine the presence of AgCA9 protein in untreated Ag55 cells or those treated with AgCA9 dsRNA or GFP dsRNA for 24, 48, 72, or 96 hours (Figure 4-3B). The presence of a second protein which cross-reacted with the antibody was used as a loading control; this protein was distinguishable from AgCA9 by its slightly higher molecular weight. The antibody 5340 recognized AgCA9 at the expected molecular weight of 31.5 kDa in all control lanes (Figure 4-3B, lanes 2 and 3 at each time point).

However, AgCA9 protein levels in cells treated with AgCA9 dsRNA were considerably reduced (90% after 96 hours) compared to the control samples (Figure 4-3B lane 1 at each time point).

Discussion

I used an *An. gambiae* larval cell line, Ag55, in which to silence AgCA9, a cytoplasmic CA cloned by members of the Linser laboratory and thought to have a role in pH regulation (Smith, K. E. et al., 2007). CA is an important component of larval alimentary canal alkalization and a crucial enzyme for larval survival. Numerous CA genes have been cloned and characterized to some extent by the Linser laboratory but we have yet to determine the specific functions of each member of the CA family in the alkalization process. The first step in uncovering the roles of each CA is to demonstrate that the mRNA can be stably silenced and that this silencing leads to a robust down-regulation of the corresponding protein.

The Ag55 cell line is an *An. gambiae* neonatal 1st instar larval cell line which others have used for successful RNAi silencing (Konet et al., 2007). Additionally, I verified that AgAGO2, an important gene in the RNAi pathway, is expressed in this cell line. To determine which CA to silence, I identified those CA genes which were expressed in the Ag55 cell line. Because the cells were derived from first-instar larvae, I did not expect them to express the same complement of CA genes as fourth-instar larvae, the cDNA of which I used as a control. However, I was able to detect three CAs, AgCA3, AgCA9 and AgCAb in Ag55 cDNA. I chose to silence AgCA9; it is a good candidate for having a role in alimentary canal alkalization due to its abundant protein expression in the GC and ectoperitrophic space (Smith, K. E. et al., 2007). Additionally, AgCA9 was abundant in the Ag55 cell line, and therefore likely to have an important role in pH regulation. I was not able to detect two of the twelve CAs, AgCA1 and AgCA7 in the control template (whole fourth-instar larvae cDNA). Either the predicted sequences were incorrect and

the primers did not anneal to the mRNA, or the CAs were expressed at a level too low to detect using my methods.

The literature suggests that RNAi silencing can occur in as little as 24 hours (Blitzer et al., 2005) and last up to at least ten days (Keene et al., 2004). I followed the expression of AgCA9 mRNA and protein daily from 24 to 96 hours due to the space constraint of the 6 well plates; after 96 hours, the cells began to overgrow and die. At each time point, I measured the relative abundance of AgCA9 mRNA and protein in each sample using qPCR and Northern and Western blots. Both qPCR and Northern blot indicated that cells treated with AgCA9 dsRNA expressed considerably less endogenous AgCA9 mRNA than those treated with GFP dsRNA or those that were untreated. Likewise, the Western blot showed that AgCA9 protein levels diminished in those cells treated with AgCA9 dsRNA. Similar to the cited literature, I found that this response was detectible within 24 hours of treatment and persisted throughout the 96 hours surveyed. These data demonstrate that dsRNA can be used to silence AgCA9 mRNA, as well as down-regulate the protein product, in the larval *An. gambiae* cell line, Ag55 cells.

When using RNAi to investigate protein function, the half-life of the protein must be considered. If the protein is stable, with a half-life that exceeds the length of the experiment, protein levels will remain unchanged even if mRNA expression is decreased. These results indicate that AgCA9 is a protein capable of being manipulated by RNAi and suggests that this technique can be used to silence a CA in live mosquito larvae. By down-regulating CA protein in live larvae, pH changes can be assessed and relative contributions of each CA to AMG pH regulation can be determined.

There are several methods by which RNAi has been used to knock down genes in adult mosquitoes: direct injection of dsRNA (Roy et al., 2007; Hansen et al., 2007; Boisson et al.,

2006), introduction of a transgene which produces the RNA of interest in a hairpin form (Franz et al., 2006), or infection with a virus that produces the dsRNA of interest (Adelman et al., 2001). To date there are only two reports of successful RNAi in mosquito larvae, one in *Ae. aegypti* using injection of small interfering RNAs (siRNAs) (Blitzer et al., 2005) and one using transgenic *An. stephensi* larvae (Brown et al., 2003). My Ag55 cell line studies suggest that AgCA9 silencing in *An. gambiae* larvae is possible. Further work in live *An. gambiae* larvae will yield a greater understanding of this important family of genes in the crucial process of pH regulation.

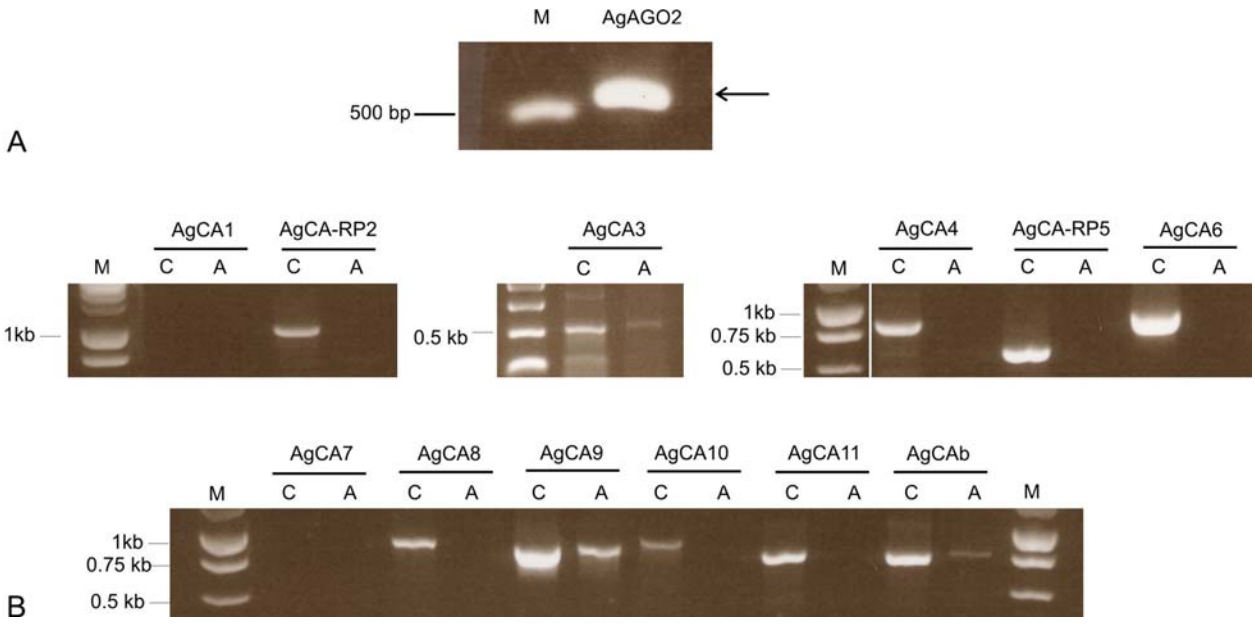

Figure 4-1. RT-PCR analysis of the expression of *An. gambiae* argonaut AgAGO2 in Ag55 cells and each of the eleven *An. gambiae* α–CAs (AgCA1-11) and one β–CA (AgCAb) in Ag55 cells and whole *An. gambiae* larvae. A) Specific primers were used to detect a 646 bp portion of the AgAGO2 gene in Ag55 cells. B) Ag55 cDNA was used in a PCR reaction with primers specific to either the whole CA transcript or the partial predicted sequence. Whole *An. gambiae* fourth-instar larvae cDNA was used as a primer control (shown by a "C" above the lane) in addition to the Ag55 experimental template (indicated by a "A" above the lane). See Table 2-3 for primer sequences and expected length of products. M: 1 kb DNA ladder® (invitrogen).

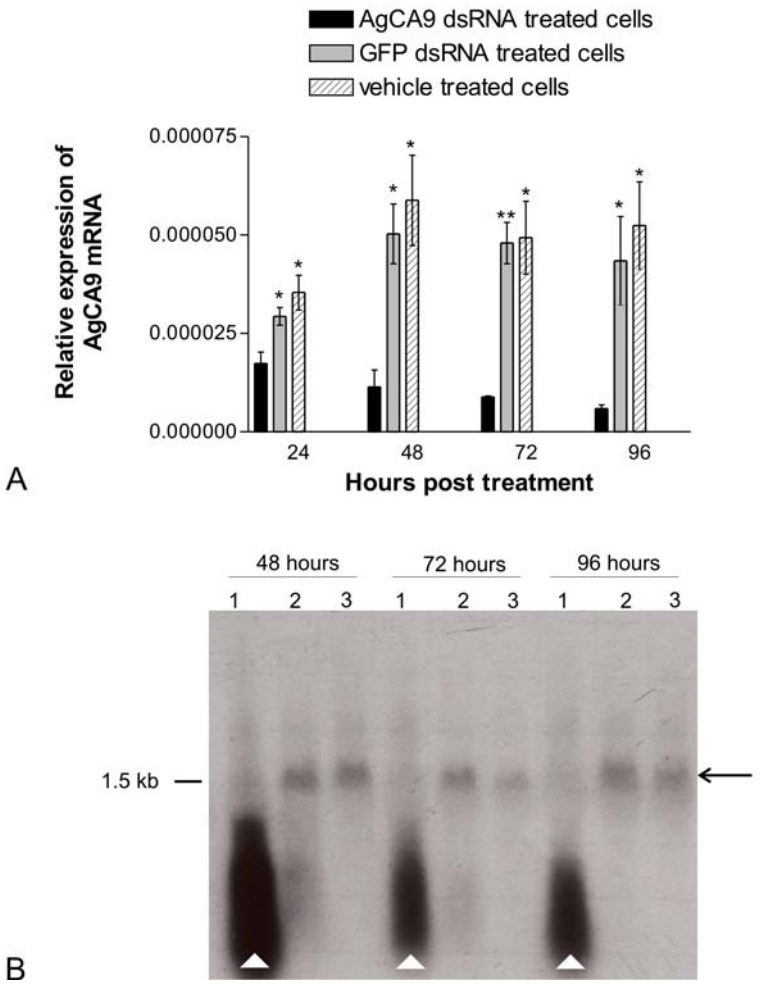

Figure 4-2. Analyses of AgCA9 mRNA expression in untreated Ag55 cells or those treated with AgCA9 or GFP dsRNA. AgCA9 mRNA was measured at 24, 48, 72, or 96 hours post-treatment using A) qPCR and at 48, 72, or 96 hours post-treatment using B) a northern blot. For the northern blot, a consistent amount of RNA was run for each sample from each time point: 48 hours (10 µg), 72 hours (6.3 µg), and 96 hours (8.0 µg). Lanes 1: cells treated with AgCA9 dsRNA; lanes 2: cells treated with GFP dsRNA; lanes 3: untreated cells. Arrow: AgCA9; arrowheads: degraded endogenous mRNA and siRNAs. *: P-Value < 0.05, **: P-Value < 0.005.

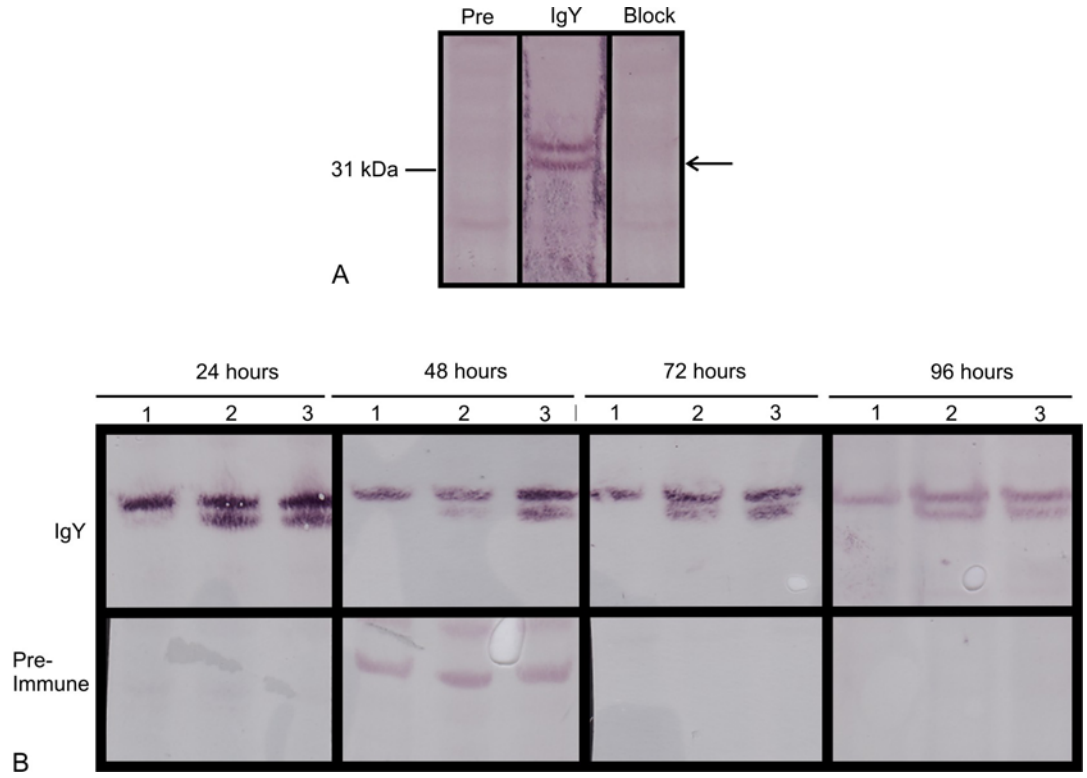

Figure 4-3. Detection of AgCA9 protein in untreated Ag55 cells or those treated with AgCA9 or GFP dsRNA. A) a blocking assay was used to verify antibody 5340 specificity. Equal amounts of whole *An. gambiae* fourth-instar protein were run in each lane. Lane 1 (pre): pre-immune IgY at a 1:1000 dilution. Lane 2 (IgY): immune IgY at a 1:1000 dilution. Lane 3 (block): immune IgY at a 1:1000 dilution blocked with peptide. AgCA9 is indicated with an arrow. The upper band represents a second protein specifically recognized by the antibody. B) a western blot was performed using protein from Ag55 cells which had been treated with either AgCA9 dsRNA (lanes 1), GFP dsRNA (lanes 2), or left untreated (lanes 3) for 24, 48, 72, or 96 hours. AgCA9 protein was detected using a 1:1000 dilution of antibody 5340. AgCA9 is indicated with an arrow.

CHAPTER 5
CHARACTERIZATION OF THE DAR AND NON-DAR CELL OF ANOPHELINE RECTA: PROTEIN LOCALIZATION

Chapters 3 and 4 have focused on larval pH regulation and the role of the CA family on this important process. I will focus Chapters 5 and 6 on another biological system which is important for larval adaptation and survival, ion regulation.

Introduction

Larval mosquitoes live in aquatic habitats that have the propensity to change drastically in both salinity and ionic composition. To survive in such dynamic environments, larvae must regulate their hemolymph osmolarity (~ 300 mosmol l^{-1}) accordingly. In freshwater, larvae tend to gain water by osmosis and lose salts by diffusion. In saline water, larvae tend to lose water to their environment and gain salts (Clements, 1992). In fresh or dilute water, all larvae hyper-regulate their hemolymph osmolarity by resorbing ions and nutrients to produce a dilute urine. By contrast, larvae in saline water respond in one of three ways, depending on the species: obligate freshwater species are restricted to waters that are iso- or hypo-osmotic to their hemolymph and cannot survive in higher osmolarities; saline-tolerant osmoregulators regulate their osmotic and ion concentrations by secreting a hyper-osmotic urine to maintain a hemolymph osmolarity of approximately 350 mosmol l^{-1} over a species-specific range of external osmolarities (Bradley, 1994); and saline-tolerant osmoconformers increase hemolymph osmolarity with increasing external osmolarity (in water exceeding 300 mosmol l^{-1}) by producing organic compounds such as proline and trehalose and accumulating them as non-toxic osmolytes in the hemolymph (Bradley, 1994). As saline-tolerant osmoconforming larvae use an osmoregulatory strategy which differs from the majority of saline-tolerant species (Bradley, 1987b), they will not be considered in the present study.

A key organ responsible for ion regulation in larval mosquitoes is the rectum. As larvae depend on ion regulation for survival, the recta of several culicine genera (including *Aedes* and *Culex*) have been studied in detail. Saline-tolerant osmoregulating culicine species have a structurally distinct rectum compared to freshwater species (Meredith and Phillips, 1973). The recta of freshwater culicines are structurally uniform and selectively resorb ions, water and nutrients from the primary urine produced by the MTs. Conversely, the recta of saline-tolerant culicines are structurally divided into distinct anterior and posterior regions. The structure and function of the anterior rectum (AR) is similar to the recta of freshwater culicines, whereas the function of the posterior rectum (PR) is to secrete a hyper-osmotic urine when larvae inhabit saline water (Meredith and Phillips, 1973; Bradley and Phillips, 1977). The idea that the larval recta of freshwater and saline-tolerant larvae are distinct in structure and function is supported by data from various culicine species (Ramsay, 1950; Asakura, 1970; Bradley and Phillips, 1975, Bradley and Phillips, 1977). To my knowledge previous work on the mosquito larval rectum was restricted to the culicine subfamily, with little data published describing the recta of anophelines.

I recently discovered a subset of cells on the dorsal anterior rectum (DAR cells) of a freshwater anopheline, *An. gambiae*, which were distinct from the rest of the rectum (non-DAR cells) with respect to localization of carbonic anhydrase (AgCA9, Smith, K. E. et al., 2007; Smith et al., 2008), V-ATPase, and Na^+K^+-ATPase (Okech et al., 2008; Smith et al., 2008). I observed similar protein localization patterns in both freshwater and saline tolerant anophelines (Smith et al., 2008). This unique type of two-part rectum was originally detected in the saline-tolerant *Anopheles salbaii* by light microscopy (Bradley, 1987a; Bradley, 1994). These data led

me to hypothesize that anopheline larvae are distinct from culicine larvae in rectal structure and ultimately in methods of ion regulation.

V-ATPase and Na^+K^+-ATPase are well known membrane energizers important for ion regulation (e. g. Wieczorek, 1992; Skou, 1990) and recent work has established the presence of one or both of these proteins in the recta of culicines (Patrick et al., 2006; Smith et al., 2008) and anophelines (Okech et al., 2008; Smith et al., 2008). Additionally, CA plays a major role in HCO_3^- secretion in the larval rectum (Strange and Phillips, 1984; Corena et al., 2002) and a specific CA isoform, CA9, localizes to the DAR cells of all anophelines examined to date including *An. gambiae*, *Anopheles albimanus*, *Anopheles farauti*, *Anopheles quadrimaculatus*, *Anopheles aquasalis*, and *Anopheles stephensi* (Smith et al., 2008), making it an excellent marker for these cells.

In the present study, I compare the distribution of three ion-regulatory proteins (CA9, Na^+K^+-ATPase, and V-ATPase) in the recta of a freshwater culicine *Aedes aegypti*, a freshwater anopheline *An. gambiae*, a saline-tolerant culcine *Ochlerotatus taeniorhynchus*, and a saline-tolerant anopheline *An. albimanus* reared in fresh water and saline water. Additionally, I determine protein distribution in larvae either reared in freshwater and exposed to saline water, or reared in saline water and exposed to freshwater, for 24, 48, and 72 hours to determine the effects of short term exposure to either of these conditions. From these analyses, I conclude that anophelines differ from culicines in larval rectal structure as well as in the regulation of protein expression. Additionally, I suggest putative functions for the DAR and non-DAR cells of anopheline larvae under both freshwater and saline water conditions.

Results

I compared the distribution of three proteins with known roles in ion regulation in the larval rectum: a specific carbonic anhydrase (CA9, Smith, K. E. et al., 2007), Na^+/K^+-ATPase,

and V-ATPase. The proteins were localized in longitudinal paraffin sections of recta from freshwater and saline-tolerant anophelines and culicines reared in varying osmotic conditions; these conditions included both fresh water and specific dilutions of ASW. The dilutions used were based on the published upper tolerance limit of each species (Bailey et al., 1981; Mosha and Subra, 1983; Mullenbach et al., 2004). I compared the freshwater mosquito species *Ae. aegypti* (culicine) and *An. gambiae* (anopheline), with the saline-tolerant mosquito species *Oc. taeniorhynchus* (culicine) and *An. albimanus* (anopheline). Additionally, I evaluated the change in Na^+/K^+-ATPase distribution in *An. gambiae*, *Oc. taeniorhynchus*, and *An. albimanus* as a ratio of Na^+/K^+-ATPase labeling intensity between the two rectal cell types in each species (either DAR cells versus non-DAR cells or AR versus PR).

The ultrastructure of both freshwater and saline-tolerant culicines is characterized by highly infolded apical lamellae and extensive basal infoldings (Meredith and Phillips, 1973). Preliminary electron micrographs indicate that the membranes of the DAR and non-DAR cells of anophelines reared in fresh water are folded in a similar way. For the present study, the cells of all recta examined are therefore assumed to possess apical lamellae and basal infoldings.

Anopheline Rectal Structure

The immunolocalization patterns of CA9 and Na^+/K^+-ATPase were used to identify anopheline DAR and non-DAR cells, respectively, in larvae reared in fresh water. No obvious differences in protein distribution were observed between the recta of freshwater anophelines (*An. gambiae, An. stephensi* and *An. quadrimaculatus*) and saline-tolerant anophelines (*An. albimanus*, *An. farauti* and *An. aquasalis*). In all larvae, CA9 localized to DAR cells and Na^+/K^+-ATPase localized to non-DAR cells (i.e. Figures 5-1B, 5-1J, 5-2B, 5-2D, and 5-4C) as described for *An. gambiae* (Smith, K. E. et al., 2007). This similarity suggests that all anopheline larvae, regardless of saline-tolerance, have DAR and non-DAR cells.

***Ae. aegypti*: Obligate Freshwater Culicine**

Ae. aegypti developed to fourth-instar in concentrations of ASW up to a maximum of 40% (~ 350 mosmol l^{-1}). After seven days post-hatch, 53% of larvae survived in 40% ASW, 82% survived in 30% ASW, and 63% survived in fresh water. Protein localization did not differ between larvae reared in freshwater versus 40% ASW: Na^+/K^+-ATPase was present on the extensive basal infoldings, whereas V-ATPase localized to the apical lamellae (Figure 5-1A). CA9 was not detectible in the non-segmented rectum of *Ae. aegypti* (Figure 5-2A).

***An. gambiae*: Obligate Freshwater Anopheline**

An. gambiae developed to fourth-instar in ASW concentrations up to 40% but could not survive in higher salinities. After six days post-hatch 16% of larvae survived 40% ASW, but were developing much slower than those in lower salinities, 87% survived in 30% ASW, and 74% survived in freshwater. However, the larvae could be acclimated from freshwater to higher ASW concentrations by slowly increasing the ASW concentration by 10% ASW each day (up to 60% ASW for a maximum of 24 hours).

The distribution of Na^+/K^+-ATPase, V-ATPase, and CA9 in *An. gambiae* reared in freshwater has been described previously (Smith, K. E. et al., 2007; Rheault et al., 2007; Okech et al., 2008). Na^+/K^+-ATPase is restricted to the basal infoldings of the non-DAR cells (Figures 5-1B, 5-2B) whereas CA9 protein is restricted to the cytoplasm of the DAR cells (Figure 5-2B). V-ATPase localizes to the apical lamellae of the non-DAR cells, and appears to be cytoplasmic in the DAR cells (Figure 5-1B). The distribution pattern of all three proteins was identical in another obligate freshwater anopheline species, *An. stephensi*, when reared in freshwater (results not shown).

Distribution patterns of the three proteins did not change in *An. gambiae* larvae reared in 10% or 20% ASW. However, the distribution of Na^+/K^+-ATPase and V-ATPase showed subtle

changes in the recta of larvae reared in 30% ASW, or acclimated to 60% ASW, compared with the recta of larvae reared in freshwater. Na^+/K^+-ATPase shifted from being undetectable in the DAR cells (Figure 5-1B) to being detectible on the basal infoldings of both DAR and non-DAR cells (Figure 5-1C). This change can be seen graphically in Figure 5-1D. When reared in freshwater, the DAR cells have significantly less Na^+/K^+-ATPase peak pixel intensity than the non-DAR cells. When acclimated to 60% ASW, there is no significant Na^+/K^+-ATPase difference between the DAR and non-DAR cells. In many larvae, this signal appeared reduced compared with that of those reared in freshwater. Additionally, V-ATPase appeared to localize to the cytoplasm of the non-DAR cells in addition to the apical lamellae (Figure 5-1C). Distribution of V-ATPase and CA9 in the DAR cells did not change.

***Oc. taeniorhynchus*: Saline-Tolerant Culicine**

The rectum of *Oc. taeniorhynchus* is composed of regionalized anterior (AR) and posterior (PR) segments in contrast to DAR and non-DAR cells, and protein localization in these regions did not appear to change drastically between larvae reared in freshwater and those reared in 100% ASW. In both cases Na^+/K^+-ATPase and CA9 localized to the AR, Na^+/K^+-ATPase localized to the basal infoldings (Figures 5-1F, G, 5-2C) and CA9 localized to the cytoplasm (5-2C). The consistency of Na^+/K^+-ATPase distribution can be seen graphically in Figure 5-1H. There is significantly more Na^+/K^+-ATPase in the AR than the PR when reared in both freshwater and 100% ASW, with no significant differences in Na^+/K^+-ATPase between the two rearing conditions. Conversely, V-ATPase localized mainly to the apical lamellae of the PR, and appeared absent from the AR (Figures 5-1F, G). However, many larvae reared in freshwater, but not 100% ASW, exhibited a low level of V-ATPase on the apical lamellae of the AR (Figure 5-1E asterisks). In all cases this signal was less intense than that in the PR.

***An. albimanus*: Saline-Tolerant Anopheline**

Protein distribution in the recta of *An. albimanus* was identical to that in *An. gambiae* when larvae were reared in freshwater: Na^+/K^+-ATPase appeared to be restricted to the basal infoldings of the non-DAR cells (Figures 5-1J, J inset, 5-2D); CA9 protein was evident only in the cytoplasm of the DAR cells (Fig 5-2D); V-ATPase localized to the apical infoldings of the non-DAR cells and the cytoplasm of the DAR cells (Figure 5-1J). This apparent cytoplasmic localization is better seen at a higher magnification in Figure 5-1I. The localization pattern of all three proteins was identical in another saline-tolerant anopheline species, *An. farauti*, when reared in freshwater (results not shown).

The distributions of CA9 and V-ATPase proteins appeared unchanged in larvae reared in 50% ASW compared with those reared in freshwater, but Na^+/K^+-ATPase underwent a dramatic shift and appeared to localize mainly to the basal infoldings of the DAR cells (Figure 5-1K and K inset), presenting a drastic increase of this protein in the DAR cells and a contrasting reduction in the non-DAR cells (compare Figures 5-1J inset and 5-1K inset). The change in Na^+/K^+-ATPase distribution is shown graphically in Figure 5-1L. When reared in freshwater, Na^+/K^+-ATPase peak pixel intensity was significantly greater in the non-DAR cells whereas when reared in 50% ASW, it was significantly greater in the DAR cells.

To determine if the Na^+/K^+-ATPase protein shift is a reversible event, larvae were reared in either freshwater or 25% ASW to second-, third-, or fourth-instar and were transferred to 25% ASW or freshwater, respectively for 24, 48 or 72 hours. For each image in Figure 5-3, the data are presented graphically as the ratio of Na^+/K^+-ATPase peak pixel intensity in the DAR cells versus the non-DAR cells (Figure 5-3H). Lowercase bar labels in Figure 5-3H correspond to the experimental group indicated by the uppercase letters (i.e. Figure 5-3A corresponds to bar "a" in Figure 5-3H). When larvae were reared in freshwater and exposed briefly (for 24 to 48 hours) to

25% ASW, the ability for larvae to shift rectal Na^+/K^+-ATPase distribution depended on the larval stage at which the exposure occurred. If exposed to ASW during the second- or third-instar stages, a change in Na^+/K^+-ATPase peak signal intensity from the non-DAR cells to the DAR cells was evident within 24 hours (Figure 5-3A, B, H bars a, b). Fourth-instar larvae exposed only for 24 hours expressed Na^+/K^+-ATPase in both DAR and non-DAR cells, as if in an intermediate stage (Figure 5-3C, H bar c). However, a change in Na^+/K^+-ATPase localization from the non-DAR cells to DAR cells was evident after 48 hours (Figure 5-3D, H bar d). In most cases, Na^+/K^+-ATPase shift was most dramatic in larvae exposed during the second larval stage. Most third- and fourth-instar larvae retained some Na^+/K^+-ATPase signal in the non-DAR after exposure to 25% ASW.

Slightly different results were found for larvae reared in 25% ASW and exposed to freshwater (for 24 to 72 hours). While second-instar larvae shifted Na^+/K^+-ATPase localization from DAR to non-DAR cells within 24 hours (Figure 5-3E, H bar e), third-instar (Figure 5-3F, H bar f) and fourth-instar (Figure 5-3G, H bar g) larvae did not fully shift Na^+/K^+-ATPase localization after 72 hours or 48 hours, respectively, and expressed the protein in both DAR and non-DAR cells. Although fourth-instar larvae exhibited very little difference in pixel intensity between the DAR and non-DAR cells after 48 hours, this difference was statistically significant.

CA Isoforms in the Anopheline Rectum

To determine if CA9 is the sole CA expressed in the rectum, the CA profile of the *An. gambiae* rectum was determined. Primers to the 12 CA sequences (11 α–CAs and one β–CA; Table 2-3) were used in individual PCR reactions. Primers were designed to amplify either the full length mRNA, in the case of those fully cloned and sequenced genes, or a portion of the mRNA predicted by the *An. gambiae* genome (www.ensembl.org). The expression of CA genes in *An. gambiae* rectal tissue was determined as well as expression of those in whole larvae

cDNA (Figure 5-4). Whole larvae cDNA was used as a control to ensure that the primers detected the CA against which they were designed. All CAs but AgCA1 and AgCA7 were detected in the whole larvae controls using the primers indicated. In the rectal tissue, AgCA3, AgCA6, AgCA9 and AgCAb were detected.

Discussion

Ion regulation by the rectum helps mosquito larvae to survive, and adapt to, a constantly changing environment. A wealth of literature has focused on the structure and function of the larval culicine rectum and the distinction between its role in freshwater and saline-tolerant species (e. g. Wigglesworth, 1972; Meredith and Phillips, 1973). However, the discovery that the anopheline rectum is structurally distinct from any culicine species described (Bradley, 1987a; Bradley, 1994; Smith, K. E. et al., 2007) suggested that anophelines may utilize a unique method of ion regulation. To test this hypothesis, I compared the localization patterns of three proteins involved in ion regulation (CA9, Na^+/K^+-ATPase, and V-ATPase) in the recta of anopheline and culicine larvae (including freshwater larvae and saline-tolerant larvae) reared in fresh versus saline water.

Three key points regarding the comparison of anopheline and culicine recta emerge from these data: (1) In contrast to obligate freshwater and saline-tolerant culicines which have structurally distinct recta, all anophelines examined (regardless of saline-tolerance) possess a similarly structured rectum, consisting of DAR and non-DAR cells (Figure 5-5). (2) Anopheline larvae undergo a dramatic shift in rectal Na^+/K^+-ATPase localization when reared in freshwater versus saline water. This shift is not seen in any culicine larvae examined. (3) With the exception of *Ae. aegypti*, the freshwater culicine examined, CA9 consistently localized to an anterior region of the rectum in both culicine and anopheline larvae regardless of the salinity of the rearing water. The first two key points, along with the localization patterns of Na^+/K^+-

ATPase and V-ATPase (discussed below), will be used to suggest putative functions for the anopheline rectal regions. Distribution of CA9 will be discussed in a separate section. Figures 5-5 and 5-6 summarize my results; Figure 5-5 illustrates the differences between anopheline and culicine recta and Figure 5-6 summarizes protein distribution in anopheline and culicine recta in a schematic form.

Freshwater–Reared Larvae: V-ATPase and Na^+/K^+-ATPase Localization

When reared in freshwater, the protein localization patterns in *An. gambiae* and *An. albimanus* recta were identical: non-DAR cells contained an apical V-ATPase and basal Na^+/K^+-ATPase whereas the DAR cells were enriched in cytoplasmic V-ATPase. The protein localization pattern of the non-DAR cells in *An. gambiae* and *An. albimanus* was similar to that of the freshwater culicine, *Ae. aegypti*, which also expressed an apical V-ATPase and basal Na^+/K^+-ATPase in its non-segmented rectum. The detection of V-ATPase in *Ae. aegypti* larval rectum confirms the finding of Filippova et al., (1998) but conflicts with the findings of Patrick et al. (2006) who detected V-ATPase mRNA in the rectum, but did not detect protein when using the same antibody against the B subunit which was used in this study. However, ultrastructural studies of the larval *Ae. aegypti* rectum identified a particulate coat on the apical lamellae (Meredith and Phillips, 1973) suggesting the presence of portasomes (Clements, 1992) which correspond to the V_1 portion of the V-ATPase (Harvey, 1992; Radermacher et al., 1999; Zhuang et al., 1999).

Ae. aegypti is a freshwater culicine that can acclimate to 50% ASW by osmoconforming in water hyper-osmotic to their hemolymph (average hemolymph of *Ae. aegypti* reared in freshwater ~ 250 mosmol l^{-1}; Edwards, 1982; Clements, 1992). Larvae possess a non-segmented rectum which selectively resorbs ions from the primary urine. Like *Ae. aegypti*, anophelines reared in freshwater actively resorb ions from the environment via their rectum to maintain

constant ionic and osmotic hemolymph concentrations (Bradley, 1994). The combination of basal Na^+/K^+-ATPase and apical V-ATPase in the rectum is ideally suited for this task. The polarity is similar to that in frog skin (Ehrenfeld and Klein, 1997), in which the V-ATPase hyperpolarizes the apical membrane, driving Na^+ into the cell from the Na^+ deficient environment. The Na^+/K^+-ATPase then transports the Na^+ across the basal membrane into the hemolymph, replenishing ions which are lost to the aquatic environment, as first suggested by Koefoed-Johnsen and Ussing (1958).

One example of V-ATPase mediated Na^+ transport into mosquito cells occurs in the alimentary canal of many species: Na^+ is driven into the cell by the electrical coupling of a V-ATPase and a Na^+: amino acid$^{\pm}$ nutrient amino acid transporter (NAT) (Boudko et al., 2005). Hyperpolarization of the apical membrane by V-ATPase drives electrophoretic Na^+: amino acid symport into the cells. The efflux of H^+ and influx of Na^+ driven by the coupling of these two proteins constitutes a Na^+/H^+ exchanger (NHE), $NHE_{V\text{-}NAT}$ (Okech et al., 2008). In addition to driving Na^+, V-ATPase hyperpolarization of the apical membrane may drive the absorption of numerous other essential ions.

In *Oc. taeniorhynchus* reared in freshwater, a similar synergy between V-ATPase (apical) and Na^+/K^+-ATPase (basal) is evident in the AR, a region that has a resorptive function (Bradley and Phillips, 1977). This finding provides further support that the physiological coupling between these ATPases is involved in resorbing essential ions from the primary urine. Importantly, when *Oc. taeniorhynchus* are reared in 100% ASW, the apical V-ATPase appears to localize to the cytoplasm, breaking the coupling with Na^+/K^+-ATPase, which may indicate that these cells decrease their resorptive function in the presence of high salinity.

The cytoplasmic localization of V-ATPase, a membrane protein, in the DAR cells of both *An. gambiae* and *An. albimanus*, as well as in the AR of saline-reared *Oc. taeniorhynchus* was unexpected, although there are several possible explanations. The rectal ultrastructure of the DAR cells has not been extensively studied, but the AR of saline-tolerant culicines exhibits a highly infolded basal membrane which constitutes the major elaboration of the surface area (Meredith and Phillips, 1973). The apparent cytoplasmic V-ATPase may instead be localizing to these basal infoldings. Alternatively, this localization could represent V-ATPase protein on the membrane of vacuoles within the cells (Harvey, 1992) or subunits that have dissociated from their membrane-bound V_0 anchors. Dissociation of V_1 from V_0 occurs during molting in caterpillars (Sumner et al., 1995) and during glucose deprivation in yeast (Kane and Parra, 2000), and indicates inactivation of the protein.

Saline Water-Reared Larvae: V-ATPase and Na^+/K^+-ATPase Localization

When anopheline larvae were reared in saline water, I observed a shift in Na^+/K^+-ATPase localization to the DAR cells (this protein was not abundant in the DAR cells of freshwater-reared larvae). Whereas in *An. albimanus* this shift was drastic, accompanied by a decrease in Na^+/K^+-ATPase in the non-DAR cells, in *An. gambiae* Na^+/K^+-ATPase was present in both DAR and non-DAR cells, suggesting an intermediate condition. In *An. gambiae* I also noted a marked reduction in the overall Na^+/K^+-ATPase signal as well as a noticeable increase in V-ATPase signal in the cytoplasm of all rectal cells. This may indicate a breakdown in the ion-transporting functions of the cells. As an obligate freshwater larva, *An. gambiae* lacks the ability to secrete a hyperosmotic urine and in fact cannot survive more than 24 hours when acclimated to 60% ASW. It is possible that the stress incurred by exposure to saline water causes a breakdown in the cellular components of the ion-regulatory organs, which would lead to death.

In saline-tolerant larvae such as *An. albimanus*, I did not observe any decrease in Na^+/K^+-ATPase protein signal or any indications of protein degradation. *An. albimanus* larvae can survive to pupation in up to 75% ASW, with about 35% of the first-instar larvae reaching pupation (Hurlbut, 1943). The dramatic shift in Na^+/K^+-ATPase (upregulation in the DAR cells and downregulation in the non-DAR cells) appears to disrupt the physiological coupling between Na^+/K^+-ATPase and V-ATPase which I predict to be responsible for Na^+ resorption in freshwater conditions. This shift renders the non-DAR cells similar in protein localization to the PR of the saline-tolerant culicine *Oc. taeniorhynchus*, and is likely to result in the ability of the non-DAR cells of *An. albimanus* to secrete a hyper-osmotic urine in a fashion similar to *Oc. taeniorhynchus* as discussed below.

Oc. taeniorhynchus larvae are highly saline-tolerant, able to survive up to 300% ASW by regulating their hemolymph to maintain a constant osmolarity of about 350 mosmol l^{-1} (Nayar and Sauerman, 1974; Bradley, 1994). The rectum of this species differs from that of the freshwater *Ae. aegypti* by the presence of an additional segment, the PR, which secretes a hyper-osmotic urine and rids the hemolymph of excess ions from a saline environment. The PR of *Oc. taeniorhynchus* expressed high levels of V-ATPase on the apical lamellae but did not appear to express Na^+/K^+-ATPase. The presence of an apical V-ATPase is supported by ultrastructural studies of other saline-tolerant culicines which described a particulate coat made up of spherical subunits on the cytoplasmic surface of the apical lamellae (Meredith and Phillips, 1973), indicating V-ATPase containing portasomes. As mentioned above and discussed in greater detail in Harvey (1992), the hyperpolarizing action of V-ATPase can be used to drive many ion transporting processes against an otherwise unfavorable concentration gradient. I hypothesize that the V-ATPase on the apical lamellae of the PR in *Oc. taeniorhynchus* and in the non-DAR

cells in *An. albimanus*, is energizing one or more transporters also present on this membrane to translocate ions from the cells to the lumen in order to excrete excess ions from the hemolymph.

The ability for *An. albimanus* larvae to shift Na^+/K^+-ATPase protein distribution in response to salinity, as well as the reversibility of this event, may be dependent on the larval stage at which exposure occurs. Younger larvae (second- and third-instars) reared in freshwater and exposed to 25% ASW exhibited a shift in Na^+/K^+-ATPase distribution from non-DAR to DAR cells in as little as 24 hours. More mature larvae (fourth-instars) exposed to 25% ASW for 24 hours expressed Na^+/K^+-ATPase in both non-DAR cells and DAR cells as if in an intermediate state between freshwater and saline water protein expression. After 48 hours, the majority of Na^+/K^+-ATPase was expressed in the DAR cells of fourth-instar larvae. This could indicate that early instar larvae are far more plastic in terms of regulating gene and/or protein expression than late larvae.

Slightly different results were obtained when rearing larvae in 25% ASW and exposing them to freshwater. Whereas second-instar larvae shifted Na^+/K^+-ATPase distribution from the DAR to non-DAR cells within 24 hours of exposure to freshwater, third-and fourth-instar larvae consistently expressed the protein in both DAR and non-DAR cells even after 72 and 48 hours, respectively. This may indicate that at the second-instar larval stages, the Na^+/K^+-ATPase protein shift is fully reversible, whereas more mature larvae cannot downregulate Na^+/K^+-ATPase expression in the DAR cells within the period of time observed. It is possible that the concentration of ASW was too low to cause a complete shift in distribution in more mature larvae, and that larvae would respond differently if reared in 50% ASW versus 25% ASW. It is interesting that a protein shift is seen at all in 25% ASW (osmolarity = 250 mosmol l^{-1}), as the osmolarity is less than that of the *An. albimanus* hemolymph (osmolarity ~ 300 mosmol l^{-1}).

This may be due to the abruptness of the salinity change, with larvae being transferred directly from freshwater to 25% ASW in the present study. Additionally, it could indicate that some event signals the rectum to shift Na^+/K^+-ATPase protein before it is actually necessary to produce a hyper-osmotic urine, as if in preparation.

CA9 is Involved in CO_2 Excretion

CA9 consistently localized to the DAR cells of all anopheline mosquitoes examined (including *An. gambiae*, *An. albimanus*, *An. farauti*, *An. quadrimaculatus*, *An. aquasalis* and *An. stephensi*), as well as to the AR of *Oc. taeniorhynchus* regardless of rearing water salinity. Members of the CA family are implicated in both ion and pH regulation in a number of organisms (e.g. Henry, 1984; Corena et al., 2004; Schewe et al., 2008) and catalyze the hydration of CO_2 to H_2CO_3 which instantaneously dissociates into H^+ and HCO_3^-. CA within the epithelial cells can convert cellular CO_2 to HCO_3^-, which can then be excreted by the action of a Cl^-/HCO_3^- exchanger (Smith, K. E. et al., 2007). Because the localization of CA9 did not change in any species in response to being reared in saline water compared with freshwater, I hypothesize that those rectal cells abundant in CA9 protein have at least one role that is independent of external water salinity.

One possible role for CA expressing cells is the transport of HCO_3^-, from blood to lumen (in preparation for excretion), or from lumen to blood (absorption). In this way, the cells may use metabolic CO_2 to regulate hemolymph HCO_3^- levels. Determining the presence and polarity of Cl^-/HCO_3^- exchangers in these cells would reveal the direction in which HCO_3^- is being transported. Alternatively, cells that are enriched in CA protein could be more metabolically active than neighboring cells which produce less CA. Cells with a robust metabolism would produce higher levels of CO_2 that in turn, could induce synthesis of high levels of CA protein to convert the toxic CO_2 to HCO_3^- prior to excretion. In support of this suggestion, there is

evidence that the AR of *Aedes dorsalis* is involved in HCO_3^- secretion (Strange et al., 1984) which is mediated by a rectal CA (Strange and Phillips, 1984).

Although I was unable to detect CA9 in the recta of *Ae. aegypti* larvae, this does not indicate a lack of CA activity in the rectum of this species. There are 13 predicted CA genes in the *Ae. aegypti* genome (www.ensembl.org), any of which could catalyze the conversion of CO_2 to HCO_3^- in the rectal cells. In support of CA activity in *Ae. aegypti* recta, alkalization of the rearing medium by starved *Ae. aegypti* larvae was reported by Stobbart (1971) who suggested that they may be excreting K^+ HCO_3^-. A similar alkalization was reported by Corena et al., (2002), who noted that the alkalization is blocked by global CA inhibitors. However, Clark et al., (2007) reported that the rectal lumen of *Ae. aegypti* is acidic (pH<6.2), and not alkaline which would be expected for a larva excreting either K^+ or Na^+ and HCO_3^-. It is possible that HCO_3^- secreted into the lumen associates with H^+ ions provided by an apical V-ATPase to form H_2CO_3, which would dissociate into H^+ and HCO_3^- when excreted from the rectum. However, as Clark et al., (2007) discuss, the pKa of H_2CO_3/HCO_3^- is 6.4 and in an environment more acidic than this pH, HCO_3^- would exist primarily in the form of CO_2. Another possibility is that CA is not present in the recta of *Ae. aegypti*. Neither Stobbart (1971) nor Corena et al., (2002) directly measured the pH of rectal excretions, and it is possible that the larvae alkalized their media by some other manner (i.e. gaseous respiration via the tracheal system). The role of CA in *Ae. aegypti* recta, as well as in other anopheline and culicine species, can be further examined by measuring the precise pH and the concentration of HCO_3^- directly from the rectal contents.

There is evidence for the expression of more than one CA in the recta of anophelines. Three additional CA isoforms are present in the recta of *An. gambiae*, AgCA3, AgCA6, and AgCAb. Whereas AgCA3 is similar to AgCA9 in that it is a predicted cytoplasmic CA, AgCA6

is a predicted secreted CA and AgCAb is a predicted β-CA. It is likely that each of these CAs has a distinct role in the rectum. At present, it is impossible to distinguish DAR from non-DAR using a dissecting microscope, and therefore I cannot determine the mRNA expression of each CA within the rectum using q-pcr, but because of the specific nature of AgCA9 localization to the DAR cells, I hypothesize that AgCA3, AgCA6 and AgCAb are likewise differentially localized in the rectum, each performing a specific role. It is possible that all three isoforms are localized to the DAR cells, as is suggested by CA enzyme histochemistry (see Chapter 3) which detects an abundance of CA activity in the DAR cells compared with the non-DAR cells. It is likely that orthologs of these CA isoforms are also present in the recta of various culicine species. The generation of specific antibodies to each of these CAs will reveal their localization patterns within the rectal cells and can offer insight into the roles of each rectal region in CA-related functions.

Conclusions: Based on the comparison of ion-regulatory protein localization in culicine and anopheline larval recta I hypothesize that saline-tolerant anophelines secrete a hyper-osmotic urine by the same rectal cells that are present in freshwater anophelines; this is in contrast to saline-tolerant culicines, which have a separate rectal region to secrete a hyper-osmotic urine. When reared in fresh water, both saline-tolerant and freshwater anopheline larvae actively resorb water and nutrients from the primary urine without excreting salt. In support of this idea, the protein localization patterns of anopheline non-DAR cells resemble those of the freshwater culicine rectal cells which are known to be active in resorbing ions. When exposed to saline water, saline-tolerant anophelines activate a region of the rectum (non-DAR cells) to secrete a hyper-osmotic urine by shifting protein localization of certain membrane energizing proteins such as Na^+/K^+-ATPase. This shift breaks the system of ion resorption in the non-DAR cells and

the rectum functions in a way that is similar to that of a salt water culicine rectum, with the DAR cells performing the task of the AR (resorption) and the non-DAR cells performing the task of the PR (excretion).

These data suggest that two subfamilies of mosquitoes, anophelines and culicines, differ greatly in rectal structure. These data also suggest that anophelines regulate protein expression differently than do culicines when reared in saline water. The present study demonstrates that data obtained from one species of mosquito cannot necessarily be applied to all species. The majority of currently available information concerning rectal structure and function, as well as ion regulation (a system crucial for larval survival), pertains to culicine species. The data presented here, along with ultrastructural and physiological research currently underway, will expand that information to include the equally important anopheline subfamily.

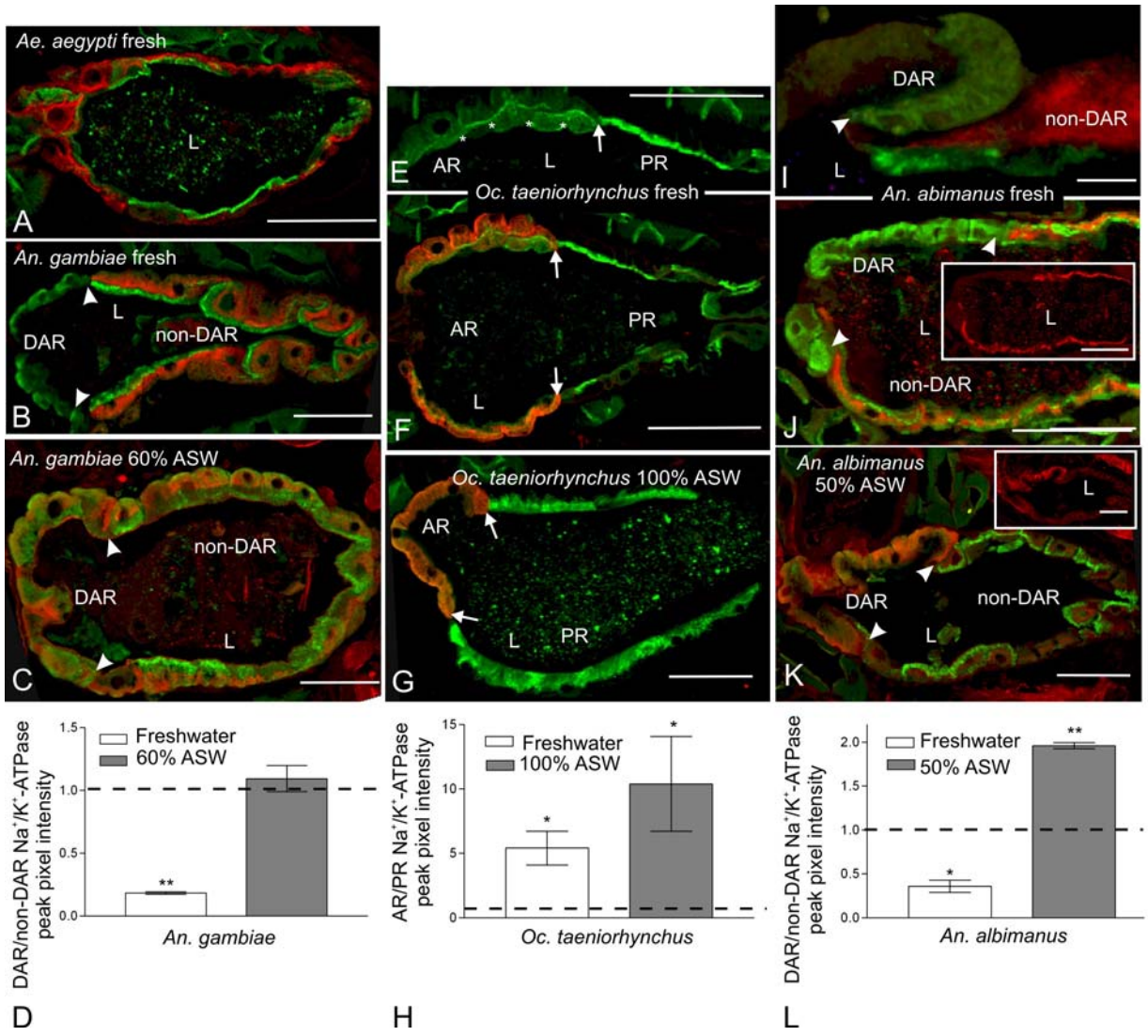

Figure 5-1. Na^+K^+-ATPase and V-ATPase protein distribution in recta of various anopheline and culicine species reared in fresh and saline water. Na^+K^+-ATPase (red) and V-ATPase (green) protein distribution was determined in longitudinal sections of the recta of A) *Ae. aegypti*; B and C) *An. gambiae*; E, F, and G) *Oc. taeniorhynchus*; and I, J, and K) *An. albimanus* reared in fresh or saline water. D, H, and L) Distribution of Na^+K^+-ATPase is indicted as a ratio of Na^+K^+-ATPase peak pixel intensity in the DAR cells (or AR) versus the non-DAR cells (or PR). Arrowheads demark the junction between DAR and non-DAR cells in anophelines and arrows demark the junction between AR and PR in culicines. The inset images in panels J and K are identical to the corresponding panel, but lack V-ATPase staining signal, thereby giving a clearer view of Na^+K^+-ATPase distribution. The apparent cytoplasmic localization of V-ATPase in *An. albimanus* is shown in higher magnification in (I). Asterisks in panel E demark weak V-ATPase signal on the apical lamellae of fresh water-reared *Oc. taeniorhynchus*. Asterisks in panels D, H, and L indicate a significant difference in the Na^+K^+-ATPase peak pixel intensities between the DAR

and non-DAR cells (or AR and PR). * P-Value > 0.05; ** P-Value > 0.005. AR: anterior rectum, ASW: artificial sea water, DAR: dorsal anterior rectum, L: lumen, PR: posterior rectum. Scale bars: 150 µm (A), 75 µm (B, J, J inset), 86.13 µm (C), 149.36 µm (E, F), 99.32 µm (G, K, K inset), 12 µm (I).

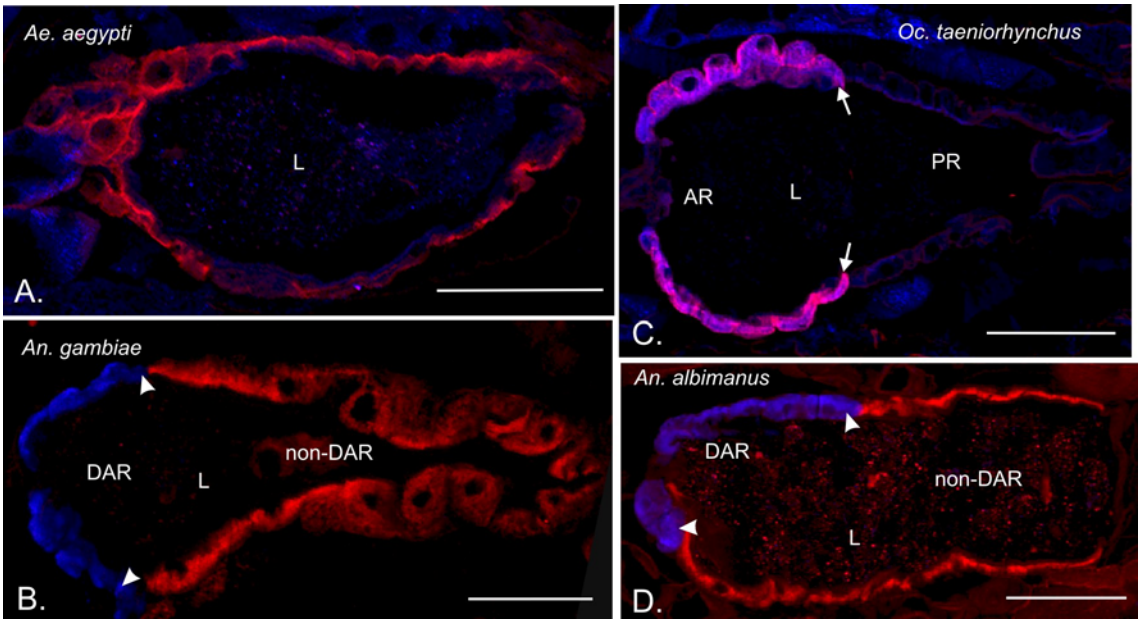

Figure 5-2. CA and Na^+K^+-ATPase protein distribution in recta of various anopheline and culicine species reared in fresh water. A) *Ae. aegypti*, B) *An. gambiae*, C) *Oc. taeniorhynchus*, and D) *An. albimanus*. Na^+K^+-ATPase (red) was used as a counterstain. CA (blue) distribution did not change in larvae reared in saline water; therefore only images of freshwater reared larvae are shown. Arrowheads indicate the junction between DAR and non-DAR cells. Arrows indicate junction between the AR and PR. AR: anterior rectum, DAR: dorsal anterior rectum, L: lumen, PR: posterior rectum. Scale bars: 150 µm (A), 75 µm (B), 149.36 µm(C), 99.32 µm (D).

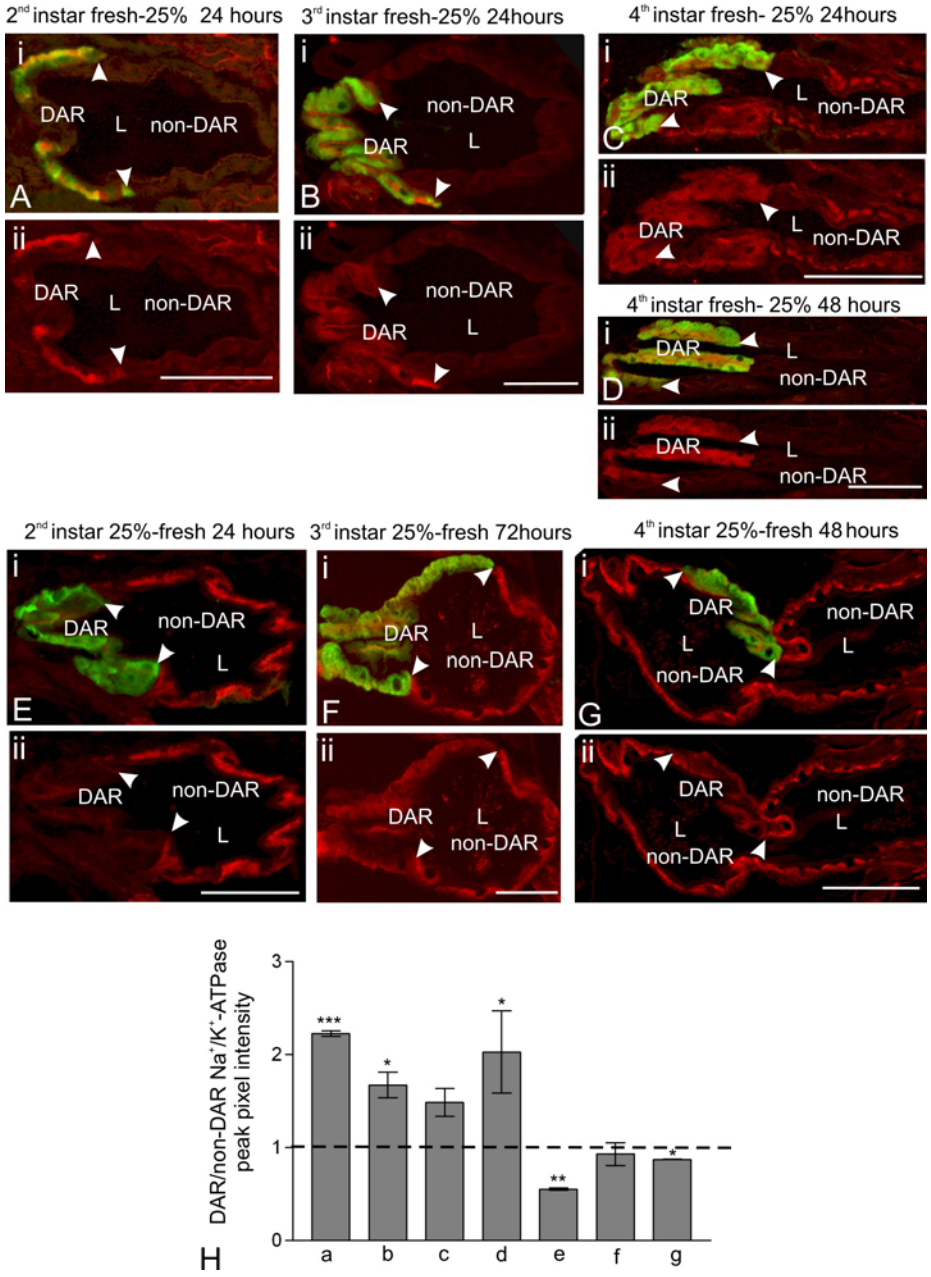

Figure 5-3. Change in CA and Na^+K^+-ATPase protein distribution in recta of *An. albimanus* given acute fresh or saline water challenges. Immunohistochemical detection of Na^+/K^+-ATPase (red) and CA9 (green) in *An. albimanus* larvae. Larvae reared in freshwater and transferred to 25% ASW during A) the second-instar stage for 24 hours, B) during the third-instar stage for 24 hours, and during the fourth-instar stage for C) 24 hours or D) 48 hours. Also shown are larvae reared in 25% ASW and transferred to freshwater during the E) second-instar stage for 24 hours, F) during the third-instar stage for 72 hours and G) during the fourth-instar stage for 48 hours. H) Distribution of Na^+K^+-ATPase in each sample is indicted as a ratio of Na^+K^+-ATPase peak pixel intensity in the DAR cells versus the non-DAR cells. Lowercase bar

labels in H correspond to the uppercase letters in Figure 5-3 panels (i.e. Figure 5-3A corresponds to Figure 5-3H bar "a"). Distribution of CA9 is indicative of DAR cells. Na^+K^+-ATPase and CA9 colocalization is indicated in yellow. In each set of images, the top panel shows both Na^+K^+-ATPase and CA9 localization, whereas the bottom panel is the same picture showing only Na^+K^+-ATPase localization. Asterisks in panel H indicate a statistically significant difference in Na^+K^+-ATPase peak pixel intensities between the DAR and non-DAR cells. * P-Value > 0.05; ** P-Value > 0.005; *** P-Value >.001. L: lumen. Scale bars: 75 μm (A, B, C, E), 150 μm (D, G), 65.17 μm (F).

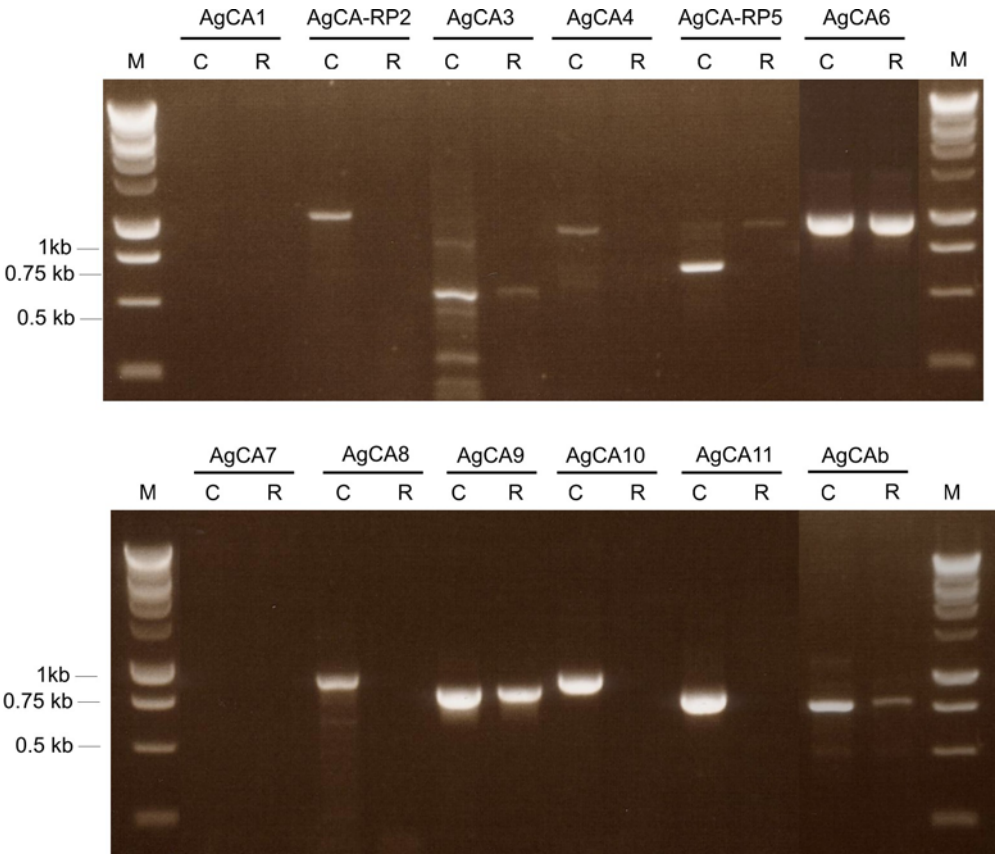

Figure 5-4. RT-PCR analysis of the expression of each of the eleven An. gambiae α–CAs (AgCA1-11) and the one β–CA (AgCAb) in *An. gambiae* rectal tissue. Rectal cDNA was used in a PCR reaction with primers specific to either the whole CA transcript or the partial predicted sequence. Whole *An. gambiae* fourth-instar larvae cDNA was used as a primer control (shown by a "C" above the lane) in addition to the rectal cDNA experimental template (indicated by a "R" above the lane). See Table 2-3 for primer sequences and expected length of products. All bands shown were the expected size for each gene amplified. M: 1 kb DNA ladder® (invitrogen).

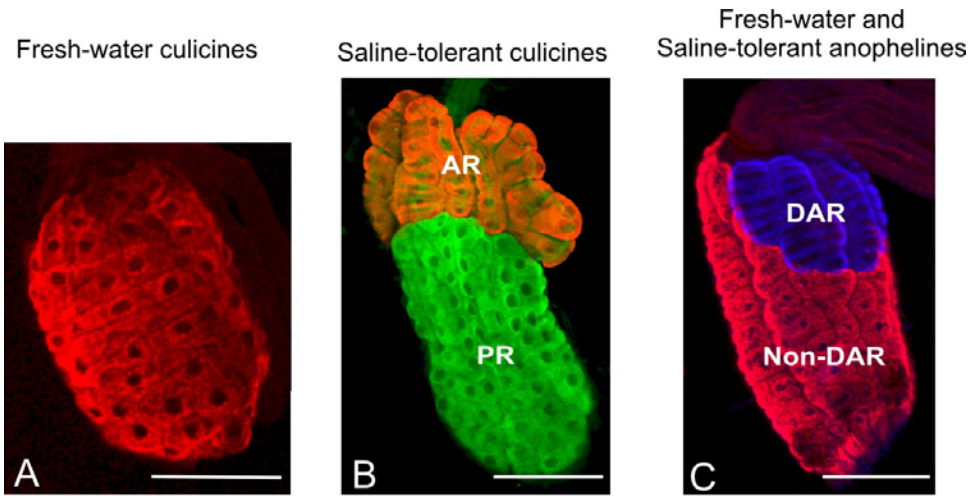

Figure 5-5. Comparison of culicine and anopheline larval rectal structure using confocal microscopy of whole mount immunohistochemical preparations. Structure of A) the freshwater culicine, *Ae. aegypti*, B) the saline-tolerant culicine, *Oc. taeniorhynchus*, and C) the freshwater anopheline, *An. gambiae*. Data similar to these have also been reported elsewhere (Patrick and Gill, 2003; Smith, K. E. et al, 2007; Okech et al., 2008). Protein localizations are shown for visual distinction of rectal segments in each species. Immunolocalizations indicate distribution of Na^+/K^+-ATPase (red), V-ATPase (green), and CA9 (blue). AR: anterior rectum, DAR: dorsal anterior rectum, PR: posterior rectum. Scale bars: 150 µm (A, C), 186 µm (B).

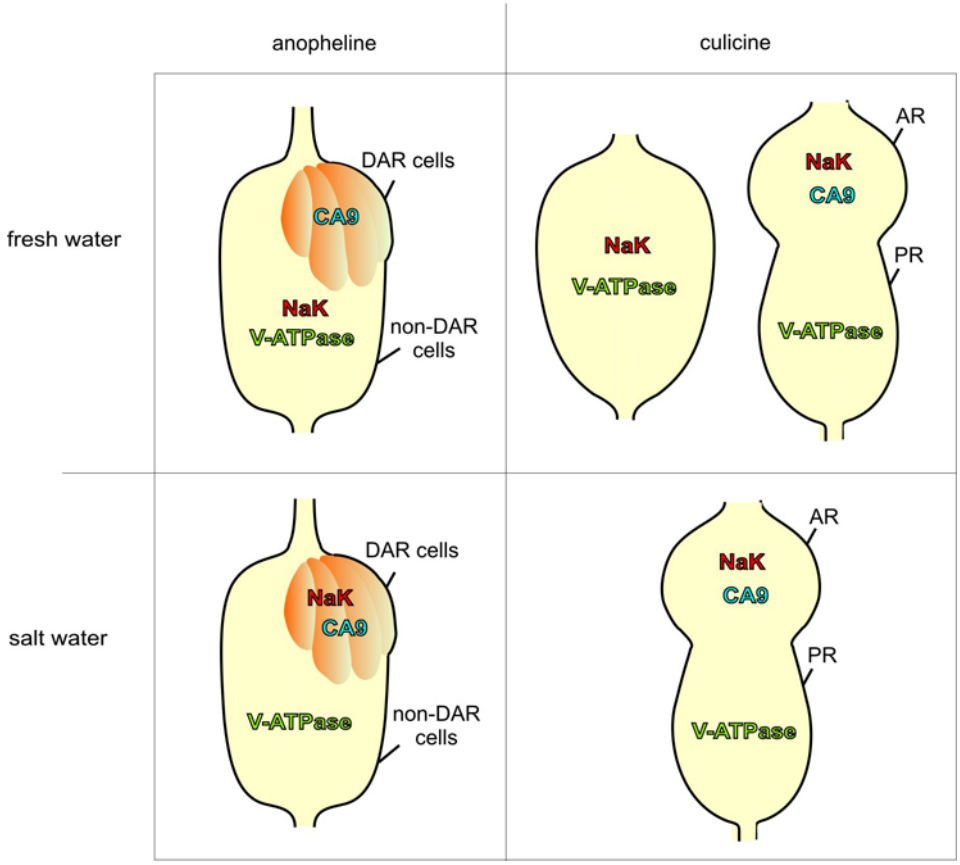

Figure 5-6. Comparison of the major protein localization patterns found in the recta of freshwater-reared culicines and anophelines to those in saline water-reared culicines and anophelines. Figure 5-6 allows an easy comparison of the proteins in the anopheline and culicine recta. In all cases CA9 localizes to the cytoplasm, Na^+K^+-ATPase (NaK) localizes to the basal membrane, and V-ATPase localizes to the apical membrane. The non-DAR cells of freshwater-reared anophelines, both freshwater and saline-tolerant, resembled the recta of freshwater culicines in protein localization; both expressed Na^+K^+-ATPase and V-ATPase. When reared in saline water, the anopheline rectum shifted Na^+K^+-ATPase localization and resembled the saline-water culicine rectum in protein localization; anopheline DAR cells and culicine AR possessed CA9 and Na^+K^+-ATPase, whereas anopheline non-DAR cells and culicine PR possessed V-ATPase.

CHAPTER 6
CHARACTERIZATION OF THE DAR AND NON-DAR CELLS OF ANOPHELINE RECTA: PHYSIOLOGICAL FUNCTIONS

Introduction

Mosquito larvae, like all aquatic organisms, must adapt to an environment which can change drastically in ionic composition and salinity. Adaptation to these varying conditions requires a highly developed system for the regulation of ions, and in mosquitoes, a major organ responsible for this regulation is the rectum. Although, to date, the majority of work on larval ion regulation has focused on the culicine subfamily, I and others have shown that the recta of anopheline larvae differ from that of both freshwater and saline-tolerant culicine species in structure (Bradley, 1987a; Bradley 1987b; Smith, K. E. et al., 2007) and in regulation of protein expression (Smith et al., 2008).

The recta of anopheline larvae are similarly structured regardless of saline tolerance, but can adapt to saline environments by shifting the distribution of at least one ion-regulatory protein, Na^+/K^+-ATPase. As a result, different salinities elicit different patterns of protein expression in the rectal regions, and may result in a change in overall function of the rectum. In this way, larvae can survive in freshwater by resorbing essential ions and nutrients, and in saline water (in the case of saline-tolerant species) by generating a hyperosmotic urine, while using the same rectal cell types.

I hypothesize that anopheline larvae shift protein distribution patterns in their rectal regions to activate the non-DAR cells, which comprise approximately 75% of the rectum, to either absorb or secrete ions based on environmental ion load. By expressing different combinations of ion-regulatory proteins, the rectal cells may favor the function of one protein over another. Many ion-regulatory transporters can activate other proteins by generating favorable electrochemical gradients across a membrane. Often, these gradients are generated by

the uneven distribution of H^+ across a membrane, and indeed many proteins facilitate the transport of H^+ across insect membranes including V-ATPase (Wieczorek et al., 1991), Na^+/H^+-exchangers (Pullikuth et al., 2006), Na^+/H^+ antiporters (Padan et al., 2001; Rheault et al., 2007), and K^+/H^+ exchangers (Harvey and Nedergaard, 1964).

The self-referencing ion-selective microelectrode technique (SIET) was developed to measure ion-specific flux across a membrane at the single cell level while virtually eliminating the artifact of voltage drift (Kühtreiber and Jaffe, 1990; Kochian et al., 1992; Smith et al., 1999). The selectivity of the electrode is based on the characteristics of commercially available ionophores suspended in a liquid membrane at the tip of a microelectrode (Smith et al., 1994). The electrode "self-references" by recording voltage values at two points within an ion gradient, a point near the ion source and a point a known distance away from the ion source. By subtracting the voltage measured at the far point from that at the near point, drift and background signals, as well as any contaminating voltages can be minimized (Smith, P. J. et al., 2007).

Here I report H^+ flux at the basal membrane of the DAR and non-DAR cells of freshwater and saline water-reared *An. albimanus* larvae using SIET, and the effects of pharmacological inhibition of that flux. My data indicate there are distinct differences between the DAR and non-DAR cells both in the direction of net H^+ flux and in the proteins mediating this flux. Additionally, there are distinct differences in the roles of several of these proteins in H^+ flux depending on the salinity of the larval rearing media. I use these results, together with previous immunohistochemical data, to generate a putative model for ion control in the larval anopheline rectum and discuss how this model relates to my previous hypothesis regarding the role of the anopheline rectum in ion regulation.

Results

H^+ Flux in Rectum

H^+ flux was determined at the basal membrane of the DAR and non-DAR cells of *An. albimanus* larvae reared in either 2% or 50% ASW using SIET (Figure 6-1). Because DAR and non-DAR cell types cannot be distinguished using a dissecting microscope, measurements were taken along the anterior-posterior axis of one side of the rectum and preparations were post-stained with rhodamine 123 to visualize DAR and non-DAR cell types (Figure 6-1A). H^+ flux was measured at points approximately 5-10 μm from the membrane in 50 μm increments along the axis of the rectum (Figure 6-1B).

In all larvae a significant H^+ efflux was observed averaging 1.3 x 10^{-7} mol cm^{-2} s^{-1} in the area of the DAR cells. Although this efflux was consistent among all larvae, the magnitude of the flux varied greatly between larvae ranging from 1.38 x 10^{-8} to 3.27 x 10^{-7} mol cm^{-2} s^{-1}. As the probe neared the DAR/non-DAR boundary, the H^+ flux decreased significantly and fluctuated between an influx and efflux, averaging 9.6 x 10^{-9} mol cm^{-2} s^{-1}. Again the magnitude of this flux varied between larvae, but in each individual larva, a trend was noted in which DAR cells exhibited a large H^+ efflux which decreased considerably at the DAR/non-DAR cell boundary, and often reversed direction in the non-DAR cells (Figure 6-1C).

Pharmacology

To determine the proteins involved in H^+ flux at the basal membrane of the DAR and non-DAR cells, the effects of concanamycin A, methazolamide and DIDS were evaluated at a single point of H^+ efflux at the DAR cells and influx at the non-DAR cells (Figure 6-2). Concanamycin A is a specific inhibitor of the H^+ pump, V-ATPase; methazolamide is a specific inhibitor of CA, a known marker for DAR cells and an enzyme which catalyzes the production of H^+ and HCO_3^- within a cell; DIDS (4,4'-Diisothiocyanatostilbene-2,2'-disulfonic acid Disodium salt) is a

specific inhibitor of anion exchange and is effective against bicarbonate transporters, proteins which frequently work in synergy with CAs (McMurtrie et al., 2004). For each inhibitor, $n \geq 5$ larvae were examined.

Concanamycin A at a concentration of 10^{-6} mol l^{-1} significantly decreased efflux at the DAR cells of larvae reared in both 2% (P-value < 0.01) and 50% (P-value < 0.05) ASW and significantly decreased non-DAR cell influx in larvae reared in 50% ASW (P-value < 0.05). Concanamycin A had no significant effect on non-DAR cell influx in 2% ASW reared larvae at the concentration used.

Methazaolamide at a concentration of 10^{-4} mol l^{-1} significantly decreased H^+ efflux in the DAR cells of larvae reared in both 2% (P-value < 0.05) and 50% (P-value < 0.01) ASW, whereas it significantly increased non-DAR cell influx in larvae reared in both 2% (P-value < 0.001) and 50% (P-value < 0.01) ASW.

DIDS at a concentration of 10^{-6} mol l^{-1} significantly decreased H^+ efflux in the DAR cells of larvae reared in 2% ASW (P-value < 0.01) and significantly increased DAR cell H^+ efflux in larvae reared in 50% ASW (P-value < 0.05). DIDS significantly increased non-DAR cell influx in larvae reared in both 2% (P-value < 0.01) and 50% (P-value < 0.05) ASW. No significant effects were detected in either cell type of larvae reared in either 2% or 50% ASW using 0.1% DMSO.

In at least one case, each inhibitor (concanamycin A, methazolamide, DIDS) caused the reversal of flux, in which treatment resulted in a H^+ efflux becoming an influx. No instances were observed where treatment resulted in a H^+ influx becoming an efflux.

Discussion

I previously hypothesized that the primary function of the rectum of saline-tolerant anophelines changes based on the ionic needs of the larva, and that this change is due to a shift in

the distribution of ion-regulatory proteins (Smith et al., 2008). Here I gain insight into the functional characteristics of the anopheline DAR and non-DAR cells by measuring H^+ flux at the basal membrane of 2% and 50% ASW-reared *An. albimanus* recta using SIET. Because H^+ is coupled to many transport processes, H^+ flux at a membrane can be indicative of transport across that membrane. A large H^+ efflux was measured from the DAR cells into the hemolymph; this contrasted with the flux measured in the non-DAR cells which diminished drastically, often becoming an influx. The H^+ flux in both DAR and non-DAR cells was shown to be independent of rearing salinity and mediated in part by the actions of V-ATPase, CA and anion exchange. Here I have combined data from H^+ flux measurements and pharmacological inhibition in each region of the rectum to generate a putative model of ion regulation which will be discussed in more detail in the following sections (Figure 6-3).

H^+ Fluxes are Likely Due to Many Transport Systems

Treatment with pharmacological inhibitors strongly suggests that the measured H^+ fluxes, large effluxes at the DAR cell basal membrane and influxes at the non-DAR cell basal membrane, are the collective result of many different H^+ transport systems. Several cases were noted in which treatment of an H^+ efflux at the DAR cell membrane with an inhibitor resulted in a measured H^+ influx. These results support the idea that the measured fluxes are not the products of a single H^+ source, but the cumulative effects of many H^+ transporting proteins, likely generating numerous H^+ effluxes and influxes at the basal membrane. The large fluxes measured at the DAR cell membrane are likely the result of an excess of H^+ efflux into the hemolymph over H^+ influx into the cell.

No instances were observed in which treatment with an inhibitor resulted in an H^+ influx at the non-DAR cells becoming an efflux. This may represent a functional difference between the DAR and non-DAR cells; however, the majority of the inhibitors increased the H^+ influx in the

non-DAR cells, and therefore would not be expected to reverse the flux. It is likely that the low effluxes/influxes measured in the non-DAR cells are the result of relatively equal numbers of H^+ being translocated into the hemolymph as there were into these cells.

This observation also affects the interpretation of pharmacological data; it is impossible to discern an increase in efflux from a decrease in influx and vice versa. Here I represent changes in H^+ flux due to pharmacological inhibition as a ratio of flux with and without, treatment with an inhibitor. However, I have not reported the percent flux inhibition, as it would be an irrelevant value. The H^+ flux measurements represent a mixture of influxes and effluxes, and I cannot distinguish which are affected by the inhibitor. Therefore, speculations on inhibitor effects will be based on known and predicted protein distribution patterns and the classical view of the specific effects of the pharmacological experiments.

Pharmacology

Although H^+ flux at the basal membrane of the rectum did not appear to differ between larvae reared in 2% and 50% ASW, the effects of specific pharmacological inhibitors on that flux, specifically the effects of concanamycin A on the non-DAR cells and of DIDS on the DAR cells, indicate functional differences between the recta of larvae reared in different salinities (Figure 6-2).

Concanamycin A: V-ATPase inhibitor

Concanamycin A is a membrane permeable macrolide antibiotic that specifically inhibits V-type H^+-ATPase-mediated H^+ movement (Huss et al., 2002). V-ATPase is an H^+ pump and well known membrane energizer important for ion regulation (e. g. Wieczorek, 1992). Treatment of DAR cells with concanamycin A resulted in a significant decrease in H^+ efflux in larvae reared in both 2% and 50% ASW (Figure 6-2). This suggests the presence of a V-ATPase on the basal membrane of the DAR cells pumping H^+ into the unstirred layer of the hemolymph.

Apparent cytoplasmic localization of a V-ATPase was observed in the DAR cells of both *An. gambiae* and *An. albimanus* using immunohistochemistry (Smith et al., 2008) and it was suggested that the protein may in fact localize to the basal membrane. Preliminary evidence suggests that similar to the recta of freshwater culicines and the AR of saline-tolerant culicines (Meredith and Phillips, 1973), the basal membrane of DAR cells is elaborated into an extensive basal labyrinth which, because of an apparent lack of apical lamellae, extends throughout the majority of the cell (K. E. Smith, unpublished observations). V-ATPase protein distributed on the basal membrane may appear cytoplasmic due to the nature of the membrane.

Treatment of non-DAR cells with concanamycin A elicited no significant effect on H^+ influx in 2% ASW-reared larvae, but resulted in a significant decrease in H^+ influx in 50% ASW-reared larvae (Figure 6-2). This suggests a difference in V-ATPase protein distribution or function between the non-DAR cells of larvae reared in 2% and 50% ASW; however, V-ATPase has been shown to localize to the apical membrane of the non-DAR cells in larvae reared in both conditions (Okech et al., 2008; Smith et al., 2008). This difference in pharmacological inhibition could be explained by the differential distribution of another H^+ transporter such as a sodium-hydrogen exchanger (NHE).

In most cases, insect NHEs mediate the electroneutral exchange of intracellular Na^+ for extracellular H^+ (Beyenbach, 1995; Maddrell and O'Donnell, 1992). However, there is evidence that they can also function in the opposite direction (Pullikuth et al., 2006), exchanging extracellular Na^+ for intracellular H^+, similar to mammalian NHEs (Orlowski and Grinstein, 2004). Two NHEs, AeNHE3 and AeNHE8, have been cloned from *Ae. aegypti* and localized to the recta of larvae (AeNHE3; Pullikuth et al., 2006) and adults (AeNHE8; Kang'ethe et al., 2007). A similar NHE may provide another means of apical H^+ transport into the lumen of *An.*

gambiae non-DAR cells in the event of apical V-ATPase inhibition. If this NHE were down-regulated in 50% ASW-reared larvae, concanamycin A inhibition of the apical V-ATPase would impede H^+ transport into the lumen, thereby "backing up" the basal H^+ influx.

In support of my hypothesis that the non-DAR cells of freshwater-reared larvae absorb ions, NHE, in conjunction with a basally distributed Na^+/K^+-ATPase (Okech et al., 2007; Smith, K. E. et al., 2007; Smith et al., 2008), may mediate the uptake of sodium from the urine. The down-regulation of NHE and Na^+/K^+-ATPase proteins in the non-DAR cells of 50% ASW-reared larvae could decrease sodium resorption and may reflect the diminished ionic needs of the larvae.

Methazolamide: carbonic anhydrase inhibitor

Methazolamide is a specific inhibitor of α-CAs, one isoform of which (AgCA9) I have previously identified as a reliable marker for DAR cells (Smith, K. E. et al., 2007; Smith et al., 2008). Additionally, the mRNA of least two other α-CA isoforms and one β-CA isoform, are present in whole recta samples of freshwater-reared *An. gambiae* larvae: AgCA3, a cytoplasmic CA, AgCA6, a secreted CA, and AgCAb, a β-CA against which methazolamide is ineffective (see Chapter 3). Both α- and β-CA isoforms catalyze the conversion of cellular CO_2 to HCO_3^- and H^+.

Treatment with methazolamide resulted in a significant decrease in DAR cell H^+ efflux and a significant increase in non-DAR cell H^+ influx in larvae reared in both 2% and 50% ASW (Figure 6-2). This data supports the known distribution of AgCA9 in the DAR cells and suggests that CA(s) influence H^+ flux in the non-DAR cells as well, possibly through the presence of an extracellular or cytoplasmic CA isoform associated with the cells. Alternatively, CA activity in the DAR cells could indirectly mediate proteins involved in H^+ flux in the non-DAR cells. Many systems exhibit colocalization of CA and a membrane V-ATPase which translocates H^+

produced by the CA-mediated reaction out of the cell (Breton et al., 1996; Breton et al., 1999; Breton, 2001; Paunescu et al., 2008). Therefore, inhibition of a cellular CA would decrease H^+ available for V-ATPase transport, decreasing the V-ATPase-mediated flux. Likewise, the decrease in DAR cell H^+ efflux following methazolamide treatment supports the prediction of a basal V-ATPase in this cell type. By contrast, the non-DAR cells of *An. albimanus* larvae are known to express an apical V-ATPase when larvae are reared in both fresh and saline water (Smith et al., 2008). The methazolamide-related increase in non-DAR cell H^+ influx may indicate that a cellular CA is the main source of H^+ for the apical V-ATPase. Inhibition of this CA would deplete the V-ATPase of H^+ needed to energize the membrane, and may lead to an upregulation of other H^+ transport systems on the basal membrane to compensate for the loss of H^+. Alternatively, a decrease in CA-mediated H^+ generation could decrease intracellular H^+ concentration, altering the H^+ gradient and leading to an increase in basal H^+ influx down the concentration gradient.

DIDS: anion exchange inhibitor

DIDS is a specific inhibitor of cellular anion exchange and is effective against multiple proteins including Na^+-driven and Na^+-independent HCO_3^-/Cl^- transporters and Na^+/HCO_3^- co-transporter as well as Cl^- channels (Grassl & Aronson, 1986; Helbig et al., 1988; Boron, 2001; Matulef and Maduke, 2005). Treatment with DIDS significantly decreased DAR cell H^+ efflux in 2% ASW-reared larvae, while significantly increasing DAR cell H^+ efflux in 50% ASW-reared larvae. This suggests differential distribution of protein activity mediating the transport of HCO_3^- or Cl^- in the DAR cells of larvae reared in 2% versus 50% ASW. Treatment of non-DAR cells with DIDS significantly increased H^+ influx in larvae reared in both 2% and 50% ASW, suggesting no significant differences in protein activity mediating the transport of HCO_3^- or Cl^- in this cell type.

Three HCO_3^- transporting proteins belonging to the SLC4 family (Romero et al., 2004) are predicted to be expressed in the *An. gambiae* genome; the mRNA of only one of these proteins, AgAE1, is abundantly expressed in the hindgut (MTs and rectum) as measured by micro-array and quantitative-PCR (Neira et al., 2008; M. V. Neira, personal communication). HCO_3^- transporting proteins are often co-localized with CAs to facilitate the transport out of the cell of HCO_3^- produced by the CA-catalyzed reaction (McMurtrie et al., 2004; Sterling et al., 2001). As mosquito larvae are thought to excrete HCO_3^- from the rectum, alkalizing their media (Stobbart, 1971), I predict AgAE1 to localize to the apical membrane, transporting HCO_3^- from the cells into the lumen of the rectum. Due to the wide range of proteins inhibited by DIDS, I cannot draw any other specific conclusions regarding my model of ion transport except to say that the results strongly suggest that DIDS-sensitive anion exchange protein activity changes in the DAR cells, but not the non-DAR cells, depending on the salinity of rearing water.

Putative Model for Ion Transport in the Anopheline Rectum

I have generated a putative model for ion transport in the larval rectum of anopheline mosquitoes (Figure 6-3) based on current physiological and pharmacological data as well as previous immunohistochemical data (Rheault et al., 2007; Okech et al., 2008; Smith et al., 2008). This model supports my hypothesis that the primary function of the non-DAR cells, the cell type which comprises approximately 75% of the cells in the rectum, changes in response to the ionic needs of the larvae. Anophelines reared in fresh water actively resorb ions via their rectum to maintain constant ionic and osmotic hemolymph concentrations (Bradley, 1994). By contrast, anophelines reared in saline water must excrete the excess ions ingested while feeding via rectal production of a hyperosmotic urine. A potential mechanism for Na^+ resorption is evident in the non-DAR cells of 2% ASW-reared larvae, whereby Na^+ is transported from the lumen into the cell via an NHE and is then transported into the hemolymph in exchange for a K^+ via a Na^+K^+-

ATPase. Basal Na^+K^+-ATPase is considerably down-regulated in the non-DAR cells of larvae reared in 50% ASW (Smith et al., 2008), and I predict that the apical NHE may also be downregulated in saline conditions. This change in protein distribution would interfere with Na^+ resorption in the non-DAR cells and may indicate a shift in primary rectal function, from resorption in fresh water, to secretion in saline water.

The DAR cells comprise approximately 25% of the cells in the rectum and are hypothesized to have a main role in HCO_3^- excretion (Smith et al., 2008). However, this hypothesis is based on the idea that CA exclusively localizes to the DAR cells. As pharmacological data now suggests that CA is present in both DAR and non-DAR cells, it is likely that DAR cells have a role in basal resorption of essential ions and nutrients from the primary urine, similar to that suggested for the AR of culicine larvae (Meredith and Phillips, 1973; Bradley and Phillips, 1977). Changes in the response of DAR cell H^+ flux to DIDS in larvae reared in 2% and 50% ASW cannot readily be explained without further analysis of protein distribution. It is possible that the effects of DIDS are related to the absence or presence of a basal membrane Na^+K^+-ATPase in DAR cells of larvae reared in 2% and 50% ASW, respectively. The shift in localization of this protein may regulate the rate or type of ion resorption mediated by the DAR cells.

Conclusions: I have further characterized the DAR and non-DAR cell types of the anopheline larval rectum using SIET. I have demonstrated that the two cell types differ in basal membrane H^+ flux and that V-ATPase, CA, and anion exchanger proteins have a major role in mediating H^+ flux in both cell types. Additionally, differences in the response of H^+ flux to inhibitors in larvae reared in 2% versus 50% ASW indicate changes in protein function between the two rearing conditions. These data, along with previous immunohistochemical results,

support a model of rectal ion regulation in which the non-DAR cells have a resorptive function in freshwater-reared larvae and a secretive function in saline water-reared larvae. In this way, anopheline larvae may adapt to varying salinities.

Ion regulation is a biological process crucial to the survival of mosquito larvae. The ability to shift protein distribution, thereby altering cell function, affords larvae the ability to survive and flourish in a wider range of habitats. This work has begun to characterize the function of the anopheline rectum as it relates to adaptation and ion regulation. Only through a full understanding of the proteins involved in, and the mechanisms responsible for these adaptive abilities can we take advantage of this vital process for the development of vector control.

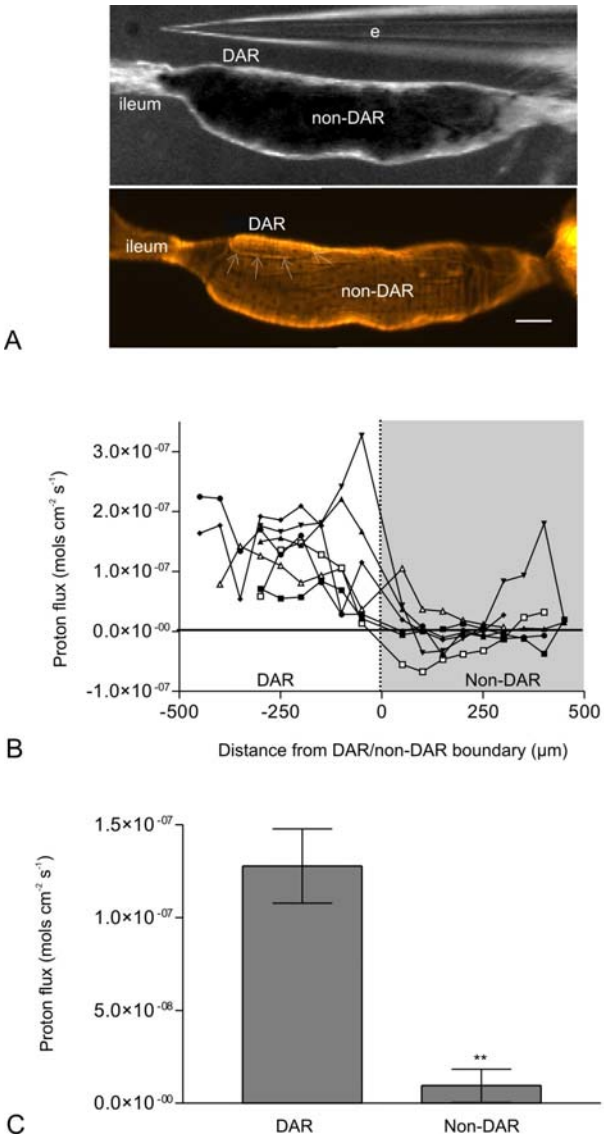

Figure 6-1. Measure of H^+ flux at the basal membrane of the DAR and non-DAR cells of *An. albimanus* larvae using SIET. A) Image illustrating the larval rectum as viewed through a dissecting microscope during H^+ flux measurements (top panel), and post-stained with rhodamine 123 to visualize the DAR/non-DAR boundary (arrows; bottom panel). B) H^+ flux for seven individual preparations beginning at the rectum-ileum junction and stoping at the end of the rectum, measured in 50µm intervals. Each data point represents an average of continuous measurements taken over five minute periods. C) Averaged DAR and non-DAR H^+ flux measurements. Error bars indicate standard error of the mean. Difference in H^+ flux between the DAR and non-DAR cells was statistically significant ($P < 0.01$) as determined using a paired t-test and reported as a two-tailed P-value. Scale bar: 100µm. e: electrode.

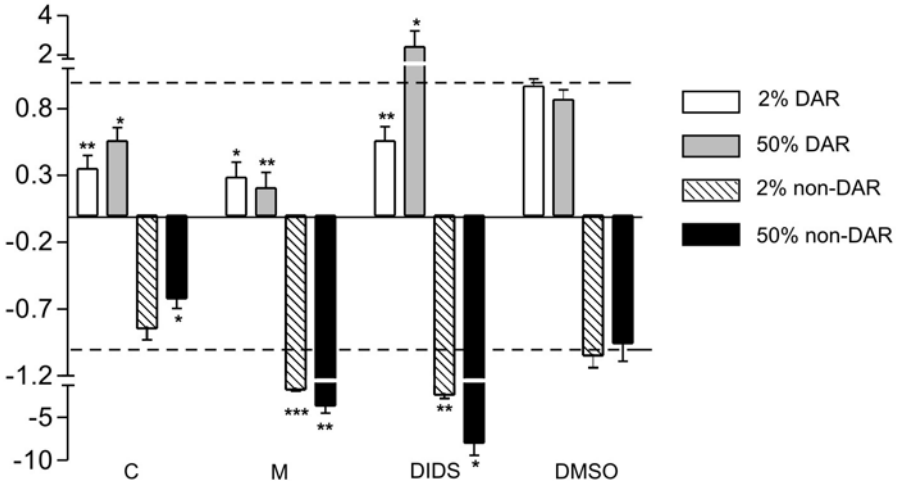

Figure 6-2. Pharmacological inhibition of H^+ flux at the basal membrane of 2% and 50% ASW-reared *An. albimanus* recta. Inhibitors include a V-ATPase inhibitor, concanamycin A (C), a carbonic anhydrase inhibitor, methazolamide (M), and an anion exchange inhibitor, DIDS, as well as a DMSO vehicle control. Asterisks indicate a significant difference between H^+ flux with and without inhibitor.

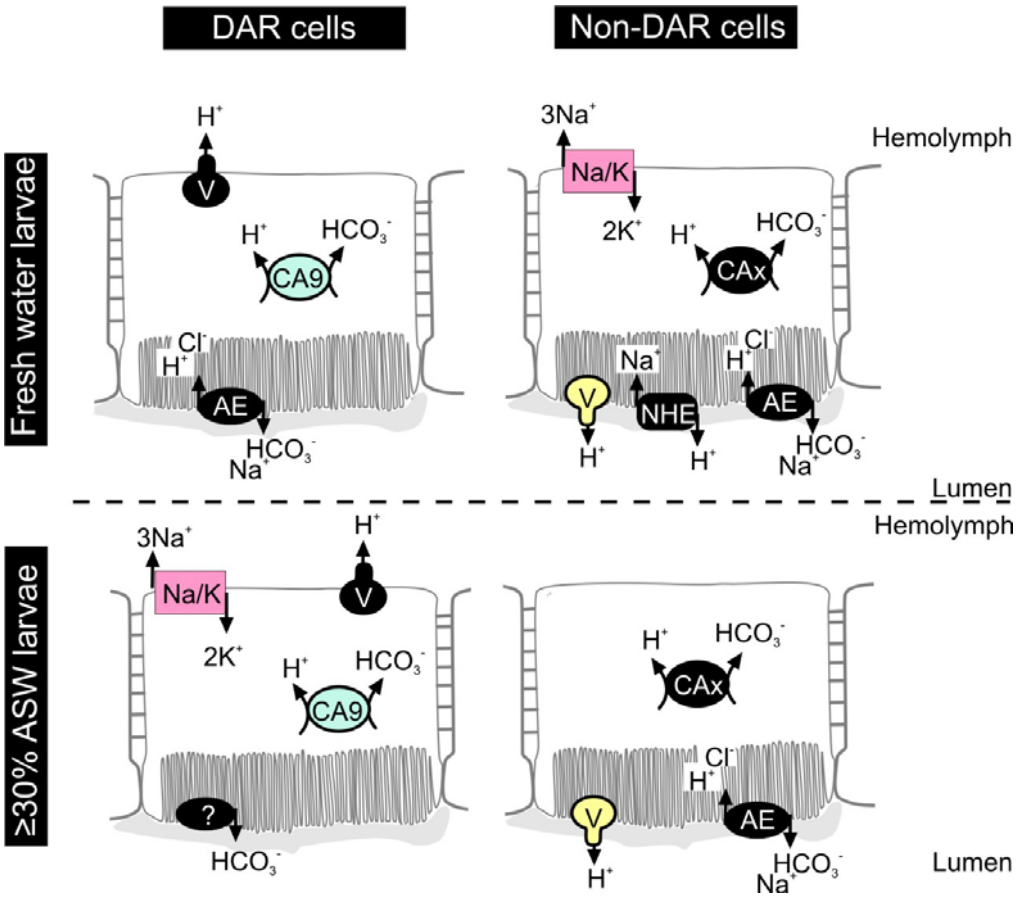

Figure 6-3. Putative model for ion transport in the anopheline rectum of larvae reared in fresh or saline water. Proteins in color are those which have been previously immunolocalized, whereas proteins in black are those which are predicted. This model suggest that the non-DAR cells of 2% ASW-reared larvae function in resorbing ions from the urine as indicated by the NHE/Na^+K^+-ATPase-mediated sodium resorption pathway. This function likely changes to a secretive one in larvae reared in 50% ASW. AE: anion exchanger; CA: carbonic anhydrase; Na/K: sodium/potassium ATPase; NHE: sodium/hydrogen exchanger; V: V-ATPase.

CHAPTER 7
CONCLUSIONS AND FUTURE DIRECTIONS

pH Regulation in the Larval Alimentary Canal

Conclusions: I have cloned the full-length transcripts of four CA genes from the *An. gambiae* alimentary canal including two α–CAs predicted to translate to secreted (AgCA6) and cytoplasmic (AgCA9) proteins, one CA-RP (CA-RP2), and one β–CA (AgCAb). mRNA localization of three of these genes indicates a significant abundance of AgCAb in the AMG and AgCA6, AgCA9 and AgCAb in the rectum. Through protein localization I detected one CA, AgCA9, in the GC, transitional region, ectoperitrophic space, MT and DAR cells of the rectum. Additionally, I have demonstrated AgCA9 mRNA silencing and protein down-regulation in an *An. gambiae* larval cell line, paving the way for functional studies in live larvae. This work has advanced the current model of AMG alkalization in mosquito larvae and has linked CA function with ion-regulation as well as pH-regulation.

The previous model of midgut alkalization in mosquito larvae relied on plasma membrane HCO_3^- transporters to translocate cellular HCO_3^- into the lumen where it buffered the near neutral milieus of the GC and PMG. An apically located V-ATPase in the AMG would cause HCO_3^- to be stripped of a H^+ to form CO_3^{2-} which could buffer the highly alkaline AMG lumen. The inability to localize a HCO_3^- transporter to the apical membrane of the alimentary canal challenged the validity of this model. However, localization of a CA to the ectoperitrophic space modified the original model such that HCO_3^- transporters are no longer essential. The ectoperitrophic space is continuous in pH with the endoperitrophic space and therefore can control pH across the whole width of the alimentary canal.

A simplified version of the new model for luminal pH buffering of larval mosquito alimentary canal is illustrated in Figure 3-12. Epithelial cells are metabolically active and

produce CO_2. CO_2 can diffuse through the epithelial cells and into the lumen where a luminal CA in the ectoperitrophic space catalyzes the conversion of CO_2 to HCO_3^-. CA catalyzes the same reaction within the epithelial cells, generating H^+. In the GC and PMG, an apically located V-ATPase hyperpolarizes the membrane by pumping H^+ from the cells into the lumen. By contrast, in the AMG epithelium, a basally located V-ATPase is positioned to move H^+ ions vectorally out of the cells (Zhuang et al., 1999), resulting in a transepithelial potential that is lumen-negative (Clark et al., 1999). This results in the loss of H^+ from HCO_3^-, forming CO_3^{2-}.

In addition to revising the model for midgut alkalization, I have demonstrated the potential for RNA interference-mediated CA silencing. Although there has been little success in down-regulating protein expression in anopheline mosquito larvae, I have shown that it is possible in an *An. gambiae* larval cell line. Because the half life of the protein of interest is an important factor in RNAi, not all proteins can be down-regulated using this mechanism. Through my cell culture work I have shown that at least one CA has the potential to be down-regulated in live larvae using RNAi.

Future directions: There remain at least six uncharacterized CA genes present by the *An. gambiae* genome. The cloning and characterization of these genes will further complete the model for midgut alkalization in mosquito larvae. Additionally, although the localization of a CA in the ectoperitrophic space offers an alternative mechanism for HCO_3^- access to the lumen, localization of predicted anion exchangers is still a major goal of the laboratory. Some progress towards this goal is described in appendix A of this manuscript.

Whereas demonstration of AgCA9 mRNA silencing in the Ag55 cell line was a first step in identifying the role of this CA, similar experiments in live larvae have not been as successful. To investigate the reasons for poor RNAi success in larvae, I suggest silencing AgCA9 using

RNAi in adult mosquitoes. This technique is used often and is widely successful in adults, and will indicate if there is an inherent problem with the gene being silenced, or with the larval stages of the mosquito life cycle, which makes RNAi silencing of AgCA9 in larvae a difficult endeavor. An alternative approach to RNAi silencing in mosquito larvae is the development of transgenic larvae. By microinjecting preblastoderm embryos with a CA gene linked to a genetic drive system such as a transposable element, larvae can be genetically manipulated to express CA-specific inverted-repeat sequences which form dsRNA in the larvae (see Franz et al., 2006).

Ion Regulation in the Larval Rectum

Conclusions: Through AgCA9 protein localization, I revealed an unexpected staining pattern which identified a novel subset of cells in the larval anopheline rectum. I discovered that the larval anopheline rectum differs from that of the larval culicine rectum in structure and in regulation of protein expression, suggesting that anophelines and culicines regulate hemolymph osmolarity in slightly different ways. Specifically, the larval anopheline rectum appears to shift primary distribution of Na^+K^+-ATPase protein from the non-DAR cells in fresh water-reared larvae, to the DAR cells of saline water-reared larvae. This is in stark contrast to culicine larvae which do not appear to shift protein distribution in response to salinity.

Additionally, I demonstrated that the anopheline DAR cells differ functionally from the non-DAR cells in basal membrane H^+ flux, as well as in the proteins mediating that flux. Finally, I showed that an anion exchange inhibitor, DIDS, and a V-ATPase inhibitor, concanamycin A, had different effects on the DAR and non-DAR cells, respectively, of larvae reared in fresh versus saline water, suggesting a change in protein function in response to salinity.

Together my immunohistochemical, physiological, and pharmacological data support the hypothesis that the major cell type of the anopheline rectum, the non-DAR cells, changes its

primary function from that of absorption in larvae reared in fresh water, to secretion in larvae reared in saline water. This suggests a remarkable method of adaptation which has not been described in mosquitoes to date. These data not only prompt the development of a new model for anopheline ion regulation in the rectum (Figure 6-3), but also stress the differences between anopheline and culicine larvae. It is clear from this data that anophelines and culicines differ in very important ways, and that data generated in culicine species cannot necessarily be applied to anopheline species and vice versa. Importantly, these differences may affect larval response, or adaptation, to vector control strategies.

Future directions: To test my hypothesis regarding a change in anopheline rectal function, the absorptive and secretive properties of the DAR and non-DAR cells must be characterized. This can be done using *in vitro* rectal ligation studies monitoring the concentration and volume of fluid accumulated in each region over time (see Bradley and Phillips, 1977). However, the difficulty lies in identifying, and separating the DAR and non-DAR cells using a dissecting microscope.

Perhaps an easier approach to further characterizing the function of the larval anopheline rectal cell types is to perform a similar physiological study on the recta of culicine larvae, the functions of which have already been determined. By comparing basal H^+ flux and pharmacological inhibition of that flux of either the freshwater culicine rectum, or the saline-tolerant culicine AR and PR, to that of the anopheline DAR and non-DAR cells, predications regarding function can be made.

Final Thoughts

As I have stressed throughout this manuscript, a thorough and detailed understanding of mosquito biology and physiology can facilitate the development of safe and effective control methods. The cloning and characterization of several CAs from the larval mosquito alimentary

canal have emphasized the global importance of this enzyme family to mosquito survival. CA is a central player in larval pH and ion regulation, two processes crucial for larval adaptation and survival. Additionally, CA activity is important to adult disease transmission. Recent unpublished work in malaria transmission assays indicate that CA inhibitors may block *Plasmodium* infection of mosquitoes, thereby interfering with the spread of this deadly disease (M. P. Corena, P. J. Linser, personal communication). I am confident that by characterizing the remaining six *An. gambiae* CAs, we will uncover new roles for this enzyme in both larval regulation strategies and adult-plasmodium interactions.

My research has not only revealed methods of pH and ion regulation in mosquito larvae not previously known, but has also shown that previous models of these processes may have been inaccurate. Specifically, the newly characterized structure and function of of the larval anopheline rectum stresses the idea that two subfamilies of mosquitoes, culicines and anophelines, are in fact very different. Presently, much larval research, including the majority of research on ion regulation, is performed on culicine mosquitoes; my work emphasizes the importance of conducting parallel research on anopheline species, the most important malaria vectors. The differences between these two subfamilies may have profound effects on larval adaptation and/or response to vector control methods, and these differences may translate to the adult stage as well. By not fully understanding the biology, physiology, and pharmacology of anophelines, the sole vectors for human malaria, we will continue to fail at eradication of this and other vector born diseases.

APPENDIX A
CLONING AND CHARACTERIZATION OF MEMBERS OF THE SLC-4 BICARBONATE TRANSPORTER FAMILY FROM *ANOPHELES GAMBIAE* SENSU STRICTO LARVAE

This appendix describes data generated towards aim one of my proposal: to clone, characterize, and localize the expression of members of the Cl^-/HCO_3^- transporter gene family in the larval mosquito alimentary canal. The work reported here addresses several key issues in regards to this aim but must be expanded to produce a publishable story.

Introduction

The previous model for AMG alkalization in mosquito larvae proposed that HCO_3^- generated by cytoplasmic CA was translocated into the alimentary canal lumen by HCO_3^- transporters and then paired with a strong cation (X^+) to buffer the lumen as either X_2CO_3 or $XHCO_3$ (Boudko et al., 2001b). This model was recently updated based on data which suggested that a luminal CA in the alimentary canal obviates the need for plasma membrane HCO_3^- transporters in AMG alkalization (Smith, K. E. et al., 2007; Chapter 3 of this manuscript). However, CA is also expressed in the cells of the alimentary canal, particularly in the GC and rectum, catalyzing HCO_3^- production within those cells (Smith, K. E. et al., 2007; Chapter 3 of this manuscript). HCO_3^- is a membrane impermeant ion and requires a transport protein to cross the plasma membrane for absorption into the hemolymph or excretion into the lumen (McMurtrie et al., 2004). Based on this requirement, I predict that plasma membrane HCO_3^- transporters localize to the membranes of epithelial cells to translocate HCO_3^- from the cells into the hemolymph or lumen. HCO_3^- transporters belong to the solute carrier 4 (SLC4) gene family and have been described in detail in *H. sapiens* (Romero et al., 2004). Many of the characterized *H. sapiens* SLC4 genes share considerable homology with genes predicted by the *An. gambiae* and *Ae. aegypti* genomes.

As reviewed by Romero et al. (2004), the SLC4 family of HCO_3^- transporters consists of integral membrane proteins that transport bicarbonate or carbonate across the plasma membrane in exchange for at least one monoatomic ion. Proteins are characterized by 10-14 transmembrane domains which separate long N-terminal and shorter C-terminal hydrophilic domains, both of which are intracellular. Based on physiological characterization of *H. sapiens* SLC4 proteins, the family includes three functional subgroups: electroneutral Cl^--HCO_3^- exchangers, electrogenic Na^+/ HCO_3^- cotransporters and electroneutral Na^+-coupled HCO_3^- transporters.

Despite having structural and functional similarities, the three SLC4 subgroups differ in their specific transport properties (Figure A-1). The electroneutral Cl^--HCO_3^- exchangers transport Cl^- and HCO_3^- across most mammalian membranes in a 1:1 electroneutral exchange (Sterling et al., 2001). In most cell types, these exchangers drive the exchange of extracellular Cl^- for intracellular HCO_3^-, but the reaction is bidirectional and direction depends on the transmembrane chemical gradients of the substrates (Romero et al., 2004). The electrogenic Na^+/ HCO_3^- cotransporters (NBCe) mediate movement in the same direction of one Na^+ and two or three HCO_3^-. In most cases, the NBCes move one Na^+ and two HCO_3^- into a cell, thereby generating a net negative charge within that cell; however, there are notable exceptions to this rule (Romero et al, 2004). The electroneutral Na^+-coupled HCO_3^- transporters mediate the movement of Na^+ and HCO_3^- across the plasma membrane in one of three ways, defined by each of three *H. sapiens* proteins belonging to this group: (1) NBCn1 mediates the uptake of one Na^+ and one HCO_3^-, but no Cl^-; (2) NDCBE mediates the uptake of one Na^+ and two HCO_3^-, coupled with the exit of one Cl^-; and (3) NCBE was originally thought to be a Na^+-driven Cl^--HCO_3^-

transporter, although there is preliminary evidence against a Cl^- requirement (Romero et al., 2004).

Boudko et al., (2001a) reported clear evidence of an electroneutral Cl^--HCO_3^- exchanger in the AMG of *Ae. aegypti* larvae. They detected a strong Cl^-/ HCO_3^- concentration difference across the AMG epithelium, with low levels of Cl^- in the lumen and high levels in the hemolymph. By contrast, HCO_3^- had the inverse distribution. These results suggest that the lumen is being supplied with a source of HCO_3^- while simultaneously being depleted of Cl^-. Additionally, Boudko et al., (2001a) reported a strong Cl^- efflux from the epithelial cells into the hemolymph which was inhibited by the anion exchange blocker DIDS, thus providing further evidence for AE mediated Cl^- movement. They hypothesized that CA in the cytoplasm of the epithelial cells catalyzes the production of HCO_3^-, which is transported into the lumen by a HCO_3^- transporter in exchange for a Cl^- ion. The Cl^- ion is then transported from the cytoplasm into the hemolymph via a nonspecific chloride channel (Boudko et al., 2001a).

There are three SLC4 genes (AgAEs) predicted to be present in the *An. gambiae* genome. Members of the Linser laboratory have previously cloned one gene, AgAE1, from *An. gambiae* cDNA (genbank accession #AY280611) (T. J. Seron, personal communication; M. V. Neira, personal communication). This gene is orthologous to the *H. sapiens* electroneutral Na^+-coupled HCO_3^- transporters as well as to another insect gene, *D. melanogaster* Na^+-coupled HCO_3^- transporter, NDAE1 (Romero et al., 2000), which exchanges Na^+ and HCO_3^- for Cl^- and H^+. The remaining two *An. gambiae* SLC4 genes, AgAE2 and AgAE3, are predicted to be orthologous to the *H. sapiens* AE genes. Here I describe the cloning of AgAE3, and the mRNA characterization of AgAE2 and AgAE3, from the *An. gambiae* larval alimentary canal. Additionally, I suggest

putative functions for AgAE1, AgAE2, and AgAE3 based on a phylogenetic analysis comparing SLC4 proteins from *H. sapiens*, *D. melanogaster*, *Ae. aegypti*, and *An. gambiae* genomes.

Results

Phylogenetic Analysis

A phylogenetic tree was generated to compare the predicted and cloned SLC4 proteins from *H. sapiens*, *D. melanogaster*, *Ae. aegypti*, and *An. gambiae* genomes (Figure A-2). The tree showed a distinct clustering of *H. sapiens* SLC4 proteins into three main groups: electroneutral Cl^--HCO_3^- exchangers (SLC4A1-3), electrogenic Na^+-HCO_3^- cotransporters (SLC4A4 and 5), and electroneutral Na^+-coupled Cl^--HCO_3^- transporters (SLC4A7, 8, and 10). SLC4A9, a protein with uncertain function, clustered with the electrogenic Na^+-HCO_3^- cotransporters. SLC4A11, a protein with no functional data available, clustered away from all other proteins.

Insect SLC4 proteins formed clusters which were distinct from those of the *H. sapiens*. AgAE1 and its *Ae. aegypti* ortholog clustered with *D. melanogaster* NDAE1. Together these proteins clustered closer to the *H. sapiens* Na^+-dependent HCO_3^- transporters, both the electrogenic Na^+-HCO_3^- cotransporters and the elecroneutral Na^+-coupled Cl^-- HCO_3^- transporters, than to the electroneutral Cl^--HCO_3^- exchangers. AgAE2 and AgAE3 (starred) clustered with their uncharacterized *Ae. aegypti* and *D. melanogaster* orthologs, and this group of proteins clustered closely with the *H. sapiens* electroneutral Cl^--HCO_3^- exchangers.

Cloning and Characterization of Full-Length AgAE3 cDNA from *An. gambiae* Larvae

An internal fragment of the AgAE3 cDNA was cloned from the *An. gambiae* larval alimentary canal using gene specific primers; the primers were designed according to the partial cDNA sequence predicted by Ensembl. Using gene-specific sequences from this fragment, RACE was used to amplify and sequence the 3' and 5' ends of the gene (see Table 2-1 for

AgAE3 RACE primers). The full-length cDNA (genbank accession #EU068741) is 2,983 basepairs and spans both the start and stop codons. The cDNA was determined to be full length by the presence of a stop codon in the 5' UTR and the presence of a 3' poly-A tail. AgAE3 is located on chromosome 3L (www.vectorbase.org).

The full length AgAE3 cDNA is predicted to translate to a protein product of 993 amino acids with a molecular mass of 108 kDa (http://bioinformatics.org/sms/). A hydrophobicity plot (Figure A-3; DNAMAN, version 3.2, Lynnon Biosoft©, Quebec, Canada) indicated AgAE3 contains ten hydrophobic transmembrane domains (Figures A-3 and A-4). A protein alignment between AgAE3, AgAE1, *H. sapiens* SLC4A1 (electroneutral Cl^--HCO_3^- exchanger), and splice variants of *H. sapiens* SLC4A5 (electrogenic Na^+/ HCO_3^- cotransporter), *H. sapiens* SLC4A8 (electroneutral Na^+-coupled HCO_3^- transporter), and *D. melanogaster* NDae1 demonstrated that AgAE3 shares considerable homology with other known SLC4 proteins (Figure A-4). A second protein alignment between the three predicted *An. gambiae* AgAEs, AgAE1, AgAE2, AgAE3 (Figure A-5), indicated that AgAE3 shares 27% identity with AgAE1 and 59% identity with AgAE2.

AgAE mRNA Expression in Alimentary Canal Regions

Quantitative PCR (qPCR) was used to detect AgAE mRNA within the mosquito larval alimentary canal. AgAE3 and AgAE2 mRNA expression levels were evaluated from cDNA derived from either whole larval alimentary canal, GC, AMG, PMG, MT or rectum. The results were normalized to the *An. gambiae* 18s ribosomal RNA gene and reported relative to whole larval alimentary canal (Figure A-6). AgAE2 and AgAE3 mRNA were detected in every region tested; however, each region expressed the AgAEs at different levels. AgAE2 was evenly distributed in the GC, AMG, and MT, with less expression detected in the PMG and rectum. No single region expressed AgAE2 significantly above whole larval alimentary canal levels. By

contrast, AgAE3 was significantly expressed by the AMG (P-Value < 0.001) and MT (P-Value < 0.01) above whole larval alimentary canal levels.

Discussion

AgAE3, a member of the SLC4 HCO_3^- transporter family, was cloned from, and mRNA expression was characterized in, the alimentary canal of *An. gambiae* larvae. The predicted protein consists of 993 amino acids and ten predicted hydrophobic transmembrane domains. AgAE3 shares 59% identity with another *An. gambiae* HCO_3^- transporter, AgAE2, and indeed the two AgAEs cluster together in a phylogenetic analysis. AgAE3 shares less similarity with a previously cloned AgAE, AgAE1, and clusters away from this AgAE. These data support the prediction that AgAE3 and AgAE2 function as electroneutral Cl^--HCO_3^- exchangers, whereas AgAE1 functions as a Na^+-coupled HCO_3^- transporter.

The phylogenetic analysis also identified distinct groups of *H. sapiens* SLC4 proteins, and as expected, proteins known to have similar functions cluster together in one of three main groups: electroneutral Cl^--HCO_3^- exchangers, electrogenic Na^+-HCO_3^- cotransporters, and electroneutral Na^+-coupled Cl^--HCO_3^- transporters. An unexpected result was the placement of SLCA9, which clustered with the electrogenic Na^+-HCO_3^- cotransporters. Although the function of SLC4A9 is still under question, Romero et al (2004) reported that its cDNA is most closely related to the electroneutral Na^+-coupled Cl^--HCO_3^- transporters. By contrast, functional studies suggest SLC4A9 behaves as an electroneutral Cl^--HCO_3^- exchangers (Ko et al., 2002). At this time, there is no physiological evidence to support SLC4A9 clustering with the electrogenic Na^+-HCO_3^- cotransporters.

One striking property of the *H. sapiens* and *D. melanogaster* SLC4 family members is the existence of numerous splice variants for each gene. In the *H. sapiens* genome, 29 individual variants exist for a total of ten genes. In the *D. melanogaster* genome, 13 individual variants

exist for a total of two genes. Multiple splice variants may also exist for *An. gambiae* or *Ae. aegypti* SLC4 members; this prediction is supported by data indicating the presence of numerous forms of the previously cloned AgAE1, each which differ slightly at the 3' cytoplasmic tail (M. V. Neira, personal communication). Splice variants of a single gene could represent amplification products of incompletely spliced pre-mRNA, as in the case of *H. sapiens* SLC4A5 (Romero et al., 2004). Alternatively, splice variants could be functional transcripts of a single gene which differ in regions required for regulation, thereby allowing a tighter control over the expression, and subsequent activity, of certain genes.

AgAE mRNA expression was examined in the five main regions of the larval alimentary canal, the GC, AMG, PMG, MT, and rectum, using qPCR. An even distribution of AgAE2 mRNA was detected in the GC, AMG and MT with less expression in the PMG and rectum, although AgAE2 was not detected at significant levels in any region above whole alimentary canal levels. This is supported by data generated from microarray analysis which detected slightly more AgAE2 mRNA in the GC and AMG than in the PMG or hindgut (MT and rectum combined) samples (Neira et al., 2008). By contrast, AgAE3 mRNA was more abundant than AgAE2 in all regions of the alimentary canal, although only expression in the AMG and MT was considered statistically significant compared to whole alimentary canal levels. This expression pattern is not consistent with microarray data published by members of the Linser laboratory (Neira et al., 2008) which detected approximately equal concentrations of AgAE3 mRNA in all alimentary canal regions, none of which significantly express AgAE3 above the whole larval insect sample.

There are several possible explanations for the contradicting AgAE3 mRNA expression data. Each technique detects a specific, but distinct sequence of AgAE3 cDNA. If, as predicted,

there are several splice variants of AgAE3, the two techniques may have identified two individual forms of the mRNA. Additionally, the microarray analysis compared mRNA expression in each alimentary canal region to whole insect, whereas qPCR analysis compared mRNA expression in each region to whole alimentary canal. If there is significant AgAE3 mRNA expression in the larval carcass, these two quantitative techniques would report different results. Finally, the qPCR data is questionable in that the sum of mRNA expression in the alimentary canal parts exceeds that of the whole. This data represents an average of four biological replicates each of which consistently indicated similar expression patterns. Presently there is no explanation for such results and this issue will need to be resolved prior to publishing AgAE mRNA characterization.

Conclusions: In conclusion, I have cloned a full-length version of an *An. gambiae* SLC4 family member, AgAE3. Phylogenetic analysis suggests that AgAE3 is homologous to another *An. gambiae* SLC4 member, AgAE2, and that both AgAEs are most similar to the *H. sapiens* electroneutral Cl^--HCO_3^- exchangers. QPCR analyses indicate that mRNA of both AgAEs is present throughout the alimentary canal, although at different levels in each region. Additionally, it is predicted that the two genes express multiple transcripts; numerous splice variants of an AgAE could potentially increase the mRNA in each region, and may also increase the level of regulation possible. These two AgAE genes, along with the previously cloned AgAE1 gene, are likely to be responsible for the transport of HCO_3^- from the epithelial cells into the lumen or hemolymph of the alimentary canal. Identification of protein localization and demonstration of activity will shed new light on an important step in both pH- and ion-regulation in the larval mosquito alimentary canal.

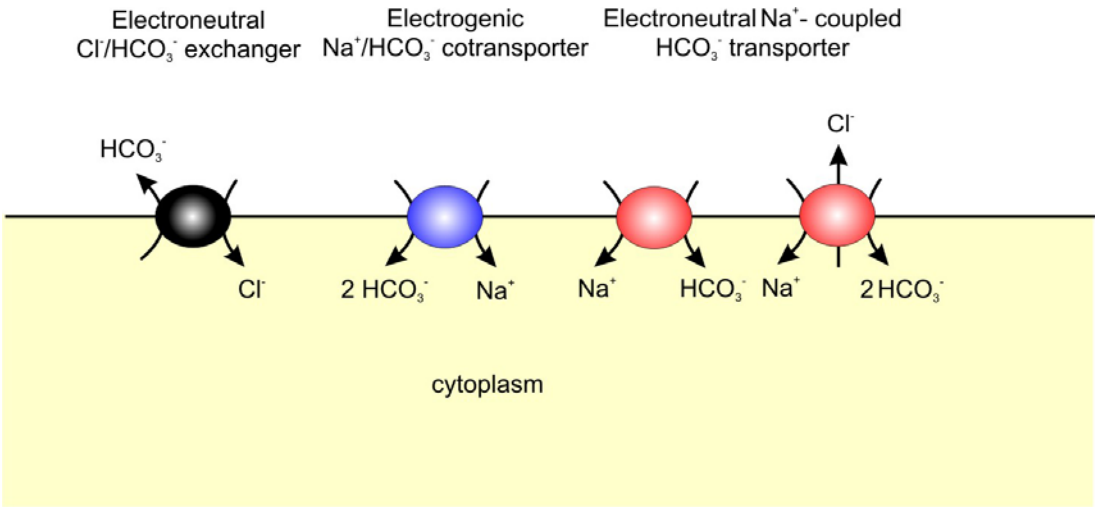

Figure A1. Function of *H. sapiens* SLC4 proteins. Electroneutral Cl^--HCO_3^- exchangers transport Cl^- and HCO_3^- across most mammalian membranes in a 1:1 electroneutral exchange, usually exchanging extracellular Cl^- for intracellular HCO_3^-. Electrogenic Na^+/ HCO_3^- cotransporters mediate movement in the same direction of one Na^+ and two or three HCO_3^-, usually transporting both ions into of the cell. Electroneutral Na^+-coupled HCO_3^- transporters mediate the movement of Na^+ and HCO_3^- across the plasma membrane by at least two known mechanisms. One mechanism includes the uptake of one Na^+ and one HCO_3^-, but no Cl^-, transporting both ions into the cell. The second mechanism includes the uptake of one Na^+ and two HCO_3^- into the cell, coupled with the exit of one Cl^-.

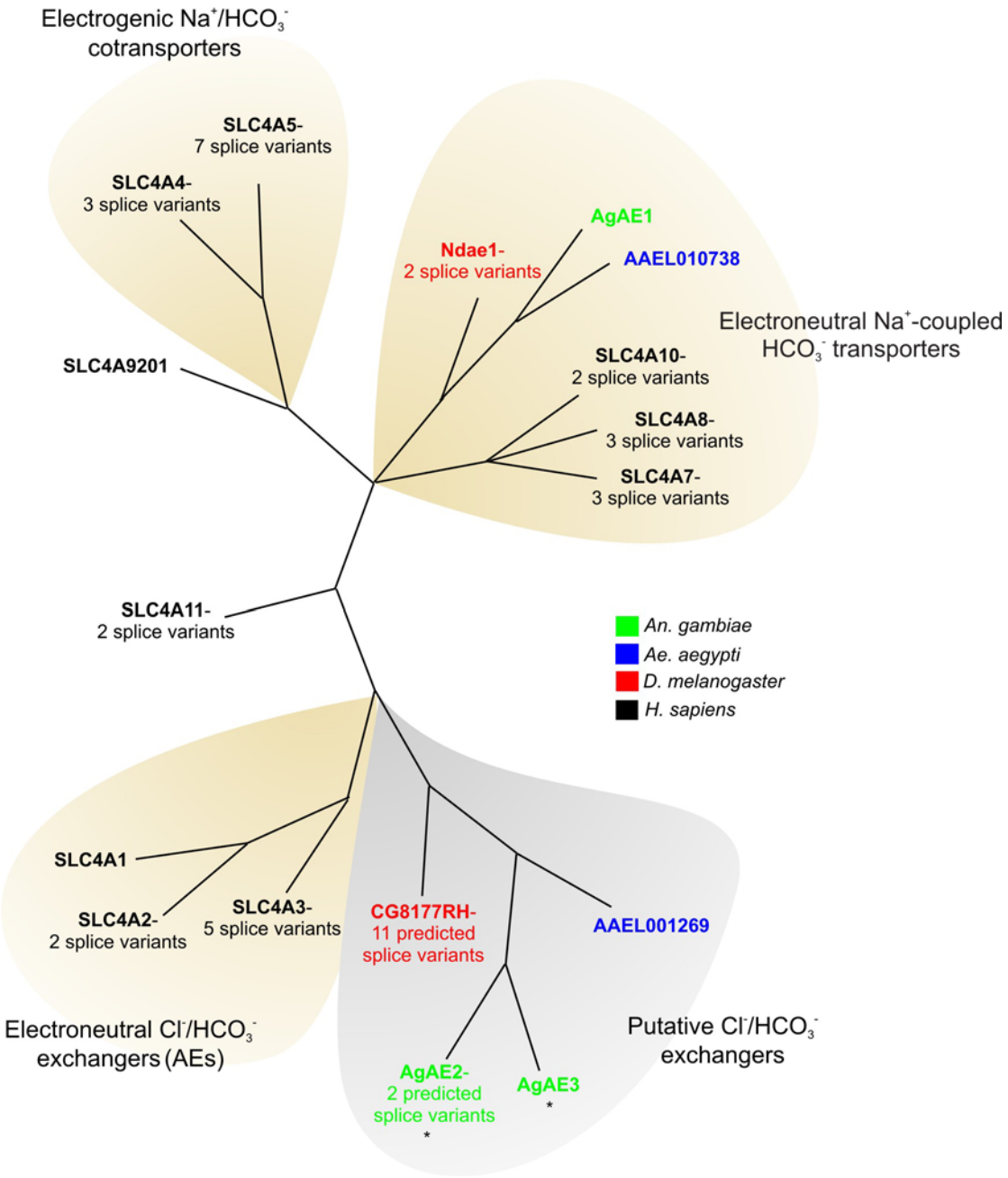

Figure A-2. Phylogenetic analysis of members of the SLC4 family in *H. sapiens* (black), *D. melanogaster* (red), *Ae. aegypti* (blue), and *An. gambiae* (green) genomes. Phylogeny was prepared using MrBayes with the JTT amino acid substitution model and 1.5 million iterations. AgAE2 and AgAE3 are starred.

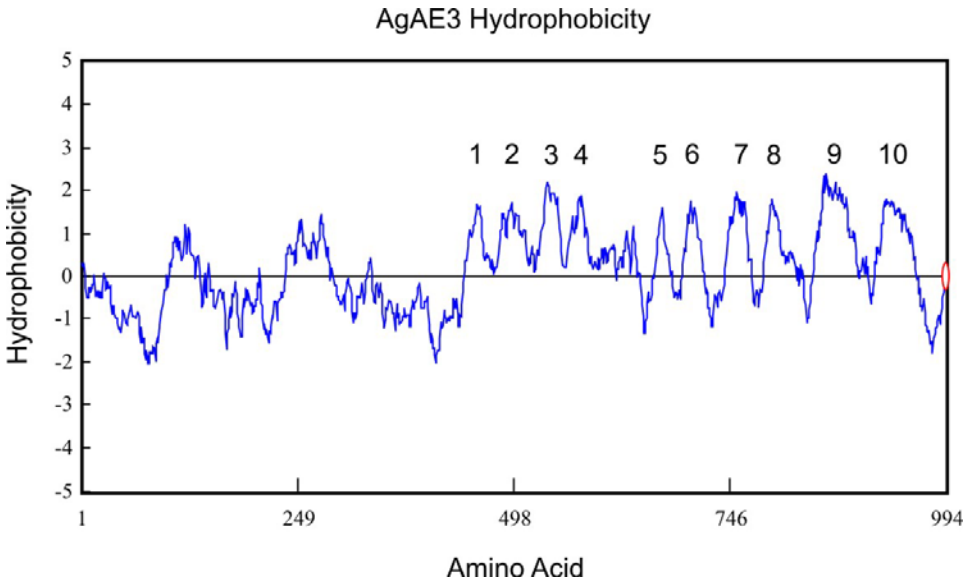

Figure A-3. Hydrophobicity plot of AgAE3. The graph plots the predicted hydropathy (Y-axis) of a protein against the amino acid sequence (X-axis). AgAE3 is predicted to consist of ten transmembrane domains which are identified numerically.

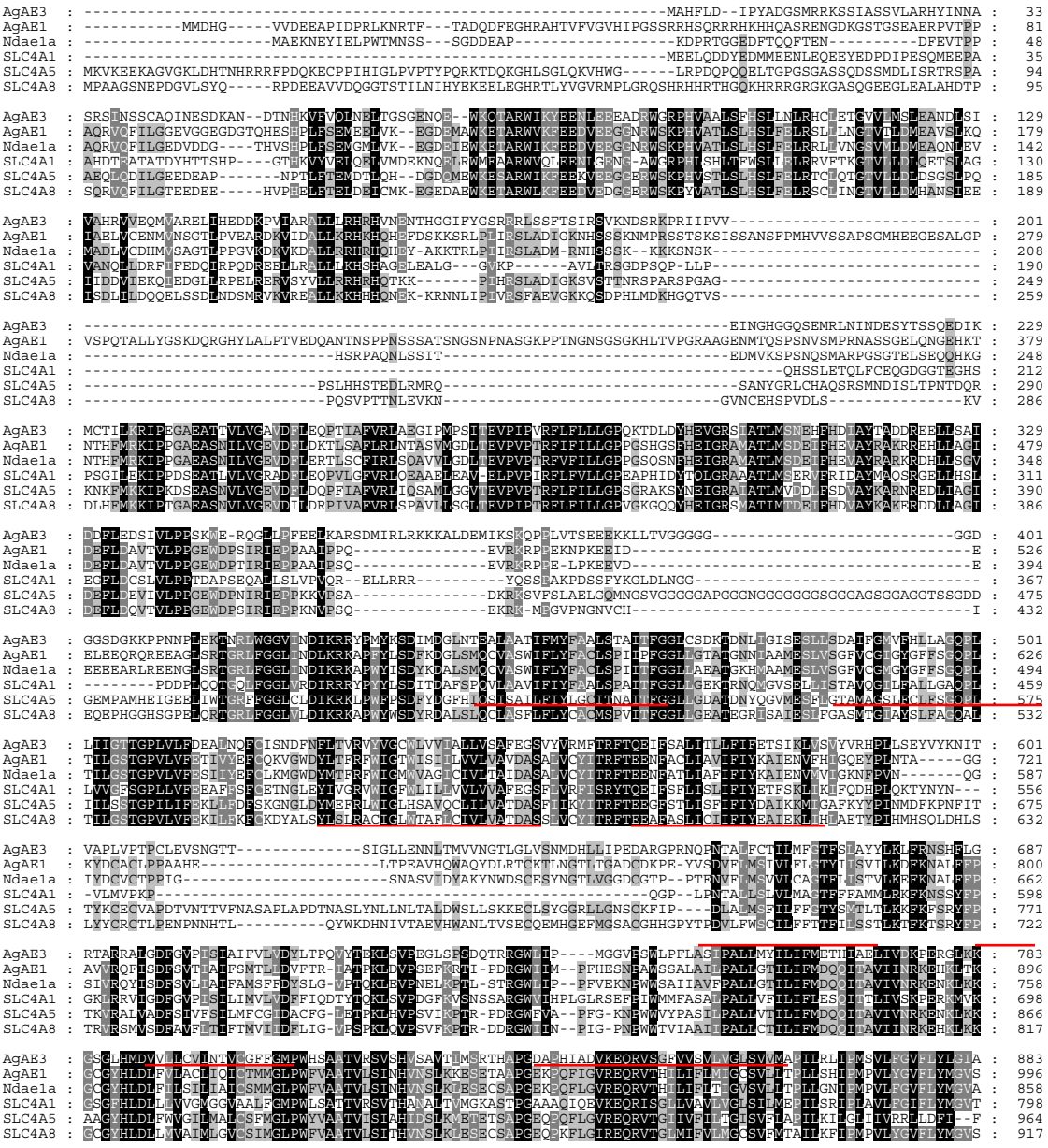

Figure A-4. Protein alignment between *An. gambiae* AgAE3 and AgAE1, *H. sapiens* SLC4A1, and splice variants of *H. sapiens* SLC4A5, *H. sapiens* SLC4A8, and *D. melanogaster* NDae1. Alignment demonstrates that AgAE3 shares significant homology with other known SLC4 proteins. Regions with high similarity are highlighted in black (100%). Regions of lesser similarity are highlighted in grey (>80%) and light grey (>60%). Predicted transmembrane domains are indicated with red bars.

```
AgAE1  : ADDLHQLEDGEDSGRHSADNLQLPLENGTVNEKGKINISEEVNRTTIWKQVNNCNVLFTKKQTPVKHSQQQLSKLSETEKRLSTMREEDEVADEPSRQLS : 1196
Ndae1a : ADDLHKLDAEVG-----------------------------------------LLARIFPWGKGSR------------------SRVVTKPP---- :  991
SLC4A1 : EGRDEYDEVAMPV-------------------------------------------------------------------------------------- :  911
SLC4A5 : ---------------------------------------------------------------------------------------------------- :    -
SLC4A8 : LDDAKKKAKEEE-------------------------------------------------------------------------------------- : 1027

AgAE3  : ------------------------------------------------------------------ :    -
AgAE1  : HQKRTQKMKREFWMNSRSGSSNGRANSNNSASSTTAAAGGKIVCAEESAALSRGSSKSASETQV : 1260
Ndae1a : ------------------GLDDGIVGSGG------AVGAGLITCTTSNANEKEFEAQSSLLKK- : 1030
SLC4A1 : ------------------------------------------------------------------ :    -
SLC4A5 : ------------------------------------------------------------------ :    -
SLC4A8 : ----------------------------------------VIVLAPTVYLGASNYRT------ : 1044
```

Figure A-4. Continued.

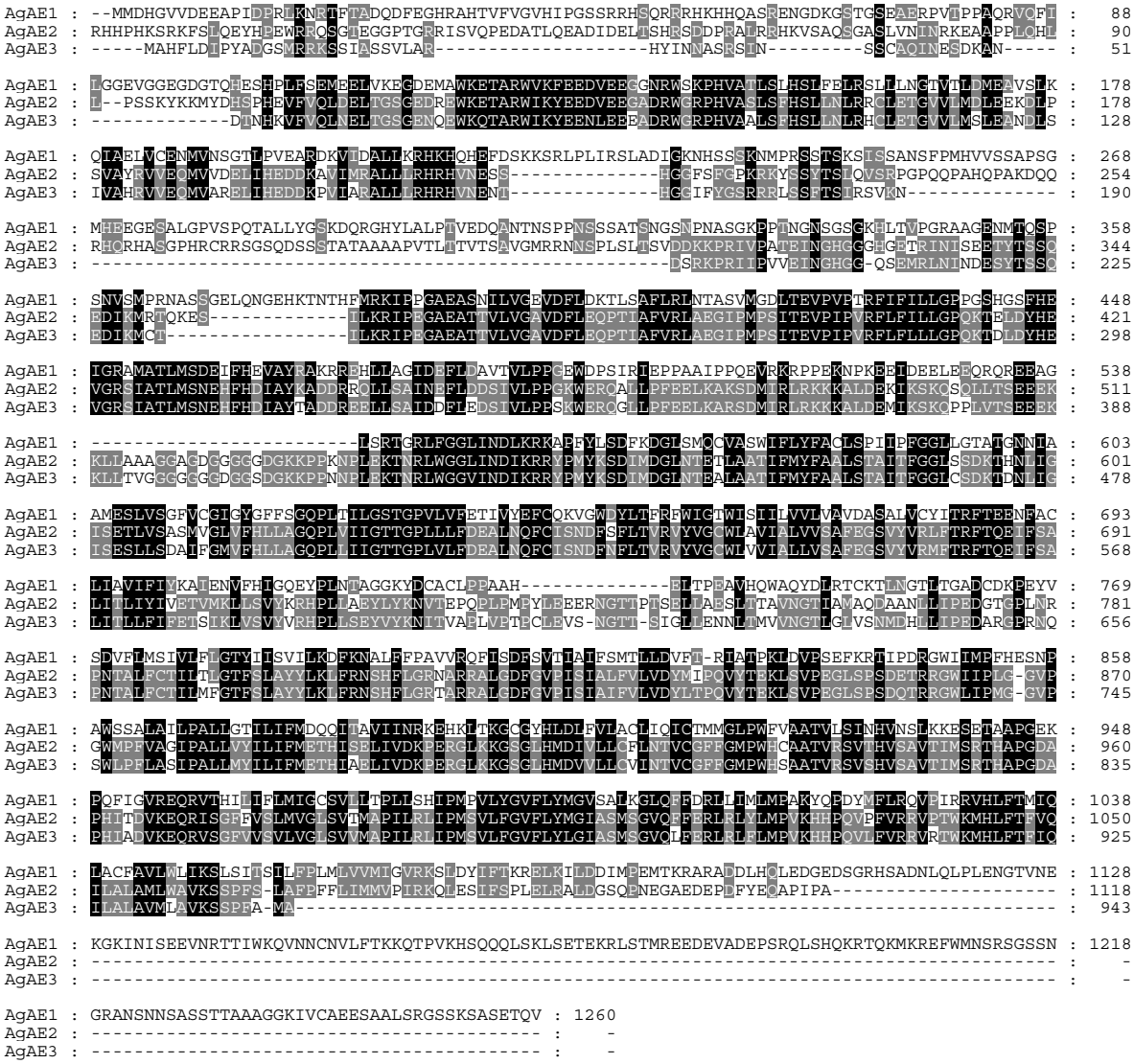

Figure A-5. Protein alignment between *An. gambiae* AgAE1, AgAE2, and AgAE3. Alignment demonstrates that AgAE3 shares a higher sequence identity with AgAE2 (59%) than with AgAE1 (27%). Regions with high similarity are highlighted in black (100%). Regions of lesser similarity are highlighted in grey (>80%) and light grey (>60%).

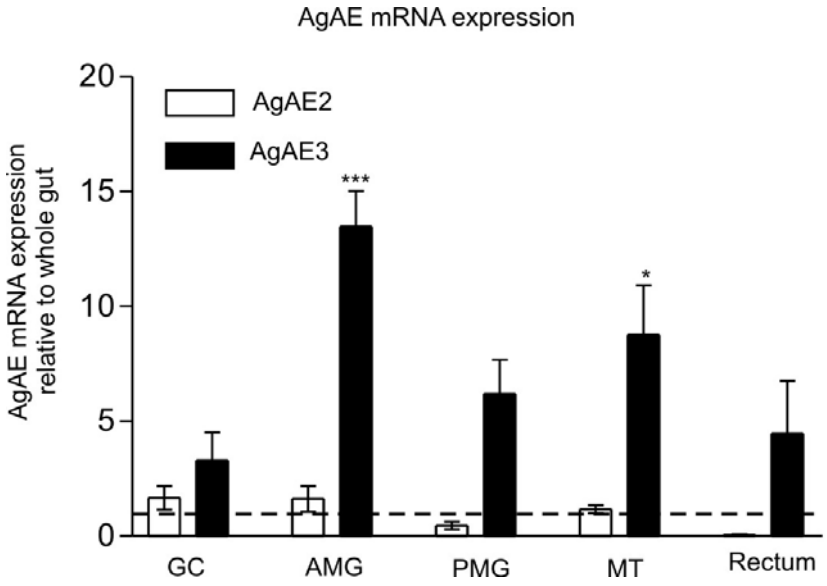

Figure A-6. AgAE mRNA expression in the regions of *An. gambiae* alimentary canal ad determined by qPCR. Results were normalized to the *An. gambiae* 18s ribosomal RNA gene and reported relative to whole larval alimentary canal. 'Whole alimentary canal' sample was normalized to a value of "1" and is indicated by a dashed line. Error bars indicate standard error between three (AgAE2) or four (AgAE3) individual runs. Abbreviations: AMG, anterior midgut; GC, gastric caeca; MT, Malpighian tubules; PMG, posterior midgut. *: P-Value < 0.05; ***: P-Value < 0.001.

LIST OF REFERENCES

Adelman, Z. N., Blair, C. D., Carlson, J. O., Beaty, B. J. and Olson, K. E. (2001). Sindbis virus-induced silencing of dengue viruses in mosquitoes. *Insect Mol. Biol.* **10**(**3**), 265-73.

Alber, B. E. and Ferry, J. G. (1996). Characterization of heterologously produced carbonic anhydrase from Methanosarcina thermophila. *J Bacteriol*. **178(11)**, 3270-3274.

Anderson, R. E., Gay, C. V. and Schraer, H. (1982). Carbonic anhydrase localization by light and electron microscopy. *J. Histochem. Cytochem.* **30(11)**, 1135-1145.

Asakura, K. (1970). Studies on the structural basis for ion- and water-transport by the osmoregulatory organs of mosquitoes. I. Fine structure of the rectal epithelium of *Aedes albopictus* larvae. *Sci. Rep. Kanazawa Univ.* **1**, 37-55.

Azuma, M., Harvey, W. R. and Wieczorek, H. (1995).Stoichiometry of K^+/H^+ antiport helps to explain extracellular pH11 in a model epithelium. *FEBS Lett.* **361**, 53–156.

Bailey, D. L., Kaiser, P. E., Focks, D. A. and Lowe, R. E. (1981). Effects of salinity on *Anopheles albimanus* ovipositional behavior, immature development, and population dynamics. *Mosquito news*. **41(1)**, 161-167.

Berenbaum, M. (1980). Adaptive significance of midgut pH in larval Lepidoptera. *Am. Nat.* **115**, 138-146.

Beyenbach, K. W. (1995). Mechanisms and regulation of electrolyte transport in Malpighian tubules. *J. Insect Physiol.* **21**, 197-207.

Beyenbach, K. W. (2003). Transport mechanisms of diuresis in Malpighian tubules of insects. *J. Exp. Biol.* **206**, 3845-3856.

Blandin, S., Moita, L. F., Köcher, T., Wilm, M., Kafatos, F. C. and Levashina, E. A. (2002). Reverse genetics in the mosquito *Anopheles gambiae*: targeted disruption of the Defensin gene. *EMBO reports*. **3**, 852-856.

Blitzer, E. J., Vyazunova, I. and Lan, Q. (2005). Functional analysis of AeSCP-2 using gene expression knockdown in the yellow fever mosquito, *Aedes aegypti*. *Insect Molec.Biol*. **14**, 301-307.

Boisson, B., Jacques, J. C., Choumet, V., Martin, E., Xu, J., Vernick, K. and Bourgouin, C. (2006). Gene silencing in mosquito salivary glands by RNAi. *FEBS Lett.* **580**(**8**), 1988-92.

Boron, W. F. (2001) Sodium-coupled bicarbonate transporters. *JOP*. **2**, 176-181.

Boudko, D. Y., Moroz, L. L., Harvey, W. R. and Linser, P. J. (2001a). Alkalinization by chloride_bicarbonate pathway in larval mosquito midgut. *Proc. Nat. Ass. Sci*. **98(26)**, 15354-15359.

Boudko, D. Y., Moroz, L., Linser, P. J., Trimarchi, J. R., Smith, P. J. S. and Harvey, W. R. (2001b). In situ analysis of pH gradients in mosquito larvae using noninvasive, sefl-referencing, pH-selective microelectrodes. *J. Exp. Biol.* **204**, 691-699.

Boudko, D. Y., Stevens, B. R., Donly, B. C. and Harvey, W. R. (2005). Nutrient amino acid and neurotransmitter transporters. In *Comprehensive Molecular Insect Science*. Vol. 4 (ed. K. Latrou, S. S. Gill and L. I. Gilbert), pp. 255-309. Amsterdam: Elsevier.

Bradley, T. J. (1987a). Evidence for hypo- and hyperosmotic regulation in the larvae of an anopheline mosquito. *Amer. Zool*. **27(4)**, 130A.

Bradley, T. J. (1987b). Physiology of osmoregulation in mosquitoes. *Ann. Reb. Entomol*. **32**, 439-462.

Bradley, T. J. (1994). The role of physiological capacity, morphology, and phylogeny in determining habitat use in mosquitoes. In *Ecological Morphology*, ed. P. C. Wainwright and S. M. Reilly, 303-318, Chicago and London: The University of Chicago Press.

Bradley, T. J. and Phillips, J. E. (1975). The secretion of hyperosmotic fluid by the rectum of a saline-water mosquito larva, *Aedes taeniorhynchus*. *J. Exp. Biol*. **63**, 331-342.

Bradley, T. J. and Phillips, J. E. (1977). The location and mechanism of hyperosmotic fluid secretion in the rectum of the saline-water mosquito larvae *Aedes taeniorhynchus*. *J. Exp. Biol.* **66**, 111-126.

Breton S. (2001). The cellular physiology of carbonic anhydrases. *JOP*. **2(4 suppl)**, 159-164.

Breton, S., Smith, P. J., Lui, B. and Brown, D. (1996). Acidification of the male reproductive tract by a proton pumping (H^+)-ATPase. *Nat. Med.* **2(4)**, 470-472.

Breton, S., Tyszkowski, R., Sabolic, I. and Brown, D. (1999). Postnatal development of H^+ ATPase (proton-pump)-rich cells in rat epididymis. *Histochem. Cell Biol.* **111(2)**, 97-105.

Brown, A. E., Crisanti, A. and Catteruccia, F. (2003). Comparative analysis of DNA vectors at mediating RNAi in Anopheles mosquito cells and larvae. *J. Exp. Biol*. **206(Pt 11)**, 1817-823.

Brown, D. (1980). Carbonic anhydrase localization in mounted cryostat sections. *Stain Technol*. **55(2)**, 115-8.

Brown, D. and Kumpulainen, T. (1985). Immunocytochemical localization of carbonic anhydrase on ultrathin frozen sections with protein A-gold. *Histochem*. **83**, 153-158.

Brown, D., Kumpulainen, T., Roth, J. and Orci, L. (1983). Immunohistochemical localization of carbonic anhydrase in postnatal and adult rat kidney. *Am. J. Physiol.* **245(1),** F110-8.

Chegwidden, R.W. and Carter, N. D. (2000). Introduction to the carbonic anhydrases. In: Chegwidden, W.R., Carter, N.D., Edwards, Y.H. (Eds.), The Carbonic Anhydrases. New Horizons. Birkhäuser, Basel, pp. 105–120.

Clark, T. M., Koch, A. and Moffet, D. F. (1999). The anterior and posterior 'stomach' regions of larval *Aedes aegypti* midgut: regional specialization of ion transport and stimulation by 5-hydroxytryptamine. *J. Exp. Biol.* 202, 247-252.

Clark, T. M., Flis, B. J. and Remold, S. K. (2004). pH tolerances and regulatory abilities of freshwater and euryhaline Aedine mosquito larvae. *J. Exp. Biol*. **207**, 2297-2304.

Clark, T. M., Hutchinson, M. J., Huegel, K. L., Moffett, S. B. and Moffett, D. F. (2005). Additional morphological and physiological heterogeneity within the midgut of larval *Aedes aegypti* (Diptera: Culicidae) revealed by histology, electrophysiology, and effects of *Bacillus thuringiensis* endotoxin. *Tissue and Cell*. **37**, 457-468.

Clark, T. M., Vieira, M. A., Huegel, K. L., Flury, D. and Carper, M. (2007). Strategies for regulation of hemolymph pH in acidic and alkaline water by the larval mosquito Aedes aegypti (L.) (Diptera; Culicidae). *J. Exp. Biol*. **210(Pt 24)**, 4359-4367.

Clements, A. N. (1992). *The Biology of Mosquitoes*, vol 1 (ed. A.N. Clements). London,: Chapman & Hall.

Corena, M. P., Seron, T. J., Lehman, H. K., Ochrietor, J. D., Kohn, A., Tu, C. and Linser P. J. (2002). Carbonic anhydrase in the midgut of larval *Aedes aegypti*: cloning, localization and inhibition. *J. Exp. Biol.* **205 (Pt 5)**, 591-602.

Cronk, J. D., Cronk, M. R., O'Neill, J. W. and Zhang, K. Y. (2001). Crystal structure of E.coli beta-carbonic anhydrase, an enzyme with an unusual pH-dependent activity. Protein Sci. 5, 911-922.

Cronk, J. D., O'Neill, J. W., Cronk, M. R., Endrizzi, J. A. and Zhang, K. Y. (2000). Cloning, crystallization and preliminary characterization of a beta-carbonic anhydrase from *Escherichia coli*. *Acta Crystallogr. D. Biol. Crystallogr*. **56(Pt 9)**, 1176-1179.

Dadd, R. H. (1975). Alkalinity within the midgut of mosquito larvae with alkaline-active digestive enzymes. *Insect Phys.* **21**, 1847-1853.

Dow, J. A. T. (1984). Extremely high pH in the biological systems: a model for carbonate transport. *Am. J. Physiol.* **246,** R633-R635.

Edwards, H. A. (1982). Ion concentration and activity in the haemolymph of *Aedes aegypti* larvae. *J. Exp. Biol.* **101**, 143-151.

Edwards, M. J. and Jacobs-Lorena, M. (2000). Permeability and disruption of the peritrophic matrix and caecal membrane from *Aedes aegypti* and *Anopheles gambiae* mosquito larvae. *Insect Phys*. **46**, 1313-1320.

Ehrenfeld, J. and Klein, U. (1997). The key role of the H^+ V-ATPase in acid-base balance and Na^+ transport processes in frog skin. *J. Exp. Biol.* **200**, 247-256.

Filippova, M., Ross, L. S. and Gill, S. S. (1998). Cloning of the V-ATPase B subunit cDNA from *Culex quinquefasciatus* and expression of the B and C subunits in mosquitoes. *Insect Mol. Biol.* **7(3)**, 223-232.

Franz, A. W., Sanchez-Vargas, I., Adelman, Z. N., Blair, C. D., Beaty, B. J., James, A. A. and Olson, K. E. (2006). Engineering RNA interference-based resistance to dengue virus type 2 in genetically modified *Aedes aegypti*. *Proc. Natl. Acad. Sci*. **103(11)**, 4198-203.

Goodchild, A. J. P. (1969). The rectal glands of *Halosalada lateralis* (Fallen) (Hemiptera: Saldidae) and *Hydrometra stagnoum* (L.) (Hemiptera: Hydrometridae). *Proc. Roy. Ent. Soc. Lond.* (A) **44**, 62-70.

Grassl, S. M. and Aronson, P. S. (1986). Na^+/HCO_3^-co-transport in basolateral membrane vesicles isolated from rabbit renal cortex. *J Biol Chem*. **261(19)**, 8778-8783.

Gringorten, J. L., Crawford, D. N. and Harvey, W. R. (1993). High pH in the ectoperitrophic space of the larval lepidopteran midgut. *J. exp Biol*. **183**, 353-359.

Gubler, D. J. Insects in Disease Transmission. In: Strickland G. T., editor. Hunter tropical medicine, 7th edition. Philadlphia: W. B. Saunders; 1991. p. 981-1000.

Hansen, I. A., Sieglaff, D. H., Munro, J. B., Shiao, S. H., Cruz, J., Lee, I. W., Heraty, J. M. and Raikhel, A. S. (2007). Forkhead transcription factors regulate mosquito reproduction. *Insect Biochem. Mol. Biol*. **37(9)**, 985-97.

Hansson, H. P. J. (1967). Histochemical demonstration of carbonic anhydrase activity. *Histochemie*. **11**, 112-128.

Harvey, W. R. (1992). Physiology of V-ATPases. *J. Exp. Biol.* **172**, 1-17.

Harvey, W. R. and Nedergaard, S. (1964). Sodium-independent active transport of potassium in the isolated midgut of *Cecropia* silkworm. *Proc. Natn. Acad. Sci. U.S.A.* **51**, 757–765.

Harvey, W. R., Cioffi, M., Dow, J. A. T. and Wolfersberger, M.G. (1983). Potassium ion transport ATPase in insect epithelia. *J.Exp. Biol*. **106**, 91–117.

Helbig, H., Korbmacher, C., Kühner, D., Berweck, S. and Wiederholt, M. (1988). Characterization of Cl^-/HCO_3^- exchange in cultured bovine pigmented ciliary epithelium. *Exp Eye Res*. **47(4)**, 515-23.

Henry, R. P. (1984). The role of carbonic anhydrase in blood ion and acid-base regulation. *Am. Zool.* **24**, 241–251.

Hewett-Emmett, D. and Tashian, R. E. (1996). Functional diversity, conservation and convergence in the evolution of the alpha-, beta-, and gamma–carbonic anhydrase gene families. *Mol. Phylogenet. Evol.* **5(1)**, 50-77.

Hoa, N. T., Keen, K. M., Olson, K. E. and Zheng, L. (2003). Characterization of RNA interference in an *Anopheles gambiae* cell line. *Insect Biochem. Mol. Biol*. **33**, 949-57.

Hopp, T. P. and Woods, K. R. (1981). Prediction of protein antigenic determinants from amino acid sequences. *Proc. Natl. Acad. Sci.* **78(6)**, 3824-3828.

Hung, C., Lin, T. and Lee, W. (2000). Morphology and ultrastructure of the alimentary canal of the oriental fruit fly, *Bactrocera dorsalis* (Hendel) (Dipteria: Tephritidae) (2): The structure of the midgut. *Zoological Studies.* **39(4)**, 387-394.

Hurlbut, H. S. (1943). Observations on the use of sea water in the control of *Anopheles albimanus* wied. *J. Parasitol.* **29(5)**, 356-360.

Huss, M. Ingenhorst, G. König, S., Gassel, M., Dröse, S., Zeeck, A., Altendorf, K. and Wieczorek, H. (2002). Concanamycin A, the specific inhibitor of V-ATPases, binds to the V(o) subunit c. *J. Biol. Chem.* **277(43)**, 40544-40548.

Kane, P. M. and Parra, K. J. (2000). Assembly and regulation of the yeast vacuolar H^+-ATPase. *J. Exp. Biol*. **203(Pt 1)**, 81-87.

Kang'ethe, W., Aimanova, K. G., Pullikuth, A. K. and Gill, S. S. (2007). NHE8 mediates amiloride-sensitive Na^+/H^+ exchange across mosquito Malpighian tubules and catalyzes Na^+ and K^+ transport in reconstituted proteoliposomes. *Am. J. Physiol. Renal Physiol.* **292**, F1501-1512.

Keene, K. M., Foy, B. D., Sanchez-Vargas, I., Beaty, B. J., Blair, C. D. and Olson, K. E. (2004). RNA interference acts as a natural antiviral response to O'nyong-nyong virus (Alphavirus; Togaviridae) infection of *Anopheles gambiae*. *Proc. Natl. Acad. Sci*. **101**, 17240-17245.

Killeen, G. F., Fillinger, U. and Knols, B. G. J. (2002a). Advantages of larval control for African malaria vectors: Low mobility and behavioural responsiveness of immature mosquito stages allow high effective coverage. *Malaria Journal*. **1**, 8-15.

Killeen, G. F., Fillinger, U., Kiche, I., Gouagna, L. C. and Knols, B. G. J. (2002b). Eradication of Anopheles gambiae from Brazil: lessons for malaria control in Africa? *Lancet Infect. Dis.* **2(10)**, 618-627.

Kimber, M. S. and Pai, E. F. (2000). The active site architecture of *Pisum sativum* beta-carbonic anhydrase is a mirror image of that of alpha-carbonic anhydrases. *EMBO journal*. **19(7)**, 1407-418.

Ko, S. B., Luo, X., Hager, H., Rojek, A., Choi, J. Y., Licht, C., Suzuki, M., Muallem, S., Nielsen, S. and Ishibashi, K. (2002). AE4 is a DIDSsensitive Cl^-/HCO_3^- exchanger in

the basolateral membrane of the renal CCD and the SMG duct. *Am J Physiol*. **283**, C1206– C1218.

Kochian, L. V., Shaff, J. E., Kühtreiber, W. M., Jaffe, L. F. and Lucas, W. J. (1992) Use of an extracellular, ion-selective, vibrating microelectrode system for the quantification of K^+ H^+, and Ca^{2+} fluxes in maize roots and maize suspension cells. *Planta*. **188,** 601–610.

Koefoed-Johnsen, V. and Ussing, H. H. (1958). The nature of the frog skin potential. *Acta. Physiol. Scand.* **42**, 298-308.

Konet, D. S., Anderson, J., Piper, J., Akkina, R., Suchman, E. and Carlson, J. (2007). Short-hairpin RNA expressed from polymerase III promoters mediates RNA interference in mosquito cells. *Insect Mol. Biol*. **16(2)**, 199–206.

Kühtreiber, W. M and Jaffe, L. F. (1990). Detection of extracellular calcium gradients with a calcium-specific vibrating electrode. *J Cell Biol*. **110**, 1565–1573.

Kyte, J. and Doolittle, R. F. (1982). A simple method for displaying the hydropathic character of a protein. *J. Mol. Biol.* **157**, 105-132.

Lane, T. W., Saito, M. A., George, G. N., Pickering, I. J., Prince, R. C. and Morel, F. M. (2005). Biochemistry: a cadmium enzyme from a marine diatom. *Nature*. **435(7038)**, 42.

Larkin, M. A., Blackshields, G., Brown, N. P., Chenna, R., McGettigan, P. A., McWilliam, H., Valentin, F., Wallace, I. M., Wilm, A., Lopez, R., Thompson, J. D., Gibson, T. J. and Higgins, D. G. (2007). Clustal W and Clustal X version 2.0. *Bioinformatics*. **23(21)**, 2947-2948.

Lebovitz, R. M., Takeyasu, K. and Fambrough, D. M. (1989). Molecular characterization and expression of the (Na^++K^+)-ATPase alpha-subunit in Drosophila melanogaster. *EMBO J.* **8,** 193-202.

Lepier, A., Azuma, M., Harvey, W. R. and Wieczorek, H. (1994). K^+/H^+ antiport in the tobacco hornworm midgut: the K($^+$)-transporting component of the K^+ pump. *J Exp Biol.* **196,** 361-73.

Liljas, A., Kannan, K. K., Bergsén, P. C., Waara, I., Fridborg, K., Strandberg, B., Carlbom, U., Järup, L., Lövgren, S. and Petef, M. (1972). Crystal structure of human carbonic anhydrase C. *Nat. New Biol*. **235(57)**, 131-137.

Linser, P. J., Seron, T. J., Hill, J. and Lehman, H. K. (2003). Characterization of novel carbonic anhydrases in larval mosquitoes. *Am. J. Trop. Med. Hyg.* **69(A319)**, 335.

Lutjen-Drecoll, E. and Lonnerholm, G. (1981). Carbonic anhydrase distribution in the rabbit eye by light and electron microscopy. *Invest. Ophthalmol. Vis. Sci.* **21**, 782-797.

Maddrell, S. H. P. and O'Donnell, M. J. (1992). Insect Malpighian tubules: V-ATPase action in ion and fluid transport. *J. Exp. Biol.* **172**, 417-429.

Mann, T. and Keilin, D. (1940). Sulfanilamide as a specific inhibitor of carbonic anhydrase. *Nat.* **146**, 164-165.

Maren, T. H. (1980). Kinetics, equilibrium and inhibition in the Hansson histochemical procedure for carbonic anhydrase: a validation of the method. *Histochem. J.* **12**, 183-190.

Matulef, K. and Maduke, M. (2005). Side-dependent inhibition of a prokaryotic ClC by DIDS. *Biophys.* **89**, 1721-1730.

Matz, M. Amplification of representative amounts of cDNA pools from microscopic amounts of animal tissue. In: Ying S-Y (ed.) 2003. Methods in molecular biology, vol 221: Generation of cDNA libraries: Methods and Protocols. Humana Press, Totowa NJ.

Matz, M., Shagin, D., Bogdanova, E., Britanova, O., Lukyanov, S., Diatchenko, L. and Chenchik, A. (1999). Amplification of cDNA ends based on template-switching effect and step-out PCR. *Nucleic Acids Research*. **27(6)**, 1558-1560.

McMurtrie H., Cleary H. J., **Alvarez B. V., Loiselle F. B., Sterling D., Morgan P. E., Johnson D. E. and Casey, J. R.** (2004)**.** The bicarbonate transport metabolon. *Journal of Enzyme Inhibition and Medicinal Chemistry*. **19(3)**, 231-236.

Meleshkevitch, E. A., Assis-Nascimento, P., Popova, L. B., Miller, M. M., Kohn, A. B., Phung, E. N., Mandal, A., Harvey, W. R. and Boudko, D. Y. (2006). Molecular characterization of the first aromatic nutrient transporter from the sodium neurotransmitter symporter family. *J. Exp. Biol.* **209 (Pt 16)**, 3183-98.

Meredith, J. and Phillips, J. E. (1973). Rectal ultrastructure in salt- and freshwater mosquito larvae in relation to physiological state. *Z. Zellforsch*. **138**, 1-22.

Messerli, M. A., Robinson, K. R. and Smith, P. J. S. (2006). Electrochemical sensor applications to the study of molecular physiology and analyte flux in plants. In: Volkov AG (ed) Plant electrophysiology - Theory and Methods. Springer, New York, pp 73 – 108.

Mitsuhashi, S., Mizushima, T., Yamashita, E., Yamamoto, M., Kumasaka, T., Moriyama, H., Ueki, T., Miyachi, S. and Tsukihara, T. (2000) X-ray structure of β-carbonic anhydrase from the red alga, *Porphyridium purpureum*, reveals a novel catalytic site for CO_2 hydration, *J. Biol. Chem.* **275**, 5521−5526.

Mosha, F. W. and Subra, R. (1983). Salinity and breeding of *Culex quinquefasciatus* Say, *Anopheles funestus* Giles and *Anopheles gambiae* Giles sensu stricto (Diptera: Culicidae) on the Kenya Coast. *Cah. O.R.S.T.O.M., ser. Ent. Med. Et Parasitol.* **21(3)**, 135-138.

Mullenbach, E., Turell, D. M. and Turell, M. J. (2004). Effect of salt concentration in larval rearing water on mosquito development and survival. *J. Vector Biol.* **30(1)**, 165-167.

Muther, T. F. (1966). On the non-specificity of histochemical methods for carbonic anhydrase. *Fed. Proc.* **25**, 320.

Nayar, J. K. and Sauerman Jr., D. M. (1974). Osmoregulation of the larvae of the salt-march mosquito *Aedes taeniorhynchus*. *Entomologia Exp. Appl.* **17**, 367-380.

Neira Oviedo, M., VanEkeris, L., Corena-Mcleod, M. D. P. and Linser, P. J. (2008). A microarray-based analysis of transcriptional compartmentalization in the alimentary canal of *Anopheles gambiae* (Diptera: Culicidae) larvae. *Insect Mol. Biol*. **17**, 61-72.

Nicholas, K. B., Nicholas, H. B. Jr. and Deerfield, D. W. II. (1997). GeneDoc: analysis and visualization of genetic variation. *EMBNEW.NEWS*. 4, 14.

Okech, B. A., Boudko, D. Y., Linser, P. J. and Harvey, W. R. (2008). Cationic pathway of pH regulation in larvae of *Anopheles gambiae***.** *J. Exp. Biol.* **211**, 957-968.

O'Meara, G. F. (1976). Saltmarsh mosquitoes. In *Marine Insects* (ed. L. Cheng), North-Holland, Amsterdam, pp. 303-333.

Orlowski, J. and Grinstein, S. (2004). Diversity of the mammalian sodium/proton exchanger SLC9 gene family. *Pflugers Arch.* **447**, 549-565.

Padan, E., Venturi, M., Gerchman, Y. and Dover, N. (2001). Na^+/H^+ antiporters. *Biochim. Biophys. Acta* **1505**, 144-157.

Palatroni, P., Gabrielli, M. G. and Scattolini, B. (1981). Histochemical localization of carbonic anhydrase in Malpighian tubules of *Culex pipiens*. *Experientia*. **37,** 409-411.

Patrick, M. L., Aimanova, K., Sanders, H. R. and Gill, S. S. (2006). P-type Na^+/K^+-ATPase and V-type H^+-ATPase expression patterns in the osmoregulatory organs of larval and adult mosquito *Aedes aegypti*. *J. Exp. Biol.* **209**, 4638-4651.

Paunescu, T. G., Jones, A. C., Tyszkowski, R. and Brown, D. (2008). V-ATPase expression in the mouse olfactory epithelium. *Am. J. Physiol. Cell Physiol.* **295(4)**, C923-930.

Pfaffl, M. W. (2001). A new mathematical model for relative quantification in real-time RT-PCR. *Nucleic Acids Res*. **29(9)**, 2002–2007.

Pudney, M., Varma, M. G. R. and Leake, C. J. (1979). Establishment of cell lines from larvae of culicine (Aedes species) and Anopheline mosquitoes. *TCA manual***.** **5(1)**, 997-1002**.**

Pullikuth, A. K., Aimanova, K., Kang'ethe, W., Sanders, H. R. and Gill, S. S. (2006)**.** Molecular characterization of sodium/proton exchanger 3 (NHE3) from the yellow fever vector, *Aedes aegypti*. *J Exp Biol***. 209(Pt 18),** 3529-3544**.**

Radermacher, M., Ruiz, T., Harvey, W. R., Wieczorek, H. and Gruber, G. (1999). Molecular architecture of Manduca sexta midgut V1 ATPase visualized by electron microscopy. *FEBS Lett*. **453**, 383-6.

Ramsay, J. A. (1950). Osmotic regulation in mosquito larvae. *J. Exp. Biol*. **27**, 145-157.

Rheault, M. R., Okech, B. A., Keen, S. B. W., Miller, M. M., Meleshkevitch, E. A., Linser, P. J., Boudko, D. Y. and Harvey, W. R. (2007). Molecular cloning, phylogeny and localization of AgNHA1: the first Na^+/H^+ antiporter (NHA) from a metazoan, *Anopheles gambiae*. *J. Exp. Biol.* **210**, 3848-3861.

Ridderstråle, Y. (1991). Localization of carbonic anhydrase by chemical reactions. In: Dodgson S.J., Tashian R.E., Gros G., Carter N.D. (eds) The carbonic anhydrases: cellular physiology and molecular genetics. Plenum Press, New York, pp 133-144.

Romero, M. F., Henry, D., Nelson, S., Harte, P. J., Dillon, A. K. and Sciortino, C. M. (2000). Cloning and characterization of a Na^+-driven anion exchanger (NDAE1). *J. Biol. Chem.* **275 (32)**, 24552-24559.

Romero, M. F., Fulton, C. M. and Boron W. F. (2004). The SLC4 family of HCO_3^- transporters. *Eur. J. Physiol*. **447**, 495-509.

Roy, S. G., Hansen, I. A. and Raikhel, A. S. (2007). Effect of insulin and 20-hydroxyecdysone in the fat body of the yellow fever mosquito, *Aedes aegypti*. *Insect Biochem. Mol. Biol*. **37(12)**, 1317-26.

Sachs, J. and Malaney, P. (2002). The economic and social burden of malaria. *Nature.* **415**, 680-685.

Schewe, B., Schmälzlin, E. and Walz, B. (2008). Intracellular pH homeostasis and serotonin-induced pH changes in Calliphora salivary glands: the contribution of V-ATPase and carbonic anhydrase. *J. Exp. Biol*. **211(Pt 5)**, 805-815.

Seron, T. J., Hill, J. and Linser, P. J. (2004). A GPI-linked carbonic anhydrase expressed in the larval mosquito midgut. *J. Exp. Biol*. **207(Pt 26)**, 4559-4572.

Skou J. C. (1990). The fourth Datta lecture. The energy coupled exchange of Na^+ for K^+ across the cell membrane. The Na^+, K^+-pump. *FEBS Lett*. **268(2)**, 314-324.

Smith, K. E., VanEkeris, L. A. and Linser, P. J. (2007). Cloning and characterization of AgCA9, a novel α-carbonic anhydrase from *Anopheles gambiae* Giles sensu stricto (Diptera: Culicidae) larvae. *J. Exp. Biol*. **210**, 3919-3930.

Smith, K. E., VanEkeris, L. A., Okech, B. A., Harvey, W. H. and Linser, P. J., (2008). Larval anopheline mosquito recta exhibit a dramatic change in localization patterns of ion transport proteins in response to shifting salinity: a comparison between anopheline and culicine larvae. *J. Exp. Biol.* **211(Pt 19)**, 3067-3076.

Smith, P. J. S, Sanger, R. H. and Jaffe, L. F. (1994). The vibrating Ca^{2+} electrode: a new technique for detecting plasma membrane regions of Ca^{2+} influx and efflux. In: Wilson L, Matsudaira P, editors. Methods in cell biology. a practical guide to the study of Ca^{2+} in living cells. San Diego: Academic Press, p115–134.

Smith, P. J. S, Hammar, K., Porterfield, D. M., Sanger, R. H. and Trimarchi, J. R. (1999). Self-referencing, non-invasive, ion selective electrode for single cell detection of trans-plasma membrane calcium flux. *Microsc. Res. Techniq*. **46**, 398-417.

Smith, P.J.S., Sanger, R.S. and Messerli, M.A. (2007). Principles, Development and Applications of Self-Referencing Electrochemical Microelectrodes to the Determination of Fluxes at Cell Membranes. In: Methods and New Frontiers in Neuroscience. Ed. Adrian C. Michael. CRC Press. Ch. 18: 373-405.

So, A. K., Espie, G. S., Williams, E. B., Shively, J. M., Heinhorst, S. and Cannon, G. C. (2004). A novel evolutionary lineage of carbonic anhydrase (epsilon class) is a component of the carboxysome shell. *J Bacteriol*. **186(3)** 623-30.

Sterling, D., Reithmeier, R. A. F and Casey J. R. (2001). Carbonic anhydrase: in the driver's seat for bicarbonate transport. *JOP. J. Pancreas*. **2(4 suppl)** 165-170.

Stobbart, R. H. (1971). Evidence of Na^+/H^+ and $Cl^-/HCO3^-$ exchanges during independent sodium and chloride uptake by the larvae of the mosquito *Aedes aegypti. J. Exp. Biol.* **54**, 19-27.

Stothard, P. (2000). The sequence manipulation suite: JavaScript programs for analyzing and formatting protein and DNA sequences. *BioTechniques*. **28**, 1102-1104.

Strange, K. and Phillips, J. E. (1984). Mechanisms of CO_2 transport in rectal salt gland of *Aedes*. I. Ionic requirements of CO_2 secretion. *Am. J. Physiol.* **246(5 Pt 2)**, R727-734.

Strange, K., Phillips, J. E. and Quamme, G. A. (1982). Active HCO_3^- secretion in the rectal salt gland of a mosquito larva inhabiting $NaHCO_3$-CO_3 lakes. *J. Exp. Biol.* **101**, 171-186.

Strange, K., Phillips, J. E. and Quamme, G. A. (1984). Mechanisms of CO_2 transport in rectal salt gland of *Aedes*. II. Site of Cl^--HCO_3- exchange. *Am. J. Physiol.* **246(5 Pt 2)**, R735-740.

Sumner, J-P., Dow, J. A. T., Earley, F. G. P., Klein, U., Jäger, D. and Wieczorek, H. (1995). Regulation of plasma membrane V-ATPase activity by dissociation of peripheral subunits. *J. Biol. Chem.* **270(10)**, 5649-5653.

Tashian, R. E., Hewett-Emmett, D., Carter, N. D. and Bergenhem, N. C. H. (2000). Carbonic anhydrase (CA)-related proteins (CA-RPs), and transmembrane proteins with CA or CA-RP domains. In: Chegwidden, W.R., Carter, N.D., Edwards, Y.H. (Eds.), The Carbonic Anhydrases. New Horizons. Birkhäuser, Basel, pp. 105–120.

Terra, W. R. and Ferreira, C. (1981). The physiological role of the peritrophic membrane and trehalase: digestive enzymes in the midgut and excreta of starved larvae of *Rhynchosciara*. *J. Insect Physiol.* **27(5)**, 325-331.

Terra, W. R., Ferreira, C. and Bianchi, A. G. (1979). Distribution of digestive enzymes among the endo- and ectoperitrophic spaces and midgut cells of *Rhynchosciara* and its physiological significance. *J. Insect Physiol.* **25**, 487-494.

The World Health Report 1996: fighting disease, fostering development. Geneva: World Health Organization; 1996. p. 46.

Toyosawa, S., Ogawa, Y., Inagaki, T. and Ijuhin, N. (1996). Immunohistochemical localization of carbonic anhydrase II in rat incisor epithelial cells at various stages of amelogenesis. *Cell Tissue Res*. **285**, 217-225.

Volkmann, A. and Peters, W. (1989). Investigations on the midgut caeca of mosquito larvae-I. Fine Structure. *Tissue and Cell*, **21**. 253-261.

Wessing, A. and Zierold, K. (1997). The formation of type-I concretions in Drosophila Malpighian tubules studied by electron microscopy and X-ray microanalysis. *J Insect Physiol*. **45(1)**, 39-44.

Wessing, A., Zierold, K. and Bertram, G. (1999). Carbonic anhydrase supports electrolyte transport in Drosophila Malpighian tubules. Evidence by X-ray microanalysis of cryosections. *J. Insect Physiol.* **43(1)**, 17-28.

Wieczorek, H. (1992). The insect V-ATPase, a plasma membrane proton pump energizing secondary active transport: molecular analysis of electrogenic potassium transport in the tobacco hornworm midgut. *J. Exp. Biol*. **172**, 335-43.

Wieczorek, H., Cioffi, M., Klein, U., Harvey, W. R., Schweikl, H. and Wolfersberger, M. G. (1990). Isolation of goblet cell apical membrane from tobacco hornworm midgut and purification of its vacuolar-type ATPase. *Methods Enzymol*. **192**, 608-616.

Wieczorek, H., Putzenlechner, M., Zeiske, W. M. and Klein,U. (1991). A vacuolar-type proton pump energizes K^+/H^+- antiport in an animal plasma membrane. J. Biol. Chem. 266, 15340–15346.Wigglesworth V. B. 1972. The Principles of Insect Physiology, 7th Edition. Chapman & Hall, London.

Wigglesworth, V. B. 1972. The Principles of Insect Physiology, 7th Edition. Chapman & Hall, London.

Zhang, Y. and Frohman, M. A. (1997). Using rapid amplification of cDNA ends (RACE) to obtain full-length cDNAs. *Methods Mol. Biol.* **69,** 61-87.

Zhuang, Z., Linser, P. J. and Harvey, W. R. (1999). Antibody to H^+ V-ATPase subunit E colocalizes with portasomes in alkaline larval midgut of a freshwater mosquito. *J. Exp. Biol*. **202**, 2449–2460.

BIOGRAPHICAL SKETCH

Kristin E. Smith was born in Somers Point, NJ and raised in West Chester PA. She is the oldest of three half-siblings, a sister and two brothers. She received her Bachelor of Science degree from Pennsylvania State University in 2004, graduating with a major in microbiology and a minor in biochemistry and molecular biology. It was during her undergraduate studies that she participated in the co-operative education program, working for a total of 18 months at GlaxoSmithKline Pharmaceuticals at the Collegeville and King of Prussia, PA branches. At GlaxoSmithKline she developed a love for the industrial work setting. Following graduation, Kristin moved to Gaivesville, FL to pursue an advanced degree at the University of Florida College of Medicine. A love for the smaller community at Whitney and isolated environment brought her to the Whitney Laboratory where she worked under the direction of Prof. Paul Linser characterizing various ion- and ph-regulatory proteins in the larval mosquito alimentary canal. Upon completion of her doctorate degree, she has secured a post-doctoral position at Mayo Clinic in Jacksonville FL, investigating the mechanisms of action of various psychotropic drugs.